Release Areas of Snow Avalanches: New Methods and Parameters

Dissertation

zur

Erlangung der naturwissenschaftlichen Doktorwürde
(Dr. sc. nat.)

vorgelegt der

Mathematisch-naturwissenschaftlichen Fakultät

der

Universität Zürich

von

Jochen Veitinger

aus

Deutschland

Promotionskomitee

Prof. Dr. Ross Purves (Vorsitz)
Dr. Betty Sovilla (Leitung der Dissertation)
Prof. Dr. Robert Weibel

Zürich, 2015

Abstract

Location and extent of avalanche starting zones are of crucial importance in order to correctly estimate the potential danger that avalanches pose to roads, railways or other infrastructure. Presently, release area assessment is based on terrain analysis, combined with expert judgement. Tools for the automatic definition of release areas are scarce and exclusively based on parameters derived from summer topography, such as slope and curvature; this leads to several limitations concerning the performance of such algorithms. One reason for this is that they neglect the effect of the snow cover on terrain morphology. In alpine terrain, the snow-covered winter surface deviates from its underlying summer terrain due to the progressive smoothing caused by snow. It is assumed that this may change the potential release area size and location – especially in the case of surface slab avalanches; therefore, it seems very likely that release area calculations performed on a summer terrain may strongly differ from calculations on a more realistic winter terrain. Introducing the snow distribution into release area definition therefore may significantly improve the definition and partitioning of potential release areas for hazard mapping purposes, as well as going towards closing the gap concerning the implementation of avalanche dynamics simulations in short-term hazard assessment. The main aim of this thesis is therefore centred on assessing the effect of snow distribution on surface morphology, and accordingly integrating this into a new algorithm with the objective to estimate the size and location of slab avalanche release areas.

In an effort to quantify terrain smoothing, high-resolution lidar measurements of the snow distribution in a high alpine catchment were performed throughout three winter seasons, comprising several acquisitions per winter season. A method was developed geared towards quantifying terrain smoothing by combining roughness calculations of snow surfaces and their corresponding underlying terrain with snow depth measurements. The evaluation of terrain smoothing showed that surface roughness at scales larger than fine-scale drift features is, to some degree, persistent between winter seasons. Further, the degree and scale of terrain smoothing processes in a topographical basin could be linked to snow distribution, namely mean snow depth and its variability. This allows approximating the winter terrain from the summer terrain as a function of snow depth.

In a next step, the effect of snow distribution on the potential size and location of slab avalanche release areas was assessed. On the one hand, examination centred on

establishing the extent to which a homogeneous terrain surface is more favourable to produce larger avalanche release areas than irregular ones. Slab properties, such as thickness and its variability, as measured by airborne laser scanning both prior to and after artificial slab avalanche release, were compared to surface roughness of underlying bed surface and snow-free terrain. The results show quantitatively, that the potential size of avalanche release areas may be linked to the surface roughness of the winter terrain. Further, winter terrain roughness appeared to be highly capable of delimiting release areas. On the other hand, the relevance of terrain smoothing was statistically assessed by relating point snow depth measurements to observed avalanche release area sizes in single avalanche paths. We observed that very large surface slab release areas occurred only in relatively thick snow covers, whilst very large slab release areas, running on weak basal layers, also occurred in shallow snowpacks. This suggests that the effect of terrain smoothing is mainly relevant for surface slab avalanches.

Based on the scale-dependency of terrain smoothing processes, we finally integrated a snow depth-dependent roughness parameter into a new fuzzy logic framework for the estimation of potential slab avalanche release areas. The validation process demonstrated an improved estimation of avalanche release areas – especially for more frequent avalanches; several case studies further illustrated the practical usefulness of this approach for hazard mapping and short-term hazard assessment. The algorithm allows capturing fine-scale topography and its attenuation under snow influence, thus providing valuable information on the partitioning of potential release areas. In addition, a wind direction-dependent sheltering parameter enables the user to define release area scenarios as a function of single storm or drift events; yet, the application of the algorithm in real case situations remains limited as snowpack stability is not integrated. In order to make this approach amenable, future research activity could therefore focus on the coupling of the algorithm with snowpack conditions.

Zusammenfassung

Lage und Grösse von Lawinenanrissgebieten sind wichtige Faktoren um das Gefahrenpotential von Lawinen für Strassen, Bahnlinien oder sonstige Infrastruktur zu beurteilen. Im Moment basiert die Abschätzung von Lawinenanrissgebieten auf Geländeanalysen und Expertenwissen. Methoden für eine räumliche Berechnung von Anrissgebieten sind rar und basieren hauptsächlich auf grobskaligen Geländeparametern, welche von einem Sommergeländemodell abgeleitet werden, wie zum Beispiel Neigung oder Krümmung. Dies hat zur Folge, dass die Leistungsfähigkeit solcher Methoden oft eingeschränkt ist. Ein möglicher Grund dafür ist, dass der Einfluss der Schneedecke auf die morphologischen Eigenschaften einer Geländeoberfläche nicht erfasst wird. Eine wachsende Schneedecke bewirkt eine zunehmende Glättung der Winteroberfläche, welche oft stark von der darunter liegenden Geländeoberfläche abweicht. Es ist anzunehmen, dass dadurch Lage und Grösse von potentiellen Anrissgebieten, vor allem oberflächennaher Lawinen, massgeblich beeinflusst wird. Auf einem Sommergelände basierende Berechnungen von Lawinenanrissgebieten könnten deshalb stark von Berechnungen auf einem wirklichkeitsgetreuen Wintergeländemodell abweichen. Die Integration der Schneedecke in solche Berechnungsmodelle könnte deshalb zu einer verbesserten Bestimmung und Unterteilung des Anbruchgebiets führen, was sowohl für die Gefahrenzonenplanung als auch hinsichtlich der Anwendung numerischer Lawinendynamikmodelle in realitätsnahen Situationen, was eine sehr genaue Abschätzung des Lawinenanrisses erfordert, sehr nützlich sein könnte. Vor diesem Hintergrund beschäftigt sich diese Arbeit vor allem damit, den Glättungseffekt der Schneedecke auf die Geländeoberfläche zu erfassen und in einen neuen Algorithmus zur räumlichen Bestimmung potentieller Anrisszonen zu integrieren.

Zu diesem Zweck wurde während dreier Winterhalbjahre, Lidar-basierte, hochaufgelöste Schneehöhenmessungen in einem hochalpinen Einzugsgebiet durchgeführt. Darauf basierend wurde eine Methode entwickelt, welche die Glättung der Geländeoberfläche erfasst und quantifiziert. Basierend auf einem Rauigkeitsparameter, wurden Sommer- und Wintergeländeoberfläche mit Schneehöhenmessungen verknüpft. Es konnte gezeigt werden, dass die Winteroberfläche zwischen verschiedenen Wintern, auf einer Grössenskala welche die Grösse von Rauigkeitselementen wie Dünen oder Wechten übersteigt, zu einem gewissen Anteil ähnlich ist. Des Weiteren konnte der Glättungsgrad, und die Skala der von Glättungsprozessen beeinflussten Oberflächenrauigkeit, mit der mittleren Schneehöhe und deren Variabilität verknüpft werden. Dies erlaubt eine schneehöhenabhängige Anpassung der Winteroberfläche ausgehend von einem Sommergelände.

Nachfolgend wurde der Einfluss der Schneeverteilung auf die Grösse von Lawinenanrisszonen untersucht. Einerseits wurde der Frage nachgegangen, inwiefern sich eine homogene Geländeoberfläche eher für grosse Anrissgebiete eignet, als eine unregelmässige. Dazu wurden Schneebretteigenschaften wie Mächtigkeit und deren Variabilität mit der Rauigkeit der Gleitfläche sowie der darunter liegenden Geländeoberfläche verglichen. Die Auswertungen zeigen zum ersten Mal quantitativ, dass die Grösse eines Lawinenanrisses mit der Oberflächenrauigkeit des darunter liegenden Geländes zusammenhängen könnte. Ausserdem erwies sich die Rauigkeit der Winteroberfläche als sehr geeignet um potentielle Anrissgebiete abzugrenzen und zu unterteilen. Andererseits wurde der Einfluss der Geländeglättung statistisch untersucht, indem Messungen der Gesamtschneehöhe mit der Lawinenbreite von dokumentierten Lawinenereignissen in einzelnen Lawinenzügen verglichen wurden. Während grosse Lawinenanrisse in oberflächennahen Schichten der Schneedecke nur in relativ mächtigen Schneedecken auftraten, wurden sie in bodennahen Lawinen auch bei sehr geringer Schneehöhe beobachtet. Das deutet darauf hin, dass der Einfluss der Geländeglättung auf die Lawinenanrissfläche vor allem für Oberflächenlawinen relevant ist.

Die Abhängigkeit von Schneehöhe und Grössenskala einer geglätteten Winteroberfläche wurde abschliessend genutzt, um einen schneehöhenabhängigen Rauigkeitsparameter in einen neuen, auf der Fuzzy-Set Theorie basierten, Algorithmus zur Bestimmung von potentiellen Lawinenanrisszonen zu integrieren. Die Validierung mit dokumentierten Lawinenereignissen zeigte vor allem für die Abschätzung von häufigen Lawinen verbesserte Ergebnisse. Mehrere Fallstudien belegen ausserdem den zusätzlichen praktischen Nutzen dieses neuen Werkzeugs sowohl für die Gefahrenzonenplanung als auch für die regelmässige Gefahrenbeurteilung z.B. einer Verkehrsachse. Die Erfassung der Oberflächenrauigkeit und deren Glättung unter Einwirkung der Schneedecke liefert zusätzliche Anhaltspunkte für mögliche Unterteilungen des Anrissgebiets. Zusätzlich erlaubt ein ebenfalls integrierter Windeinflussparameter, Szenarien für Anrisszonen in Abhängigkeit von einzelnen Wetterereignissen zu definieren. Jedoch ist der Nutzen des Algorithmus für die Berechnung einzelner Lawinenereignisse, unter Berücksichtigung der aktuellen Lawinensituation limitiert, da Information über Schneedeckenaufbau und Schneedeckenstabilität nicht enthalten sind. Zukünftige Weiterentwicklungen könnten somit vor allem durch die Koppelung mit Informationen über den Schneedeckenaufbau erzielt werden.

Acknowledgements

First of all, I am very grateful to Betty Sovilla, my main supervisor, for her trust and support, for plenty of feedback, discussions and corrections and for always finding a storyline in my writing.

I also would like to thank Ross Purves for supervising this thesis with countless valuable advice on scientific and organisational issues. In particular, I would like to thank him for making it possible for me to spend some time within his research group, which brought a lot of input to my work from outside the "avalanche community".

I owe a debt of gratitude to Robert Weibel for supervising the thesis and the valuable feedback in the beginning of my thesis.

I also like to thank Curdin and Christian, who provided me with more than enough working space within their office, and, more important, with ideas, help and good humour making my visits in Zurich a fruitful and, at the same time, a very enjoyable time for me.

I would like to thank all colleagues from SLF, for their help and the great working ambiance. This work would have never been possible without all of you: Michael, Marc, Yves, Cesar, Tom F., Claudia, Anselm, JP, the best office colleagues Linda, Lisa, Martina and James, Luki, Stefan, Perry, Andi, Tom G., Frank, Gian, Christoph, Ben, Martin and many others.

I also thank all my friends, who made this time in Davos unforgettable. A special thanks goes to Walter, Fabiano, Christoph, Johan, Benni, Kiki, Sanni, Maren, Christiane and Laura for sharing the flat, good times (and good food!!) with me.

I would not be where I am today without the everlasting support of my parents, which always encouraged me in following my interests and giving me the freedom to do so. Thank you for teaching me skiing when I was not even three years old and for awakening the fascination for snow in me!

Finally, I like to thank you, Sabrina, for sharing so many great moments, always reminding me of what really matters...

Contents

List of Figures

List of Tables

Chapter 1

Introduction

1.1 History and motivation

Snow avalanches still nowadays threaten human life and property all over the world. They endanger settlements, transportation links but also recreationists travelling in mountainous terrain. Alpine and North American countries such as Austria, Switzerland, France or the US nowadays observe a mean annual number of fatalities between 20 and 30 (Whiteman, 2011). But also many Asian and South American countries deal with avalanche hazard. As an example, data collected in the Western Himalaya indicates that 30 - 40 fatalities and property worth several million US dollars is lost every year in avalanches (Ganju and Dimri, 2004). However, actual numbers are likely to be significantly larger since many events occur unreported or are not documented in less developed parts of the world.

One trend that is observed in alpine countries during the last decades is the decrease of avalanche victims in settlements. This can be attributed to significant efforts directed towards protecting society and infrastructure from avalanche danger. As a consequence of the catastrophic avalanche winter of 1950/1951, which resulted in approximately 100 deaths in Austria and Switzerland (SLF, 1951), mountain communities in the Alps began to build defence structures in an attempt to hinder avalanches from starting or otherwise to protect endangered houses or transport networks. At the same time, local people, such as those from forest services, began to systematically map the outlines of observed snow avalanches; the so-called avalanche cadastre was born. Based on the information of this database, the first hazard map was established in 1953 in Switzerland, delineating the area that could potentially be threatened by avalanches. Soon, the importance of this planning tool for land use planning was recognised and its development pushed further forward. Different danger levels, dividing a threatened area into different danger

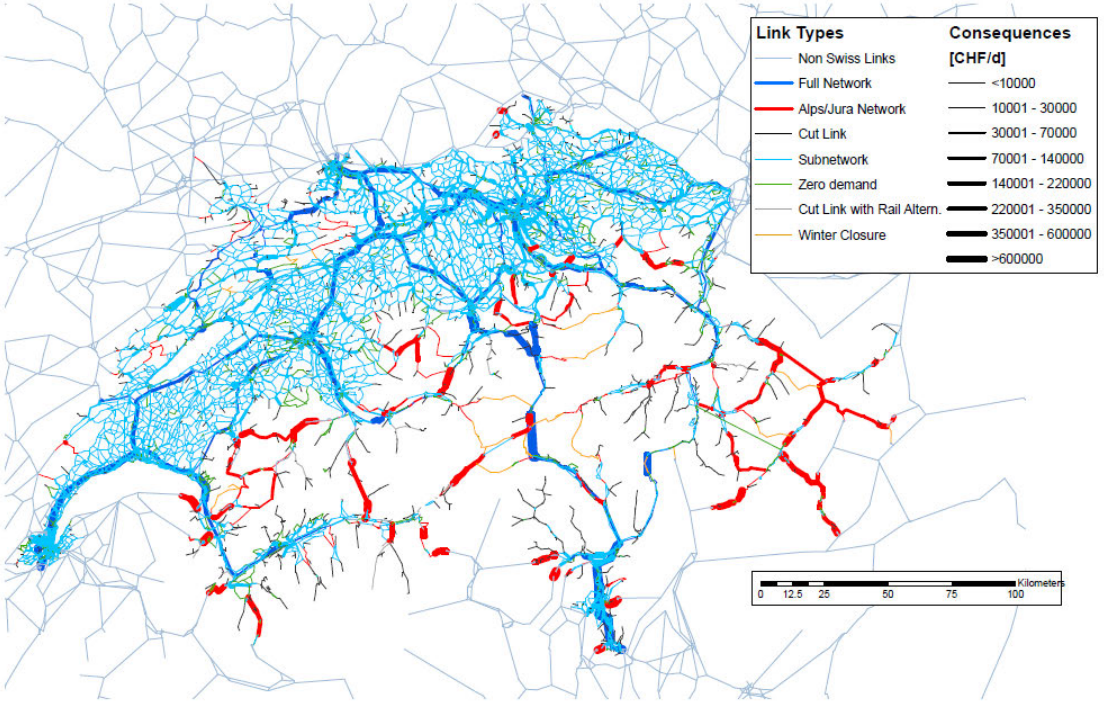

FIGURE 1.1: Vulnerability assessment for the Swiss road network. Indirect failure consequences based on the Swiss National Transport Model (Erath et al., 2009).

zones, and an official guideline for the consideration of avalanche danger for land-use planning, was issued in 1984 (BBF and SLF, 1984). It defines rules for the definition of the different hazard zones, considering not only the intensity of an avalanche event but also its frequency of occurrence (return period). Avalanche hazard mapping therefore mainly focuses on large avalanche events reaching valley floors and villages, and is today operational in many countries, such as Austria, Norway and Iceland (Jóhannesson et al., 2009). Together with important investments into structural mitigation measures (Switzerland invested around CHF 1.5 billion between 1951 and 1999 (SLF, 2000)), the avalanche hazard for mountain communities has been significantly reduced.

Although the last catastrophic avalanche winter of the years 1998/1999 demonstrated a good performance of hazard mapping and structural protection measures (Gruber and Margreth, 2001), in a very extreme situation (97% of the avalanches stopped within the marked avalanche hazard zones in Switzerland), one particular difficulty of hazard mapping remains today – that is, the definition of appropriate scenarios for shorter return periods (e.g. a 30 year return period). Throughout this process, the intensity of an avalanche event within a given return period has to be defined, including an estimation of the release area. Whilst the definition of extreme release areas is already challenging, release area definition for more frequent avalanches additionally requires the partitioning of the whole potential release zone into adequate sub-areas. This very complex task remains subject to the individual judgement of avalanche experts.

Nowadays, although the most dangerous avalanche paths have been mitigated using permanent protection structures, a large number of avalanche paths remain, posing a danger for roads, railways or ski resorts (Maggioni et al., 2012). Since resources for structural protection measures are quite limited (Margreth et al., 2003), temporary protection measures, such as road closures, are often favoured over structural mitigation measures due to their better cost-efficiency (Bründl et al., 2006; Wilhelm, 1998). Temporary protection measures heavily rely on a short-term assessment of possible locations and sizes of avalanche events; this necessitates experienced avalanche specialists with sound process understanding, as well as understanding and knowledge relating to nivo-meteorological conditions in a given area. This is especially important as tools for short-term hazard assessment at the level of single avalanche paths do not exist. Therefore – and in combination with the major difficulty of predicting avalanches– temporary mitigation measures, such as road closures, continue to produce many false alarms. Schweizer (2008) estimates the false alarm ratio in the order of 2–10 for road closures. Further, a closed transport way in mountainous regions is often linked to high financial damage. As an example, Figure 1.1 shows that, in Switzerland, a closed transport way in the alpine part of the country induces similar damage potential than the closure of a main transport axis in the Swiss plateau.

Numerical models of avalanche dynamics are well established tools in the current engineering practice of hazard mapping. They allow the assessment of run-out, velocity, flow height or impact pressure of avalanches, and are especially important when historical data is sparse or completely lacking; however, avalanche dynamics models cannot be applied for short-term hazard assessment as they are not coupled with snowpack conditions (Steinkogler et al., 2014). Nonetheless, it would be highly desirable to do so, such as in the case of estimating avalanche run-out in a given snow situation. In order for this approach to be considered amenable, considerable effort is currently being directed towards the implementation of snow cover parameters, such as the flow regime (Bartelt et al., 2011) or snow temperature (Vera Valero et al., 2012) into existing snow avalanche dynamics models. However, this requires a very precise definition of the release zone. Recent studies of modelling small and frequent avalanches, including snow cover parameters (Dreier et al., 2014), have shown a high sensitivity of the model for small changes of release area size and location.

With the increasing availability of geographic information systems (GIS) and digital elevation models, the development of algorithms to automate the process of release area definition was already initiated (Gruber, 2001). Although they are fairly suitable for the definition of extreme avalanche scenarios with very high return periods, they fail to estimate more frequent avalanches with smaller release areas. Current algorithms do not take into account the snow distribution as, for example, morphological changes

introduced by a snow-covered winter terrain surface. Therefore, it seems very likely that release area calculations performed on a summer terrain may strongly differ from calculations on a more realistic winter terrain. Introducing the snow distribution into release area definition therefore may significantly improve the definition and partitioning of potential release areas for hazard mapping purposes, and could also go towards closing the gap concerning the implementation of avalanche dynamics simulations in short-term hazard assessment.

1.2 Scientific questions and objectives

The basic rationale of this research is that the integration of morphological changes introduced by a snow-covered terrain into release area definition can significantly contribute to both long- and short-term avalanche hazard assessment. The successful application of avalanche dynamics models in hazard mapping procedures, as well as their potential integration into short-term avalanche mitigation practice, is highly dependent on an improved release area estimation; therefore, this thesis aims to develop techniques to assess the effect of snow distribution on surface morphology and to integrate it within a new framework of avalanche release area definition. In this process, the following research questions are addressed:

1. How does snow distribution influence surface morphology of alpine terrain and how can such an effect be captured?

2. What is the influence of the morphological differences between the snow free summer terrain and the snow-covered winter terrain on avalanche release area size and location?

3. How can potential release area modelling be improved by taking into account the influence of snow distribution on surface morphology?

In order to address the aforementioned research questions, several consecutive work packages are defined, each representing a separate research objective.

1. The development and evaluation of a methodology to quantify the effect of snow distribution on surface morphology in alpine terrain.

2. The assessment of the effect of morphological changes introduced by a snow-covered terrain on avalanche release area size.

3. The development of a new algorithm for release area definition, including morphological changes introduced by snow distribution.

1.3 Structure and outline of the thesis

Chapter 2 introduces all important concepts and theories adopted in the analysis of snow influence on geomorphology and avalanche release area modelling. This includes avalanche formation processes, geomorphometric parametrisation of terrain and natural hazards modelling. Chapter 3 presents the field sites, describes the techniques for performing the field measurements, and presents an overview of the obtained field data. Chapters 4 – 6 address the three main research questions. Chapter 4 describes how snow distribution influences surface morphology in a winter terrain. Chapter 5 investigates the influence of snow distribution on avalanche release area size and location. Chapter 6 presents the developed GIS tool and the chosen validation process. Chapter 7 discusses the strengths and weaknesses of the new release area algorithm, and recalls the main research questions in the context of the obtained results. In chapter 8, the achievements and insights from the research of this thesis are presented, with possible future research directions proposed.

Chapter 2

State of the art

In this chapter, an overview is provided of the principal theoretical concepts used in this thesis. In the first two sections, fundamental definitions and concepts in avalanche formation and hazard management are recalled. The third section comprises a review of how the interaction between terrain and snow distribution influences slab avalanche formation. The fourth section discusses different approaches of terrain modelling and the calculation of geomorphological parameters. The last section provides an overview on how natural hazards can be spatially modelled.

2.1 Avalanche hazard management

Avalanche risk management consists of protecting people, settlements and infrastructure from avalanches. A great variety of protection measures and planning instruments exist. Generally, one can distinguish structural (barriers, dams, sheds), planning (hazard mapping) or temporary measures (artificial avalanche release, road closures), whereas long term measures (hazard mapping, structural measures) require the detailed assessment of potential avalanche locations (starting zones and run-out), whilst temporary measures, such as road closures, additionally require the forecast of the time of occurrence and an assessment of current snow and meteorological situation. In this chapter, the differences between the two approaches are highlighted, particularly emphasising the different methodologies and tools used.

2.1.1 Hazard mapping

Hazard mapping is an important long-term land-use planning instrument, preventing humans from building in avalanche-prone terrain. A hazard map consists of different

zones, corresponding to different danger levels. The danger level is based on the frequency of the events (return period) and their magnitude. The return period (T) is technically the mean time (usually in years), separating two events of a given intensity, assuming independence and the same probability distribution for the successive events (Eckert et al., 2007). Several measures for the magnitude or intensity of an event exist, such as run-out distance, velocity, or impact pressure (p). Avalanche hazard mapping mainly focuses on large avalanche events reaching valley floors and villages. Normally, avalanches with return periods of 30 years and longer are considered.

Producing a hazard map is a complex task and requires a great deal of experience to be held by the individual in charge (BBF and SLF, 1984). The main points to be considered are as follows:

- Consultation of historical avalanche events in avalanche cadastre,
- Analysis of terrain characteristics,
- Field survey to recognize old avalanche traces,
- Assessment of snow climatological conditions,
- Expected type of avalanche and its return period,
- Definition of release depth and potential release area, and
- Evaluation of avalanche dynamics parameters and calculations.

Based on these criteria, design events are defined as a function of return period, which is related to a certain magnitude. Gradual hazard levels are then defined based on these design events. Many countries worldwide recognise hazard mapping procedures, yet the danger levels, return periods and intensity thresholds vary from one country to the next. In Switzerland, for example, four different danger zones, depending on the return period (T) and impact pressure (p) are defined (Fig. 2.1). In the red zone, the construction of new buildings is forbidden, whereas in the blue zone construction is only permitted for buildings with reinforced structure to resist possible avalanche impacts. The yellow zone is possibly affected by the powder cloud part of powder avalanches, whilst the white zone is considered safe, with no limitations applicable. The criteria defining the different danger zones are shown in Table 2.1.

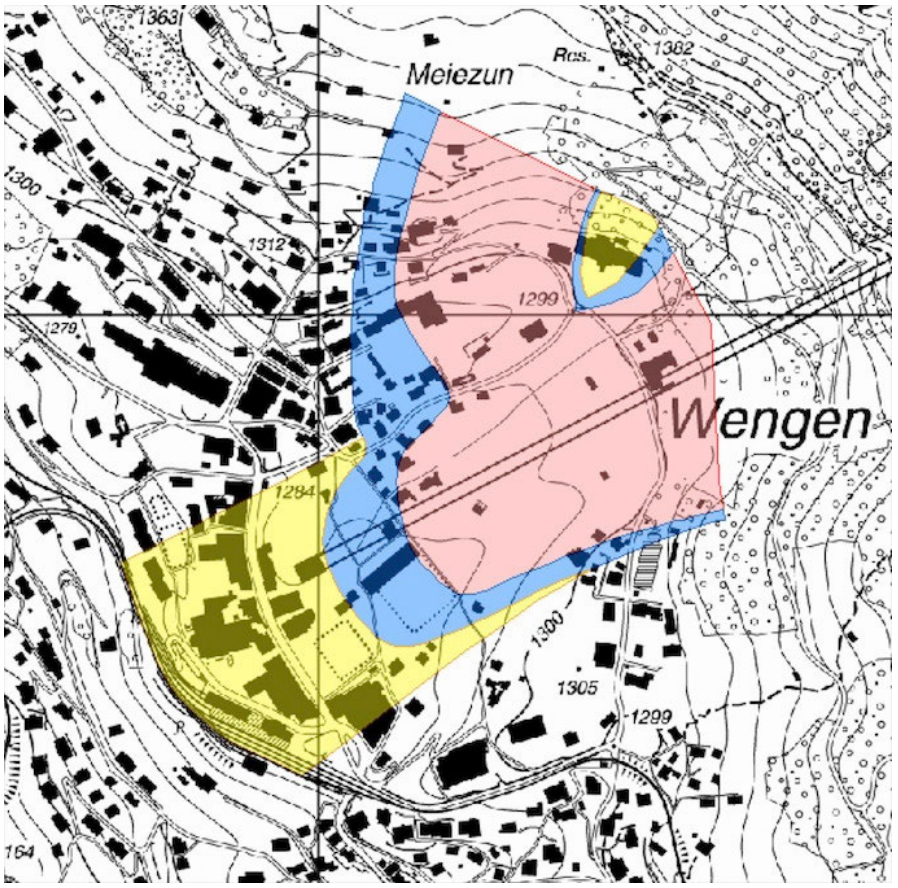

FIGURE 2.1: Example of a hazard map in Switzerland.

TABLE 2.1: Definition of different hazard levels and its corresponding danger zones (BBF and SLF, 1984).

Danger zone	Definition of hazard level
Red	$T < 30$ yr or $T > 30$ yr and $p > 30$ kPA
Blue	30 yr $< T < 300$ yr or $T < 30$ yr and $p < 3$ kPa
Yellow	powder avalanches with $T > 30$ y and $p < 3$ kPa or very extreme avalanches $T > 300$ yr
White	no avalanches expected

2.1.2 Avalanche dynamics modelling

Numerical models of avalanche dynamics, such as RAMMS (Christen et al., 2010) or SAMOS-AT (Sampl and Granig, 2009; Sampl and Zwinger, 2004) are well-established tools in the current engineering practice of hazard mapping. They allow the assessment of an avalanche's velocity, flow-height or impact pressure (Fig. 2.2).

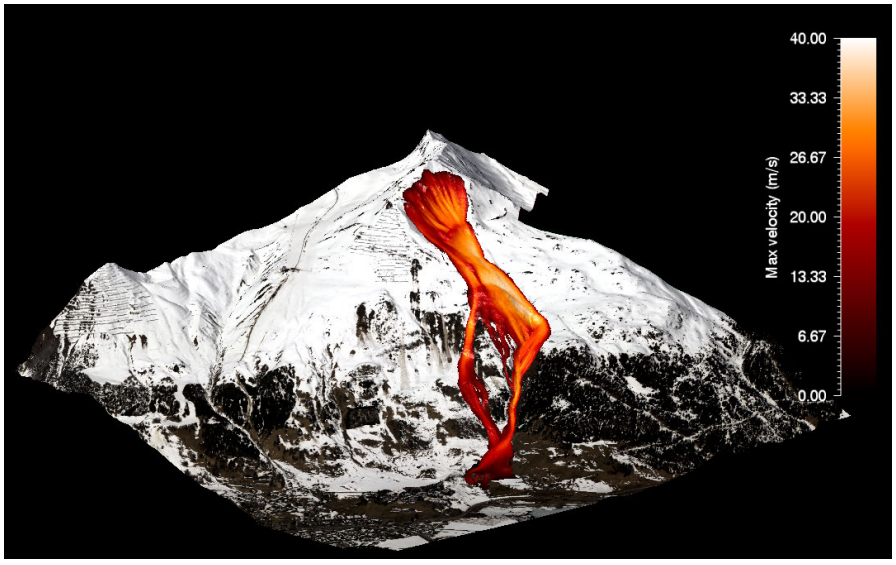

FIGURE 2.2: Avalanche dynamics simulation at the Dorfberg near Davos, using the numerical model RAMMS (Christen et al., 2010)

.

Numerical models are especially important when historical data is sparse or completely lacking. The input parameters for numerical avalanche simulations are a detailed digital elevation model (DEM), the release volume and the friction parameters in the avalanche path. Although the procedure of running such simulations is relatively simple, the choice of input parameters is crucial and requires an experienced user. The release volume is particularly important, as it is the parameter with the highest degree of freedom for the user. The release volume comprises two complementary parameters, the release area and the fracture depth. In order to determine fracture depth for a given return period, empirical formulas exist. Fracture depth is mainly based on the 3-day new snow sum, which is statistically interpolated for different return periods (Salm et al., 1990); however, no procedures exist for the definition of the release area. It has to be estimated by experienced avalanche specialists based on terrain analysis and areal pictures from the winter surface. Nonetheless, lately, with the increasing availability of geographic information systems (GIS) and digital elevation models, the development of algorithms centred on automating the process of release area definition is attempted: for example, Maggioni and Gruber (2003) established a GIS based procedure to automatically detect potential release areas (PRAs) using a Digital Elevation Model and information about

densely forested areas. The comparison with historical events revealed that release areas of extreme avalanches, with an expected return period of 300 years, coincide with the PRAs of the algorithm, whereas release areas for avalanches with a 100-year return period comprised only parts of the PRA. Thus fur, such algorithms are based on coarse resolution DEMs and therefore only represent the macrotopography. Further, they are based on the summer terrain and do not take into account the morphological changes introduced by a snow-covered winter terrain.

2.1.3 Short-term hazard assessment

Short-term hazard assessment deals with the evaluation of potential avalanche size in a given situation, as for example, estimate avalanche run-out in a given situation. In contrast to hazard mapping procedures, where avalanche dynamics models offer valuable support in assessing avalanche hazard, they cannot be applied for short-term hazard assessment. One reason is the difficulty to assess input parameters related to snow cover properties, since avalanche dynamics models are not yet coupled with snow pack conditions. In an effort to correctly predict the run-out of an avalanche, especially in small and medium-sized paths, the precise state of the snow cover must be known. Various processes, such as erosion and deposition along the avalanche path (Sovilla et al., 2006), or the flow regime (Bartelt et al., 2011), are very important. Steinkogler et al. (2014) reports the huge effect that snow cover conditions can have on avalanche run-out for similar initial release volume. This is not yet included in current avalanche dynamics models, such as RAMMS (Christen et al., 2010). Nevertheless, considerable effort is currently being directed into the implementation of snow cover parameters, such as flow regime or snow temperature (Vera Valero et al., 2012), which are being incorporated into existing snow avalanche dynamics models. At the same time, the problem of a precise estimation of the release zone remains, which is currently not addressed in avalanche research.

Beside the estimation of potential avalanche size, the question of whether or not an avalanche releases cannot be answered by avalanche dynamics models; this depends on avalanche forecasting, which is generally performed on a regional scale ($1000\,\mathrm{m}^2$). At the present day, avalanches cannot be forecasted in a single avalanche path, as the probability of occurrence of an event, even at very high danger levels (Fig. 2.3) at a regional scale, is only between 1% and 10% (Schweizer, 2008). Further, avalanches are generally rare events, thus meaning it is very difficult to establish robust relationships between the occurrence of an avalanche event and its contributory variables in an avalanche path. In most of the cases, observation data is only sparsely available, and the observation periods are quite short. One parameter commonly used in forecasting is the 3-day new

snow sum, which has been shown to be best related with avalanche activity (Ancey et al., 2003). However, not every critical snowfall event produces an avalanche. Typically, the return period of an avalanche event is 2–5 times larger than its corresponding 3- day new snow event (Schweizer et al., 2009).

Consequently, preventive avalanche mitigation measures, such as road closures, still produce many false alarms. Schweizer (2008), for example, estimates the ratio between avalanche non-event and event in the order of 2–10 for road closures. The use of avalanche dynamics models could potentially improve temporary protection measures and could, to some extent, reduce closure times for transportation ways. Nonetheless, the challenge remains in terms of assessing the probability that a single avalanche path produces an avalanche.

	Danger level	Snowpack stability	Avalanche triggering probability	Consequences for transportation routes and settlements / recommendations	Consequences for persons outside secured zones / recommendations
5	very high	The snowpack is poorly bonded and largely unstable in general.	Many large and multiple very large natural avalanches are expected, even in moderately steep terrain.	Acute danger. Comprehensive safety measures.	Highly unfavourable conditions. Avoid open terrain.
4	high	The snowpack is poorly bonded on most steep slopes*.	Triggering is likely even from low additional loads** on many steep slopes. In some cases, numerous medium-sized and often large-sized natural avalanches can be expected.	Many exposed sectors are endangered. Safety measures recommended in those places.	Unfavourable conditions. Extensive experience in the assessment of avalanche danger is required. Remain in moderately steep terrain / heed avalanche run out zones.
3	considerable	The snowpack is moderately to poorly bonded on many steep slopes*.	Triggering is possible, even from low additional loads** particularly on those steep slopes indicated in the bulletin. In some cases medium-sized, in isolated cases large-sized natural avalanches are possible.	Isolated exposed sectors are endangered. Some safety measures recommended in those places.	Partially unfavourable conditions. Experience in the assessment of avalanche danger is required. Steep slopes of indicated aspects and altitude zones should be avoided if possible.
2	moderate	The snowpack is only moderately well bonded on some steep slopes*, otherwise well bonded in general.	Triggering is possible primarily from high additional loads**, particularly on those steep slopes indicated in the bulletin. Large-sized natural avalanches are unlikely.	Low danger of natural avalanches.	Mostly favourable conditions. Careful route selection, especially on steep slopes of indicated aspects and altitude zones.
1	low	The snowpack is well bonded and stable in general.	Triggering is generally possible only from high additional loads** in isolated areas of very steep, extreme terrain. Only sluffs and small-sized natural avalanches are possible.	No danger	Generally safe conditions

Explanations:

* generally explained in greater detail in Avalanche Bulletin (e.g. altitude zone, aspect, type of terrain)

** Additional load:
- high (e.g. group of skiers without spacing, snowmobile/groomer, avalanche blasting)
- low (e.g. single skier, snowboarder, snowshoe hiker)

→ moderately steep terrain: slopes flatter than about 30 degrees

→ steep slopes: slopes with an angle of more than about 30 degrees

→ steep extreme terrain:: those which are particularly unfavourable as regards slope angle (usually steeper than about 40°), terrain profile, proximity to ridge, roughness of underlying ground

- natural: without human assistance
- aspect: the compass direction in which a downward slope faces
- exposed: especially exposed to danger

"conditions" refers exclusively to the avalanche danger. The avalanche bulletin only rarely remarks on the condition of the snow (powder snow, corn snow, breakable crust) and weather conditions (fog, storm force winds), which are also potentially dangerous in some circumstances.

FIGURE 2.3: European avalanche danger scale with consequences for transportation routes/settlements and persons in unsecured areas.

2.2 Slab avalanche formation

Avalanche release is the result of a series of mechanical actions involving terrain, snow cover and meteorological conditions and the understanding of avalanche release at the level of the single mechanical processes is unbelievably complex. Schweizer et al. (2003) describes five essential factors: terrain, precipitation (new snow), wind, temperature and snow stratigraphy. It is important to acknowledge that avalanche formation is the result of the complex interaction of such factors. The aim of this chapter therefore is concerned with identifying key parameters that may explain the extension and location of release areas based on the state of the art understanding of the mechanical processes involved.

2.2.1 Avalanche release types

Manifold ways exist to classify avalanches, such as based on size (Fig. 2.4), snow humidity (dry snow or wet snow avalanche), the avalanche flow (dense flow avalanche or powder cloud avalanche) or the type of release (loose snow or slab avalanche, Fig. 2.5).

Size	Name	Runout classification	Damage potential classification	Quantitative classification
Size 1	**Sluff**	Snow relocation without danger of burying (danger of falling)	Relatively harmless to people	Path < 50 m, volume < 100 m³
Size 2	**Small Avalanche**	Stops within slope	Could bury, injure or kill a person	Path < 100 m, volume < 1.000 m³
Size 3	**Medium Avalanche**	Reaches end of slope	Could bury and destroy a car, damage a truck, destroy a small building or break a few trees	Path < 1.000 m, volume < 10.000 m³
Size 4	**Large Avalanche**	Traverses flat parts (considerably below 30°) over distances >50m and can reach valley ground	Could bury and destroy a railway car, large truck, several buildings or a piece of forest	Path ~1-2 km, volume < 100.000 m³
Size 5	**Very large Avalanche**	Reaches valley ground. Largest snow avalanche known	Could gouge the landscape. Disastrous damage potential possible	Path ~3 km, volume > 100.000 m³

FIGURE 2.4: Size classification for avalanches

As a prerequisite to understanding the formation of avalanches, one has to recognise that the winter snowpack consists of layers of different density or cohesion as a result of intermittent snowfall periods and changing meteorological conditions. The layering of the snowpack, with its corresponding snow properties, is decisive in terms of defining which type of avalanche may form (McClung and Schaerer, 2002). Loose snow avalanches consist of cohesion-less snow releasing from one point and gaining more mass in the downwards motion due to their typical fan shape. However, they are often small as they are mostly limited to surface snow layers. They are also referred to as point releases. In contrast, slab avalanches form due to the failure of a cohesive layer (slab) overlaying a less cohesive layer (a so-called weak layer, Fig. 2.6).

FIGURE 2.5: Example of a loose snow avalanche (left) and a slab avalanche (right).

Slab avalanches show a typical linear fracture at the upper limit of the avalanche – the so-called crown (Fig. 2.7). The other delimiting borders defining the slab release area are the flanks (lateral limits) and the stauchwall (lower limit).

The bed surface is defined as the sliding plane of the slab, and may be either a underlying snow layer or the ground. Slab avalanches are the more dangerous type of avalanche and are responsible for most damage and avalanche fatalities (Schweizer and Lütschg, 2001). Avalanche risk management (section 2.1) mainly deals with this type of avalanche.

Different types of slab avalanches can be distinguished. Slab avalanches, where the cohesive slab is formed by new snow, are referred to as storm avalanches. As the amount of new snow is strongly associated with avalanche danger levels, it is considered the strongest forecasting parameter (Föhn et al., 2002). Large catastrophic avalanches are mostly the result of intensive snowfall periods, creating large new snow amounts; however it should be noted that not every large snowfall automatically results in the release of an avalanche in an avalanche path (Schaer, 1995); other factors such as the stratigraphy of the snowpack or the amount of old snow (Stoffel et al., 1998; Föhn et al., 2002) are also important. Generally, a critical new snow depth of between 10 cm and 20 cm under unfavourable conditions and between 30 cm and 50 cm under favourable conditions is

FIGURE 2.6: Example of a slab release. Cohesive slab overlaying a thin weak layer (buried surface hoar). Graphic from Schweizer et al. (2003).

needed in order to produce storm snow avalanches. Conditions in this context refer to meteorological factors, such as wind influence and temperature changes or the snowpack conditions before the snowfall (e.g., the presence of surface hoar).

Slabs formed due to wind drift and deposition are recognised as wind slabs. Whilst storm snow avalanches generally form everywhere on the mountain (given a steep enough slope), wind slabs, on the other hand, are mostly found in leeward aspects close to ridges or, in the case of a more intensive wind event, in the leeward of ribs and gullies (so-called cross loading). Storm snow avalanches or wind slabs normally stabilise over time, resulting in a decreasing danger; however, if the weak layer consists of so-called persistent forms (layers that are very resistant to bonding and settling, such as facets, surface hoar or depth hoar (Jamieson and Johnston, 1992)), the avalanche problem can persist over time, and then is considered a persistent slab avalanche. If such a persistent weak layer is buried deep in the snowpack or near to the ground, it is considered a deep slab avalanche. Generally, the deeper the weak layer, the more difficult it is to trigger the avalanche.

FIGURE 2.7: Parts of a slab avalanche.

However, its potential size (and thus destructive power) might increase due to the larger load, and fractures might even propagate through terrain features (Tracz and Jamieson, 2010). In continental climates, deep slabs are often identified in leeward slopes of high alpine zones; however, generally, they show little relation to specific terrain features. Summarising, it becomes evident that the type of slab avalanche is related both to the location where an avalanche potentially occurs and also to its potential size.

2.2.2 Slab avalanche formation from a mechanical point of view

From a mechanical point of view, slab avalanche release requires a chain of processes to occur within a wide range of scales. Avalanche formation can be conceptually captured by the break of single bonds and crack formation (failure initiation) at microscale (mm – cm), followed by crack propagation. This sequence of processes can finally result in slab release at macroscale (10^1–10^2m) (Schweizer et al., 2003) (Fig. 2.8).

Today, it is widely accepted that properties of slab and weak layer are crucial for failure initiation and crack propagation (Reuter et al., 2013). Most slab release models assume that deficit areas in the weak layer are responsible for crack propagation and thus for avalanche release (Schweizer, 1999). A so-called weak zone can be recognised as a weaker part within the weak layer, where the failure initiation propensity is higher and could lead to the release of a slab avalanche. However, field experiments could so far not prove

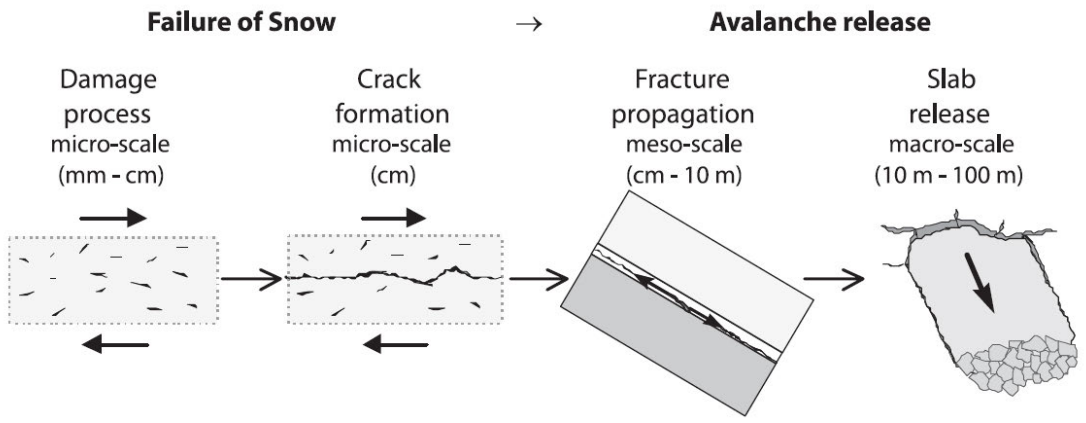

FIGURE 2.8: Conceptual model of dry slab avalanche release. Graphic from Schweizer et al. (2003).

the existence of those deficit zones, which are also probably too simplistic to represent the complex heterogeneity of weak layer mechanical properties (Gaume et al., 2014b). Further, the conditions when a local failure of snow bonds leads to crack propagation remain unclear. Snow slab failure models, for example, estimate the critical size of deficit zones necessary for crack propagation between 0.1m and 10 m, which also strongly depends on the loading rate.

Nevertheless, our understanding of the processes driving slab avalanche release have improved significantly during the last two decades. Shear was, for a long time, believed to be the only driving force in fracture initiation and crack propagation: it was held that, if shear stress of the superposed dense slab exceeds shear strength of the underlying weak layer, failure would occur and a crack would be observed (McClung, 1979); however, this concept could not explain other observations such as fractures in flat terrain or remote triggered avalanches, which have been observed by practitioners for long periods of time. As a result, Jamieson and Schweizer (2000) argue that the gravitational energy released due to the collapse of the weak layer may favour crack propagation due to the bending effects of the slab. New experiments could measure the volumetric collapse of the weak layer without a prior shear crack (van Herwijnen et al., 2010). These findings are in accordance with recent model developments (Heierli et al., 2008), adding a compressive component to the shear component for crack propagation. Both components contribute different amounts of energy to crack propagation depending on terrain and snowpack characteristics. The relative contribution of the slope-normal component (collapse) and the slope parallel (shear) mainly depends on slope angle.

Other authors have made attempts to numerically model slab avalanche release using a simplified snow cover comprising a slab and weak layer with spatially variable properties (Gaume et al., 2013b; Fyffe and Zaiser, 2007, 2004). Based on their results, the simple

idea is proposed that avalanche release area size is rather controlled by topographic than by some dynamically critical phenomena. Gaume et al. (2013a), using a mechanically -based statistical model of the slab-weak layer system, showed that, for realistic mechanical parameters, local variations in the weak layer properties are not sufficient to trigger a slab tensile fracture. Instead, they stress the importance of slope morphology, of topographic features (rocks, trees or ridges) and of the heterogeneous snow cover. This result was recently confirmed using a discrete element method and taking into account slab bending due to weak layer collapse (Gaume et al., 2014a).

Importantly, this suggests that terrain and snow distribution – at least to some extent – control the mechanical processes that occur in slab avalanche release. In the next section, we detail how these aspects influence location and the extent of slab avalanche release areas.

2.3 Terrain - snow cover interaction and its role for avalanche formation

Terrain and snow cover distribution in alpine terrain are not independent, but exert mutual influence upon each other: on the one hand, terrain affects the spatial distribution of the snow cover; on the other hand, the irregular snow distribution alters surface morphology in a snow covered winter terrain. In this section, we discuss in detail how the interaction of both terrain and snow distribution are related to slab avalanche release area size and location.

2.3.1 Spatial variability of snow cover

Snow distribution in alpine terrain varies substantially, mainly due to variation in terrain and micro-meteorological conditions. As a result of several external processes interacting with topography both during and after a snowfall, snow is transported and distributed irregularly (Pomeroy et al., 1998). Precipitations, solar radiation, air temperature and wind are the main factors (Wirz et al., 2011). The spatial heterogeneity of the snow cover is not only very relevant for avalanche formation (Birkeland et al., 1995), but is also an important factor for correctly assessing water resources for hydrological (Balk and Elder, 2000) or ecological (Wipf et al., 2009) purposes.

The mountain snow cover is generally characterised by a high spatial variability over a wide range of scales, from millimetre to kilometre scales (Blöschl, 1999). Depending on the scale of variability, the importance of single factors strongly varies. At the scale of

a mountain range, the mountain snow cover generally increases with elevation due to increasing precipitation rates with altitude and due to negative temperature gradients, thus leading to higher proportions of snow over rain (Grünewald and Lehning, 2014; Clark et al., 2011). At a slope scale, wind drift (Gauer, 2001) and preferential deposition of precipitation (Lehning et al., 2008) are the main influencing processes. They occur due to the interaction of the wind field with topographical features, such as ridges or gullies. Snow is further redistributed due to gravitative redistribution processes, such as avalanching and sluffing (Sovilla et al., 2010; Gruber, 2007). Such processes are strongly influenced by slope angle. Wind terrain interaction is also observed at finer scales at the size of single rocks or small depressions. Snow is accumulated in depressions or deposited in the leeward side of terrain features. This so-called surface roughness has a large immediate impact on snow deposition and is believed to strongly control snow distribution in alpine terrain (Lehning et al., 2011).

Based on the importance of wind-terrain interaction for snow distribution, several authors developed terrain based parameters with the aim of capturing wind shelter and exposure (Winstral et al., 2002; Purves et al., 1998). Several studies have confirmed the capacity of the wind shelter index of Winstral et al. (2002) in capturing wind sheltering effects and realistically producing accumulation patterns of snow (Schirmer et al., 2011; Erickson et al., 2005).

Further, the spatial variability of snow cover is not restricted to variations in snow depth; they further result in spatially varying snow stratigraphy. Varying internal snowpack conditions lead to the constant change of the layers (snow metamorphism). As shown in section 2.2, the layering of the snowpack is essential in terms of whether or not a slab avalanche is able to form. Hageli and McClung (2004) estimate the spatial variability of the snow cover as being one key obstacle in evaluating stability and thus avalanche forecasting. Again, wind is assumed to be the most relevant process limiting the prediction of variability at the slope scale (Schweizer et al., 2008). The role of spatial variability for avalanche formation is twofold: high variability favours the initiation of fractures but ultimately limits crack propagation and vice-versa (Schweizer et al., 2003).

This illustrates the strong control of terrain–wind interaction on snow cover distribution. Consequently, many studies with focus on avalanche formation related avalanche occurrence to geomorphological parameters. An overview of these studies and the main terrain parameters is provided in the following section.

2.3.2 Relating terrain variables to avalanche release areas

Terrain is an essential parameter for avalanche formation. The strong link between terrain and the occurrence of avalanches is obvious. The concept of hazard mapping, as well as the planning of structural protection measures, relies on the fact that avalanches occur at specific locations on the mountain, whereas other areas are not affected. It would not be possible to construct mitigation measures if there was no relation between terrain and avalanche occurrence. Extensive studies have been conducted in the past with the aim of analysing naturally triggered or skier triggered avalanches (Perla, 1977; Schweizer and Lütschg, 2001; Schweizer and Jamieson, 2001). Generally, slab avalanches release on slopes between 28° and 55°. The frequency distribution of avalanches peaks between 35° and 40°, and symmetrically decreases for flatter and steeper slopes, respectively. Figure 2.9 shows the slope distribution for skier triggered avalanches.

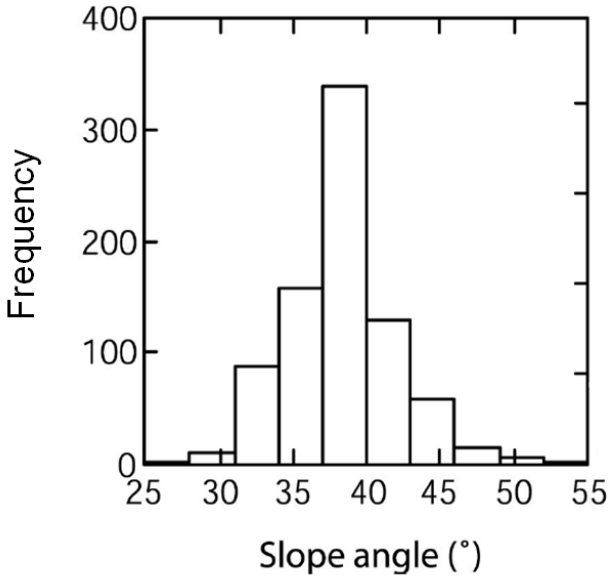

FIGURE 2.9: Slope distribution for skier triggered avalanches. Investigated cases (N=809) are from Canada and Switzerland. Graphic from Schweizer and Jamieson (2001).

An increased release probability is generally observed above 35° (Stoffel and Margreth, 2012). With respect to size, avalanches occurring below 35° are often large. For very steep regions (> 45°), release probability for large avalanches decreases because of constant sluffing and avalanching, which prevent the formation of a continuous weak layer. Mostly small, frequent avalanches are observed. Above 55°, sluffing hinders the formation of slabs (McClung and Schaerer, 2002), and only loose snow avalanches or sluffs are observed. Several studies showed that avalanches are more frequent in flat to plan concave terrain (Gleason, 1995; McClung, 2001; Vontobel, 2011; Vontobel et al., 2013). Concerning profile curvature, study results from skier triggered avalanches diverge: some

have found convex areas to be more prone to avalanche release (Jamieson and Geldsetzer, 1996), whereas concave downslope terrain has been identified by others (Vontobel et al., 2013). This may suggest that avalanches occur in transitions from convex to concave downslope curvatures; this has been confirmed by a high proportion of concave release zones identified just below convex terrain breaks (Vontobel, 2011). This could be explained that, under wind influence, snow is likely to accumulate in gullies or behind terrain breaks. Nevertheless, the occurrence of skier triggered avalanches might also reflect, to some extent, the preferences of skiers for certain slopes and terrain forms. This may bias the observed statistics, especially for skier triggered avalanches.

Other terrain parameters, such as aspect, roughness or distance to ridge, also have an effect on avalanche formation (Schweizer et al., 2003). Aspect is relevant as it reflects differences in exposure to radiation and wind, leading in general to different snowpack layering. Distance to ridge (Maggioni and Gruber, 2003) refers to wind exposure close to ridges, which hinders snow accumulation. The microtopograhy (roughness) of a slope has several effets on avalanche release areas: it provides mechanical support (anchoring effect), influences the evolution of the snowpack (metamorphism), and stability as a result. We will more closely review this parameter in section 2.3.4.

Overall, the analysis of terrain parameters for avalanche formation shows that slope is one of the most relevant parameters concerning avalanche release. Further, terrain forms able to accumulate snow under wind influence are more prone to produce avalanches than exposed terrain. Terrain further affects the layering of the snowpack, which subsequently influences the stability of the snowpack. In the next section, we will have a closer look at this effect and present studies on the effect of terrain on snowpack stability.

2.3.3 Relating terrain variables to snow stability

Another approach to assess the potential location of slab release areas is to relate potential trigger locations to terrain variables. As slab avalanche release requires the presence of a weak layer buried from a slab, linking trigger locations to morphological parameters can also deliver insight into the spatial distribution of such places. Trigger locations are defined as points of low stability assessed by point stability tests. (For a review of different snow stability tests see Winkler and Schweizer (2008)). The idea behind this approach is that weak spots can potentially be modelled a priori if a relation to terrain variables exists; therefore, this approach is of high practical interest.

Generally, all studies have shown that spatial variability of the stability test results is generally high, making it difficult to identify general patterns concerning terrain, altitude bands or snow climates. Nonetheless, interesting relationships with terrain could be

identified. Guy and Birkeland (2013) sampled 17 couloirs in steep alpine terrain, and established that terrain interacts with the snowpack differently in each couloir. However, it was also established that terrain parameters related to physical processes, such as wind deposition and erosion or sluffing are most influential. Eckerstorfer et al. (2014) studied trigger zones on wind affected slopes in central Svalbard, and highlighted the strong influence of topography on slope stability in rugged terrain. Nonetheless, he points out that this effect decreases with increasing snow depth owing to the progressive smoothing of terrain features.

The effect of terrain smoothing on avalanche formation is discussed in detail in the following chapter. More specifically, the focus will be directed towards the role of terrain roughness, which is commonly mentioned in literature in the context of snow influence on surface morphology.

2.3.4 Terrain smoothing and its role for avalanche formation

During and after a snowfall event, wind, snow gliding and avalanches redistribute snow and accordingly smooth the geomorphology of the terrain by filling irregularities. During the snow accumulation season, terrain features successively disappear, leading to the progressive smoothing of the terrain surface. Surface roughness changes modify the backscattering of visible light and microwave wavelengths, thus influencing albedo or remote sensing applications (Anttila et al., 2014). Furthermore, it influences surface heat transfer, and energy balance is affected by modifying the air flow through the snow surface (Fassnacht et al., 2009). A smoothed winter terrain also changes snow deposition patterns of snow depth, thus influencing snow distribution (Mott et al., 2010). Whilst albedo is mainly affected by millimetre to centimetre changes of the winter terrain surface (Manninen et al., 2012), snow distribution processes are modified by a changing winter topography at scales of up to several tens of metres; therefore, gaining understanding into the multi-scale effects of snow smoothing on topography is not only very important in avalanche hazard assessment, but also for run-off modelling and water resource management.

The evaluation of snow's influence on surface morphology has always been an important task in avalanche hazard assessment, and has been widely discussed in the literature, together with surface roughness.

Surface roughness has been mentioned as early as 1959, during which time it was recognised as an important parameter for avalanche release (Peev, 1959). For a shallow snowpack, terrain roughness can have a stabilising function, hindering the formation of continuous weak layers (Schweizer et al., 2003) as well as providing mechanical support

FIGURE 2.10: Surface roughness in the Steintälli area near Davos in summer and winter.

to the snowpack (McClung, 2001; van Herwijnen and Heierli, 2009). McClung (2001) studied 76 avalanche paths due to clear-cut logging in the Coast and Columbia mountains of British Columbia, subsequently establishing that ground roughness (defined in a categorical way: (1) low: ground features smaller than 1 m relief; (2) medium: ground features 1 m–2 m relief; (3) high: ground features greater than 2 m relief) beneath vegetation height and vegetation coverage is potentially important in inhibiting avalanche events. In actuality, no events were reported in areas with a roughness height greater than 2 m. Observations from the Alps showed that avalanches occurred more frequently after the farmers stopped cutting the grass on steep, open slopes (McClung and Schaerer, 2002). All these studies suggest that rough ground (boulders, logs, etc.) hinders the snowpack in the downward motion and provides certain stabilisation.

However, when the snowpack is deep enough to form a smooth surface, the stabilising effects of terrain roughness disappear or even reverse (McClung and Schaerer, 2002). Schweizer et al. (2003) estimate that a snow depth of 0.3 m to 1 m is required to eliminate terrain roughness; in such an instance, rough elements introduce additional stress to the snowpack, and snow, covering boulders, is often more susceptible to snow metamorphism owing to the greater temperature gradients. At the same time, however, a smoother surface leads to increasingly homogeneous deposition patterns during storm events (Mott et al., 2010). This facilitates the formation of continuous weak layers and slabs, which favours fracture propagation (Simenhois and Birkeland, 2008).

In recent years, airborne (Vallet, 2011; Fischer et al., 2011) and terrestrial laser scanning (Grünewald et al., 2010; Prokop, 2008; Prokop et al., 2008) have become increasingly reliable and feasible techniques for obtaining high-resolution snow depth measurements

– even in steep alpine terrain – thus allowing the analysis of snow depth distribution over multiple scales (Schirmer and Lehning, 2011; Deems et al., 2008; Trujillo et al., 2007). Although these studies provided valuable insight into snow depth distribution and its persistent topographical control in alpine terrain, little focus has been directed towards how snow depth affects the roughness of a winter terrain surface. Schirmer and Lehning (2011) interpret the two distinct fractal scaling behaviours of snow depth in combination with increasing scale breaks in the accumulation season as smoothing of terrain roughness at increasing scales.

In summary, the progressive smoothing of a terrain surface during the accumulation season reduces snowpack variability in the surface layers and reduces the mechanical support of a slab. This may increase weak layer and slab homogeneity, increasing the potential size of slab avalanches. Simenhois and Birkeland (2008) point out that a slab tends to initiate in thinner areas of the snowpack and crack propagation preferentially occurs from thinner to thicker areas as opposed to vice versa. This implies that high variable slab thickness could result in smaller avalanche sizes; on the other hand, in return, a more homogeneous slab geometry in a smoothed winter terrain could form larger avalanche release areas. Thus far, most studies and applications refer to the summer terrain – even when dealing with geomorphology in a winter terrain. As most avalanches do not release on bare ground, but rather on an underlying snow layer, the summer terrain might not be representative for the situation in a winter terrain.

2.4 Morphometric parametrization of terrain

Terrain parameters play an important role in natural hazards modelling. In the early days, information pertaining to slope was obtained from measuring distances between contour lines in printed maps; however, nowadays, this information can be accessed through Geographic Information Systems (GIS) on a computer. Surface elevations are mostly stored as a digital elevation model (DEM). A DEM is a gridded representation of sampled elevation information. This chapter summarises how geomporphometric parameters can be derived from gridded elevation models.

2.4.1 The importance of scale

Information derived from a DEM inherently depends on its resolution. This behaviour is known in geographic science as scale dependency (Wood, 1999) or scale tendency (Goodchild and Quattrochi, 1997). The latter defines it as "the effects that may or may not present when measuring a property at different scales"; in this context, scale relates

to what we identify as a small peak at fine scales as being a part of a channel at coarser scales (Figure 2.11).

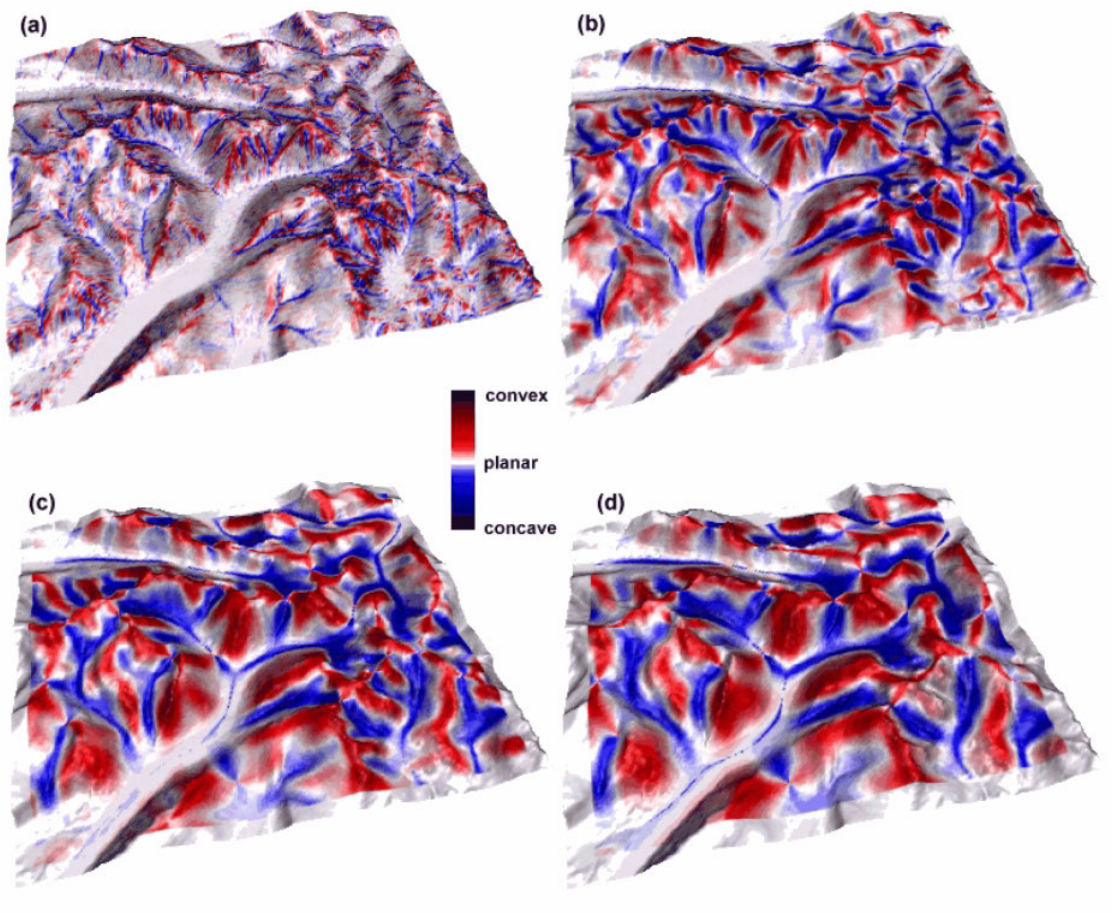

FIGURE 2.11: Curvature derived from a DEM at scales of (a) 150 m, (b) 450 m, (c) 850 m and (d) 1.25 km. The area represented in the figure is approximately 8 x 8 km. Local curvature varies considerably with scale. Graphic from Wood (1996).

With regard to a raster (pixel) based geometry, scale incorporates two components: the measurement resolution (resolution of the DTM) and the measurement extent (window size where a terrain parameter is calculated). For example, a pixel can have a convex curvature value for a small neighbourhood or high DTM resolution, whereas using a low resolution DTM or large neighbourhood, the pixel might be classified as concave. This illustrates that more information can be obtained by calculating terrain parameters at multiple scales. This concept is especially important in terms of characterising the influence of snow on terrain parameters. Snow modifies terrain parameters on certain scales (for example, rough to smooth by filling small depressions), whereas other, coarse scale terrain features might remain almost completely unchanged. Recent studies have revealed the importance of scale in terrain-snow interaction. In snow hydrology, for instance, it is recognised, that snow redistribution patterns vary over scale due to different underlying processes (Deems et al., 2006; Blöschl, 1999). Winstral et al. (2002)

admit, that one reason for the low percentage of snow depth variation which may be explained by terrain parameters, could be owing to differences in modelled processes and scales. Schirmer and Lehning (2011) discussed the effect of snow on terrain topography. They interpret the two-scale behaviour of snow depth in combination with increasing scale breaks in the accumulation season as smoothing of terrain roughness at increasing scales. Likewise, they could further distinguish between lee, cross loading and windward slopes.

2.4.2 Calculation of terrain parameters

As mentioned earlier on in this chapter, terrain parameters are derived from DEMs. In order to do so, one solution can be to calculate first- and second-order derivatives from a locally fitted surface around a point (or grid cell) of interest. For example, slope and aspect belongs to the group of first order derivatives, whereas plan and profile curvature correspond to second -order derivatives. One widely adopted method for approximating the surface is the use of biquadratic polynomials of the form

$$z = ax^2 + by^2 + cxy + dx + ey + f, \tag{2.1}$$

where z corresponds to the elevation estimate at a point (x, y) and $a - f$ are the coefficients that define the quadratic surface (Evans, 1980). Originally, the six unknown parameters $a - f$ are defined, taking into account all grid values within a 3x3 window around the central cell. Wood (1996) expanded this concept to what he refers to as a "multi-scale quadratic parametrisation", by fitting the trend surface over any arbitrarily sized window. By varying the extent of the window size, a surface parameter can be calculated for varying scales without changing the resolution of the elevation model. This is convenient for applications where surface parameters vary significantly with scale and where different estimates for different scales are needed.

In greater detail, in order to calculate slope and aspect, direction (aspect) and magnitude (slope) of the steepest gradient at the central grid cell of the fitted surface needs to be determined. To this aim, the rate of change in x and y direction is calculated and combined using, for example, the equations provided by Wood (1996):

$$\frac{\mathrm{d}z}{\mathrm{d}xy} = \left(\sqrt{\left(\frac{\mathrm{d}z}{\mathrm{d}x}\right)^2 + \left(\frac{\mathrm{d}z}{\mathrm{d}y}\right)^2} \right). \tag{2.2}$$

The partial derivatives for x and y are noted as:

$$\frac{\mathrm{d}z}{\mathrm{d}x} = 2ax + cy + d, \tag{2.3}$$

and

$$\frac{\mathrm{d}z}{\mathrm{d}y} = 2by + cx + e. \tag{2.4}$$

In order to obtain the parameter at the central point of the surface ($x = y = 0$), equations 6.3 and 6.4 are integrated into equation 6.2, and note:

$$\frac{\mathrm{d}z}{\mathrm{d}xy} = \sqrt{d^2 + e^2}. \tag{2.5}$$

Slope (α) is thus given as:

$$\alpha = \arctan \sqrt{d^2 + e^2}. \tag{2.6}$$

Likewise aspect is defined as

$$\beta = \arctan \frac{e}{d}. \tag{2.7}$$

Similar definitions exist for surface curvature (Wood, 1996). The aforementioned definitions are consistent with others, as reported in the literature (Zevenbergen and Thorne, 1987).

2.4.3 Roughness measures

Roughness has always been an important land surface parameter in earth and planetary sciences. It is used for the identification of landforms and the related processes forming them. Manifold definitions of roughness exist, depending on the application field and the scale under examination. For example, in a remote sensing application, the backscatter of an electromagnetic wave could serve as an adequate roughness measure; however, such a concept is not suited to geomorphological applications, where landform analysis is performed based on surface elevation values. In the literature, different terms are used to describe surface roughness, such as microtopography, ruggedness, rugosity or microrelief. Generally, it may be defined as "the variability of a topographic surface at a given scale" (Grohmann et al., 2011).

For geomorphological applications, different approaches to measure surface roughness do exist. Essentially, we can distinguish area ratio, vector dispersion and the variability

of surface elevation methods (Grohmann et al., 2011). Notably, other methods, such as fractal dimension or wavelets, are not directly linked to measurable geomorphological variables, and therefore require large interpretation effort, limiting its use for practical applications.

Area ratio approaches compare the area of a given land surface to a smoother underlying surface. The drawback of such methods is that they depend on slope if a flat surface is chosen; or, when choosing a smoothed terrain as an underlying surface, they depend on the scale of underlying surface used to distinguish roughness components from the underlying trend surface. Therefore, such methods are rather not suited for applications in alpine terrain.

The variability of surface elevation such as standard deviation of elevation or standard elevation of slope, is commonly used for geomorphological applications. However, they depend on slope (in the case of standard deviation of elevation) or, in the case of the standard deviation of slope, do not take into account variations in aspect for surface pitches of constant slope.

The vector dispersion methods basically compare the orientation of normal vectors of a given patch of surface with the orientations of neighbouring surface patches. The degree of variability in the orientations serves as a measure of the irregularity of the topographical surface. Figure 2.12 illustrates the principle of vector dispersion methods. This especially highlights the dependence of scale, namely the resolution of the DEM and the moving window size.

One particularly appealing vector dispersion method is the vector ruggedness measure developed by Sappington et al. (2007), based on the vector approach proposed by Hobson (1972).

Based on slope and aspect definitions (Equations 2.6, 2.7), normal unit vectors of every grid cell of a digital elevation model (DEM) are decomposed into x, y and z components (Fig. 2.14):

$$z = 1 \cdot \cos(\alpha), \tag{2.8}$$

$$d_{xy} = 1 \cdot \sin(\alpha), \tag{2.9}$$

$$x = d_{xy} \cdot \cos(\beta), \tag{2.10}$$

$$y = d_{xy} \cdot \sin(\beta). \tag{2.11}$$

A resultant vector $|r|$ is then obtained for every pixel by summing up the single components of the center pixel and its neighbours using a moving window technique. The neighbourhood size can be set by the user and is defined by the number of pixels n taken

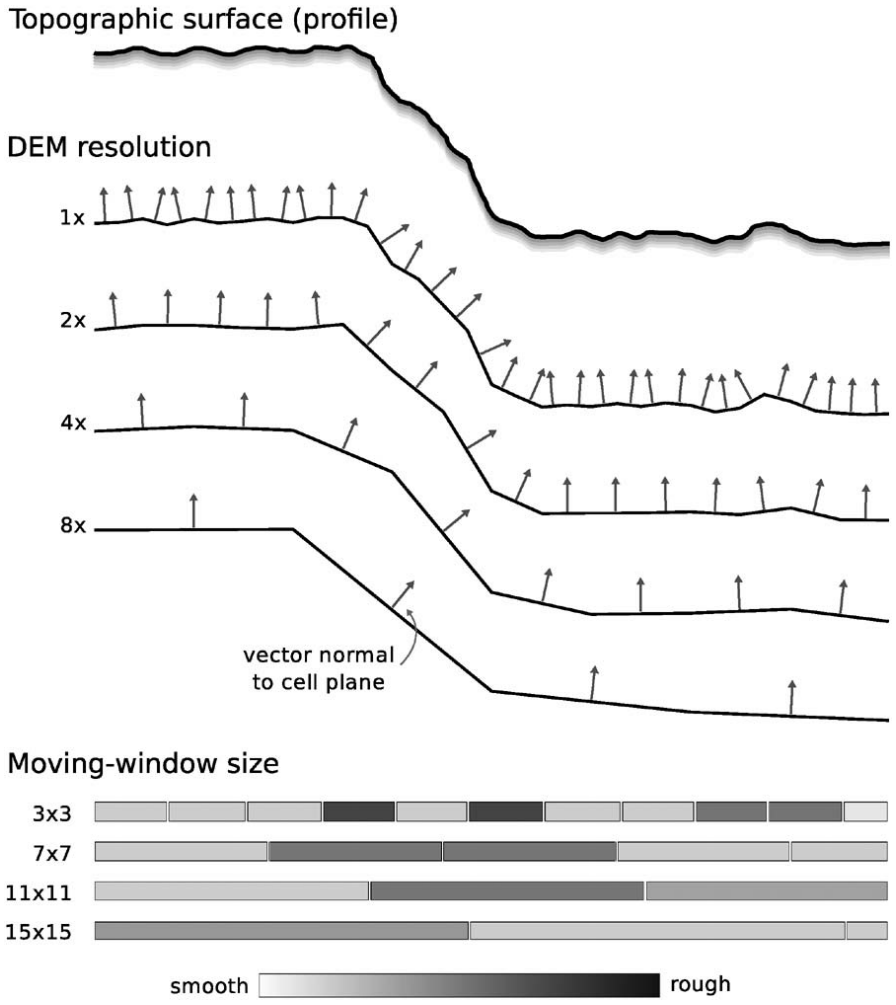

FIGURE 2.12: Vector dispersion method used to calculate surface roughness at different scales for a topographical surface. Graphic from Grohmann et al. (2011)

into account.

$$|r| = \sqrt{(\sum x)^2 + (\sum y)^2 + (\sum z)^2}, \tag{2.12}$$

as shown in Fig. 2.14b. The magnitude of the resultant vector is then normalised by the number of grid cells n and subtracted from 1:

$$R = 1 - \frac{|r|}{n}, \tag{2.13}$$

where R is the vector ruggedness measure.

The result is a measure of the surface roughness with values ranging from 0 (flat) to 1 (extremely rough). This definition makes it possible to derive roughness directly from a DEM, and the moving window technique allows us to calculate local, pixel-based estimates of roughness. Since the method incorporates both the aspect and the slope of the elevation gradient, we can distinguish between constant slope with constant aspect and constant slope with changing aspect (Fig. 2.14 c). Sappington et al. (2007) show

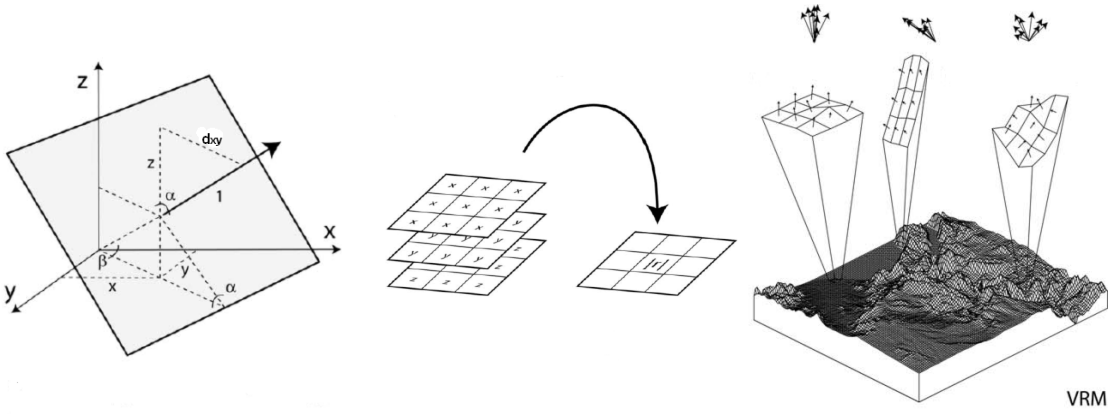

FIGURE 2.13: (c)

FIGURE 2.14: Calculation of vector ruggedness measure R. **(a)** Decomposition of normal unit vectors of a DTM grid cell into x, y, z components using slope α and aspect β. **(b)** Resultant vector r is obtained by summing up the x, y, z components of all pixels n within the neighbourhood window. **(c)** Vector ruggedness measure in flat (left), steep and even (middle) as well as steep and uneven terrain (right). Graphics from Sappington et al. (2007).

that the vector ruggedness measure is uncorrelated with slope. The measure has already been applied in different research fields, including, amongst others, animal habitat analysis (Sappington et al., 2007), avalanche dynamics (Sovilla et al., 2012) and avalanche formation (Vontobel, 2011).

2.5 Spatial modelling of natural hazards

2.5.1 Terrain based models for natural hazard processes

In general, two ways of modelling reality have been distinguished, depending on the degree of understanding of the underlying process and on the degree of the random component of the analysis (Hengl and MacMillan, 2009):

(1) Direct (or deterministic) models. These allow the prediction of the model output based on a physical law or an exact algorithm. The number of input parameters is known and can be linked to the target variable by an exact formula. In the case that the target variable is time–dependent, such as avalanche flow height within an avalanche flow, we speak about process–based models.

(2) Indirect estimation models. If the relation between target variable and input parameters is not fully understood or too complex to model, other approaches need to be

identified. As the exact number of influencing input variables is not known, the formulae to relate input and output, as well as the random component, is unknown. In such cases, the only way is to design a model that fits the measurements of the target variable and/or reflects expert knowledge. Two ways do exist: (a) Pure statistical models, which completely rely on measurements. Still, the statistical model has to be chosen; (b) Expert-based or heuristic models which build on empirical rules. In this case, some knowledge (at least at a conceptual level) on the processes involved or the location in space where these processes occur exists.

Often, applications in natural hazard modelling use indirect estimation models due to the complexity of the underlying processes and the often limited input data. Further, many natural hazards, such as debris flows, landslides or snow avalanches, are the result of a so-called slope instability (or failure), resulting in a downward mass movement. Both the starting zone, as well as the path, are strongly controlled by geomorphology, making its use in hazard models very appealing. Therefore, models based on geomophological parameters (so-called geomorphometric models) are widely used for landslide susceptibility assessment (Carrara and Pike, 2008), flow propagation in debris flow and ice avalanches (Huggel et al., 2003) or release area estimation of snow avalanches (Maggioni and Gruber, 2003). In contrast to process–based models, where the physical processes of the event are modelled, geomorphometric models rely on a simpler parametrisation of the physical processes. These have the advantage of (1) faster computation times, (2) less input data requirements, (3) easier availability and (4) the requirement of less technical know-how (Gruber et al., 2009). However, they do have the disadvantage that they cannot model the dynamical component of mass movements. In practice, a combination of different model types also exists (Hengl, 2007).

Many different types of statistical models are used in natural hazard modelling, namely classification based, tree-based or regression models. For discrete target variables, such as potential release area definition, classification approaches are particularly suited (Hengl and MacMillan, 2009). Depending on the classification rules, either a continuous (fuzzy) or a boolean (crisp) output is produced. In the next section, both techniques will be evaluated with regard to their suitability for hazard modelling.

2.5.2 Fuzzy logic modeling in natural hazard assessment

Risk-based decision making in the field of natural hazards is often supported using a land-use suitability analysis implemented in a GIS (Malczewski, 1999); in other words, the suitability of a terrain for a specific objective – as based on selected criteria, which the area under question needs to fulfil– must be determined. For example, if one seeks to map

areas prone to landslide events, a terrain analysis linking different criteria is executed. Traditionally, a suitability analysis is approached in two different ways, namely by binary intersection (boolean approach) or weighted linear combination (Eastman, 1999). In a boolean approach, binary layers for each criteria are created. They can be seen as a type of constraint, excluding areas that are not suited for a certain purpose. For example, the construction site of a new company has to fulfil the criteria "vicinity to a main road" defined as being not less than 1 km away from a main road. The resulting layer would be a 1 km buffer around each side of all main roads where potential constructions sites may be located. However, such an approach would only distinguish between "suited" or "not suited", and therefore cannot provide any subdivision, such as highly suited or poorly suited. As a result, a possible location of 200 m away from the main road would obtain the same score than a location 900 m away.

To account for such varying degrees of suitability, weighted linear combination was introduced. This treats every variable as fully continuous. In an effort to illustrate this, adopting the example used before, distance to road could be modelled in this framework as a continuous variable, with values ranging from 1 for areas located directly at the road and a value of 0 located at a distance of 1 km or more from the road. All distances in between could be assigned using, for example, linear interpolation or any other arbitrarily function.

However, natural process can rarely describe or be modelled as a result of such sharply defined variables. Mostly, rather general relations of diffuse categories prevail. For example, if we aim to model "steep and wind sheltered terrain", it is very difficult – or altogether impossible– to precisely define steep or wind sheltered terrain. Expert decision making therefore contains significant degrees of uncertainty or vagueness owing to the complex nature of the process and the parameters involved. Such issues cannot be solved through a classical logic approach; therefore, with this in mind, Zadeh (1965) introduced the fuzzy logic approach in an effort to to deal with such imprecise data or diffuse rules. This approach overcomes the concept of sharp (so-called crisp) borders by introducing the membership concept. Every element, as opposed to belonging (or not) to a class, is attributed a degree of membership (= truth value) belonging to that class (referred to as a set in fuzzy set theory). A more mathematical formulation adopted by Zadeh (1965) is as follows:

"Let X be a space of points (objects), with a generic element of X denoted by x. Thus, $X = x$. A fuzzy set (class) A in X is characterized by a membership (characteristic) function $f_A(x)$ which associates with each point in X a real number in the interval $[0, 1]$, with the value of $f_A(x)$ at x representing the "grade of membership" of x in A".

This concept is very appealing for natural hazards applications as it allows the integration of human reasoning capabilities into knowledge–based expert systems. Moreover, already it has been successfully applied to landslide susceptibility mapping (Schernthanner, 2007) and risk modelling of wet snow avalanches (Zischg et al., 2005).

At the same time, fuzzy set theory is supported by a strict mathematical framework. It defines, for example, the logical operators used to aggregate fuzzy sets. Zadeh (1965) originally defined three basic operators: the union (OR), intersection (AND) and the complement (negation). The union of two fuzzy sets A and B, is a fuzzy set C, the membership function of which is defined as follows:

$$f_C(x) = max[f_A(x), f_B(x)], x \in X. \tag{2.14}$$

The intersection of the two fuzzy sets A and B, is a fuzzy set C, the membership function of which is defined by:

$$f_C(x) = min[f_A(x), f_B(x)], x \in X. \tag{2.15}$$

The complement of a fuzzy set A is denoted by A' and is defined by:

$$f'_A(x) = 1 - f_A(x), x \in X. \tag{2.16}$$

These operators are so-called non-compensatory. Compensation in the context of set theory signifies that a low value of one fuzzy set cannot be compensated by high value of the other or vice-versa. No compensation (or trade-off) is commonly inadequate for modelling purposes when aggregating human reasoning– especially when conflicting variables are aggregated; therefore, the family of fuzzy operators was extended by so-called averaging operators (for example, arithmetic mean) (Zimmermann, 1987).

In a more generalised framework, the MIN operator constitutes the lower boundary of the intersection operators and the MAX operator the upper boundary of the union operations (both with no trade-off between variables). The arithmetic mean is situated in the middle, between the two extremes, thus allowing a full trade-off between variables; therefore, it is possible to define operators situated anywhere in between the MIN and MAX operator, with any desired level of compensation between variables. Two operators allowing to define the level of compensation between variables are, for example, the ordered weighted averaging operators by Yager (1988) and the "fuzzy OR" and "fuzzy AND" (Werners, 1988). More specifically, the ladder is particularly suited to empirical data (Zimmermann and Zysno, 1983). The "fuzzy AND" operator is defined by:

$$f_C(x) = \gamma \times min[f_A(x), f_B(x)] + \frac{(1-\gamma)(f_A(x) + f_B(x))}{2}, x \in X, \gamma \in [0,1]. \quad (2.17)$$

The "fuzzy OR" operator is defined as follows:

$$f_C(x) = \gamma \times max[f_A(x), f_B(x)] + \frac{(1-\gamma)(f_A(x) + f_B(x))}{2}, x \in X, \gamma \in [0,1]. \quad (2.18)$$

We can see that for $\gamma = 1$, the operators corresponds to the MIN and MAX operator, respectively, whilst for $gamma = 0$, the operators correspond to the arithmetic mean.

Generally, simple and computationally efficient membership functions are favoured in fuzzy logic implementations. Very simple implementations are, for example, triangular or trapezoidal functions. Owing to their computational efficiency, they are commonly used in real time applications where calculation speed is critical; however, they only comprise linear segments and introduce very sharp changes at the corner points. In an effort to overcome these drawbacks, generalised bell (also referred to as Cauchy membership function) or Gaussian functions are used (Jang and Sun, 1997). They are characterised by smooth outlines where the sharpness of transition can be set by a parameter.

In conclusion, fuzzy logic modelling is an appropriate means of assessing natural hazard processes, where the underlying physical processes are not fully understood and where empirical relations and assumptions need to be exploited for decision making purposes.

2.5.3 Assessment of model performance

Model validation is a very important step throughout the course of model development. Commonly, validation is referred to as evaluating the predictive power of a model, meaning a comparison of simulated and measured data, the so-called "operative validation" (Caswell, 1976). More generally, "validation means that a model is acceptable for its intended use because it meets specified performance requirements" (Rykiel Jr, 1996). Therefore, techniques such as the sensitivity analysis of model parameters, the comparison to other model results or, as commonly applied in the context of natural hazards, the comparison of the model output with a database of observed events of the analysed hazard in the past, can also be considered proper validation techniques (Rykiel Jr, 1996). The validation of hazard assessment is crucial for the final user to estimate the confidence in the model. Confidence in a model is commonly described in literature as

credibility, thus meaning "a sufficient degree of belief in the validity of a model to justify its use for research and decision making" (Sargent, 1984).

With respect to an operative validation, different validation techniques exist, depending on the type of model output. In a binary classification scheme (section 2.5.2) only two classes are produced – a positive one (safe zones) and a negative one (unsafe zones). The classification output (prediction) then can be compared to the actual observations obtained from the reference data. One possibility of assessing the quality of the classification is using a simple similarity index, such as the Jaccard Index (Jaccard, 1908). The Jaccard index $J(A, B)$ is defined as the ratio of the area of intersection and union between two sample sets A and B:

$$J(A, B) = \frac{A \cap B}{A \cup B}. \tag{2.19}$$

It is one of the most useful similarity indices – especially for binary data (Birks, 1987). However, the underlying distribution of the different sets is not taken into account.

In order to do so, more meaningful measures exist. Generally, four different outcomes are possible in a binary classification task. A positive observation classified as positive is considered a true positive. Vice-versa, a negative observation classified as negative is referred to as a true negative. If a positive observation is classified as negative or vice-versa, it is counted as a false negative and false positive, respectively. If these statistics are transformed into a two-by-two matrix, a so-called confusion matrix or contingency table (Stehman, 1997) is created (Table 2.2).

Table 2.2: Confusion matrix

Prediction	Observation	
	positive	negative
positive	True Positives (TP)	False Positives (FP)
negative	False Negatives (FN)	True Negatives (TN)

From this confusion matrix most performance statistics can be calculated.

$$Precision = \frac{TP}{TP + FP} \tag{2.20}$$

$$Accuracy = \frac{TP + TN}{TP + TN + FP + FN} \tag{2.21}$$

$$Sensitivity = \frac{TP}{TP + FN} \tag{2.22}$$

$$Specificity = \frac{TN}{TN + FP} \tag{2.23}$$

The interpretation of the above statistics requires some degree of special attention centred on the context of natural hazards. First, natural hazards often affect only small proportions of a whole study area, thus leading to a prevalence of negative cases in a study area (events not observed) in comparison to positive events. For example, imagine a case where 95% of an area is not susceptible for landslides but the remaining 5% is: if a model classifies the whole area as safe, the overall accuracy would still be 95%, although the classifier would neglect to highlight all dangerous areas. Thus, the accuracy measure alone is insufficient in terms of evaluating the quality of a model. The specificity and sensitivity of the model, which take into account the distribution of the two classes, should also be provided. The dependency of accuracy on the rate between positive and negative events was shown to be commonly overlooked when comparing models in various domains, such as weather forecasting (Murphy, 1993) or avalanche forecasting (Heierli et al., 2004). Second, natural hazards are often rare events, meaning that false positive results should not automatically considered as classification errors; equally, they could represent dangerous areas where the hazard has not been observed in the past but which may occur in the future. Such particularities have to be taken into account when interpreting the quality of hazard prediction results using the above defined statistics.

In the case that a hazard assessment model delivers continuous model output such as from a fuzzy logic approach (section 2.5.2), other validation techniques are recommended. As has been acknowledged earlier, the use of the confusion matrix requires the definition of a classification threshold to obtain only two classes. Accordingly, in order to correctly estimate the predictive power of a model independent of a threshold, one could plot the performance measures for all possible thresholds. Such plot is refereed to as a receiver-operating characteristic (ROC) plot (Fawcett, 2006), as shown in Fig. 2.15.

The area under curve (AUC) is commonly used as a measure for the overall accuracy of the model–independent of a certain threshold. It can be interpreted in the sense that the diagonal line corresponds to the case of a random guess (value of 0.5, thus meaning a 50% chance of correct classification. Any curve situated further towards the upper left corner would describe an improvement over the random guess.

In the case of a continuous model output, a division into several hazard classes is commonly requested by decision makers for practical reasons (such as the planning of mitigation measures, for example). The selection of such decision thresholds depends on the context of application of the hazard model and the costs associated with the two error types (false positives/negatives) rather than on the characteristics of the model itself. Nevertheless, it is very important for the final user to dispose over some accuracy measures for a hazard model under a given threshold. Accordingly, in this vein, Beguera

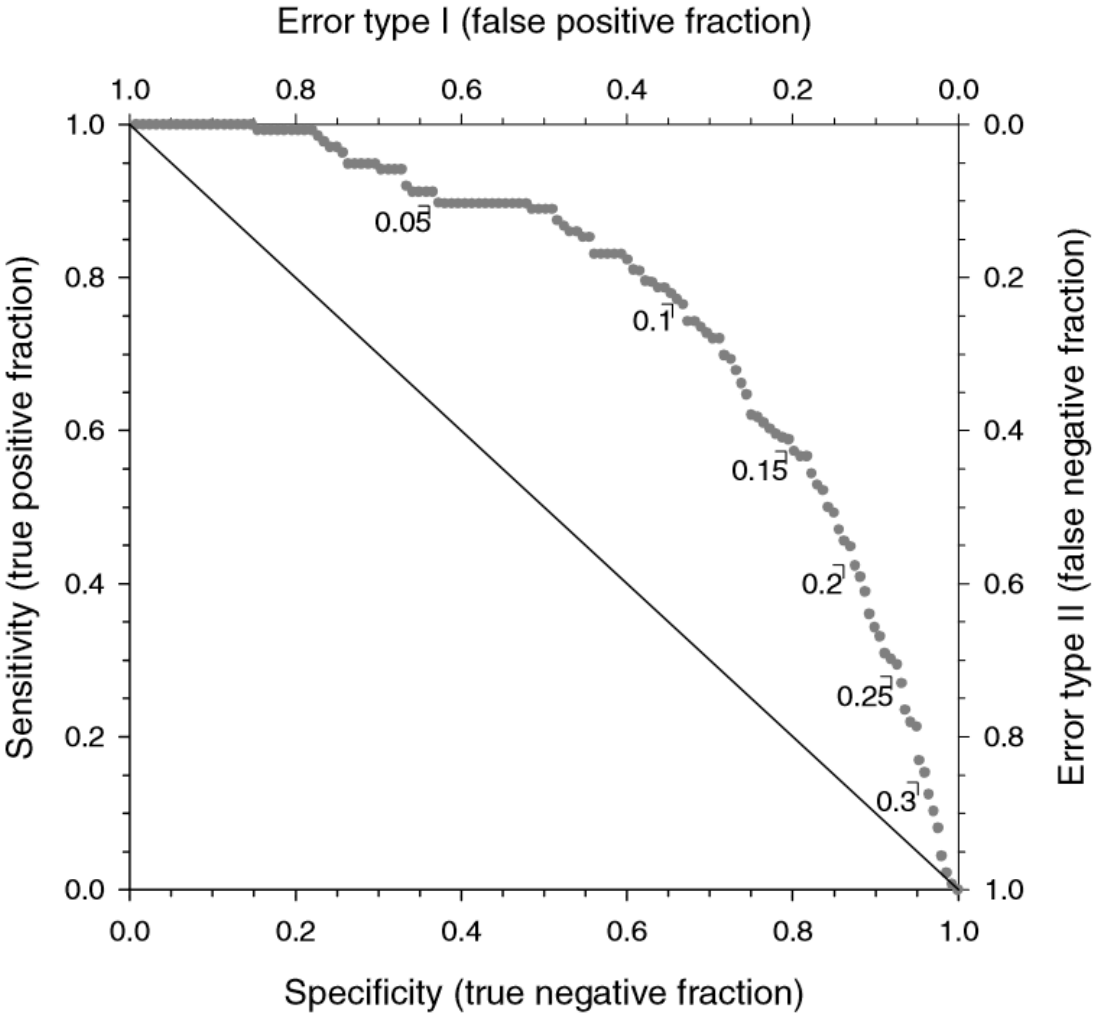

FIGURE 2.15: Example of a ROC plot. Graphic from Beguera (2006).

(2006) proposes the conduction of the model validation independently of various final thresholds, and to use such validation output to propose decision thresholds, including associated confidence measures for the end users of hazard models (Fig. 2.16).

To summarise, validation is a crucial step in model development. Several validation techniques exist, depending on the purpose of the model, the data available and the type of model output produced. With regard to natural hazards, the often uneven distribution of the different target variables (event, non-event) must be taken into consideration. A simple accuracy measure is often misleading in correctly assessing the performance of a model.

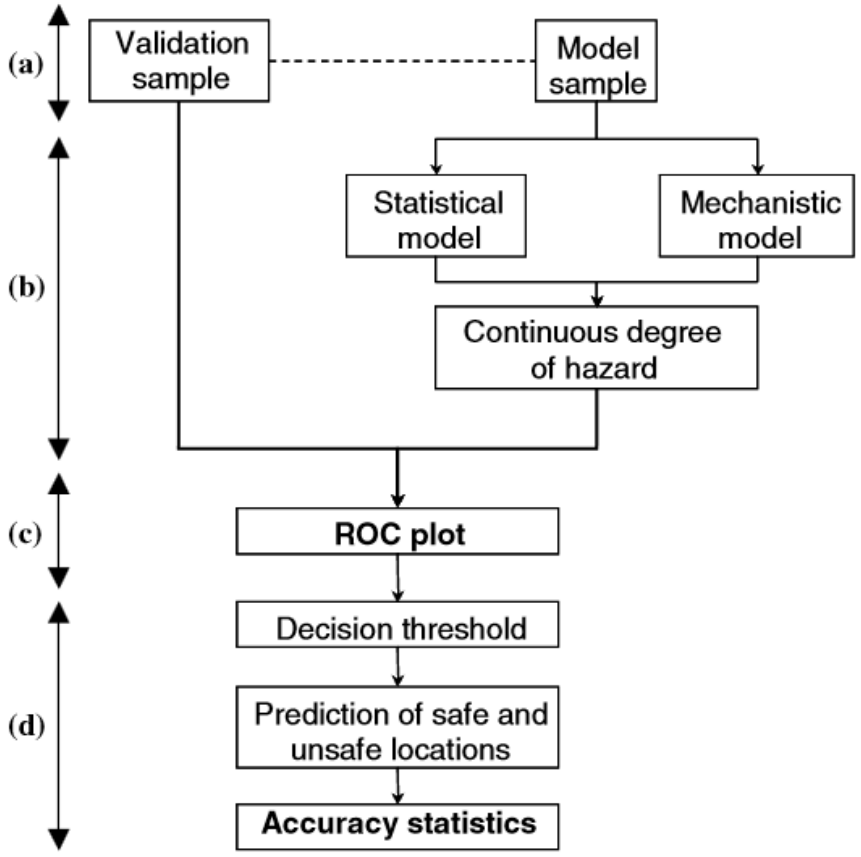

FIGURE 2.16: Threshold independent validation and evaluation of natural hazard models from Beguera (2006). **(a)** Sampling, **(b)** model construction, **(c)** model validation and **(d)** model evaluation.

2.6 Research gaps

The state of the art revealed the importance of improving the current release area definition practice for hazard mapping purposes, as well as for the application of avalanche dynamics models in short-term hazard assessment. The literature review identified the following research gaps related to the modelling of avalanche release areas:

(1) Snow distribution introduces important morphological changes in a winter terrain surface compared to its underlying summer terrain; however, thus far, no attempt has been made to establish an appropriate method to quantify the influence of the snow distribution on surface morphology of a winter terrain surface, integrating scale dependency and the temporal consistency of these processes.

(2) The literature review clearly highlights the importance of surface roughness in avalanche formation processes. It especially emphasises the progressive cancelling out of surface roughness due to snow accumulation, leading to more homogenous snow deposition patterns. It is assumed that this may lead to a more uniform slab thickness and, in combination with reduced support from the bed surface, to potentially larger release area sizes. To our knowledge, thus far, this relation between slab geometry, underlying surface and release area size has so not been explicitly and quantitatively explored – mainly due to a lack of data providing information of the snow distribution both before and after avalanche release and the slab geometry.

(3) In accordance to traditional avalanche hazard mitigation practice, recent advances in the mechanical modelling of the slab weak layer system, as well as field studies, provide some evidence for the relevance of topography for release area definition. This is very promising in the sense that practical applications for avalanche release areas can be based on terrain parameters as they are constant over time and widely available. However, several limitations of topographical influence were identified, such as the important morphological changes introduced by a snow-covered terrain surface. Current algorithms are mostly terrain- based; however, the low resolution of the terrain models (around 25 m) in such algorithms only captures the macrotopography (ridges, valleys), but neglects to consider the microtopography (small rocks, trenches, etc.). The role of the latter, however, is negligible in extreme situations; it is highly relevant for smaller, more frequent avalanches, which cause the vast majority of casualties in Switzerland and threaten mountain roads and ski runs. Such finer scale terrain features are commonly considered delimiting borders for less extreme avalanches. Simultaneously, snow accumulation strongly affects microtopography. Microtopography and its alteration under snow influence have not yet been taken into account in the current algorithms of automatic release area definition. Therefore, it seems very likely that the release area

calculations performed on a summer terrain may strongly differ from calculations on a more realistic winter terrain.

(4) The literature review of natural hazards modelling considers fuzzy logic modelling approaches as generally superior over binary classification approaches for applications where the underlying physical processes are not fully understood and where empirical relations and assumptions need to be exploited for decision making purposes (as, for example, avalanche formation). Existing algorithms for avalanche release area definition are commonly rule based, separating release area from non release area using a binary classification approach. Its performance is therefore strongly dependent on threshold selection and threshold independent evaluation or validation is not possible. The introduction of a continuous, fuzzy logic model approach, combined with a threshold independent validation procedure, would not only allow gaining more insight into the performance of such algorithms, but further optimise the definition of decision thresholds in hazard models.

These four research gaps reflect the three research questions, introduced in chapter 1 of this thesis:

1. How does snow distribution influence surface morphology of alpine terrain and how can such an effect be captured?

2. What is the influence of the morphological differences between the snow free summer terrain and the snow-covered winter terrain on avalanche release area size and location?

3. How can potential release area modelling be improved by taking into account the influence of snow distribution on surface morphology?

Chapter 3

Field measurements and experimental data

In this chapter, the data used and the selected methods to gather the data are presented. Terrestrial and airborne laser scanning at different stages of the accumulation season at two geomorphologically different mountain test sites in the Swiss Alps, Vallée de la Sionne and Steintälli were performed. In addition, data from avalanche experiments performed at the Vallée de la Sionne fieldsite are analysed. Avalanches were artificially triggered by helicopter and combined with airborne laser scanning, both prior to and following release, providing detailed information about the characteristics of the slabs and bed surfaces. In contrast to those highly detailed but rather short-term data, long-term avalanche observations from the village of Zuoz in the eastern Swiss Alps are used to analyse whether or not terrain smoothing has an effect on the observed release area size and location.

3.1 Measurement principle of airborne and terrestrial laser scanning

In recent years, airborne (Vallet, 2011; Fischer et al., 2011) and terrestrial laser scanning (Grünewald et al., 2010; Prokop, 2008; Prokop et al., 2008) have become increasingly reliable and cost-efficient techniques in terms of obtaining continuous snow depth measurements– even in steep alpine terrain – potentially allowing the analysis of snow depth distribution over multiple scales.

The basic measurement principle of laser scanning is rather simple: it is based on the time of flight of an electromagnetic wave (normally in the near infrared range) between

an emitting laser scanning device and a target object. The laser device emits a short pulse of light and, at the same time, a clock is started. The emitted pulse is then reflected by the target, which is then returned to the laser scanner instrument. A photodiode registers the pulse at the instrument and triggers the stop of the clock. Thus, the two–way travel time can be measured and ultimately the distance between laser scanner and the target object determined. Whilst a terrestrial laser scanner (TLS) is mounted at a fixed position on the ground (tripod etc.), airborne laser scanners (ALS) are mounted on an aircraft or helicopter (Fig. 3.1). This requires additional measurement devices, such as global positioning system (GPS), and an inertial measurement unit (IMU) in an effort to precisely determine the position of the aircraft in motion. TLS– measured point clouds are mostly georeferenced using control points (reflectors, prominent terrain features) or GPS. The georeferencing of ALS measurements is carried out through the localisation of the position of the aircraft, using GPS and IMU (Prokop, 2008)).

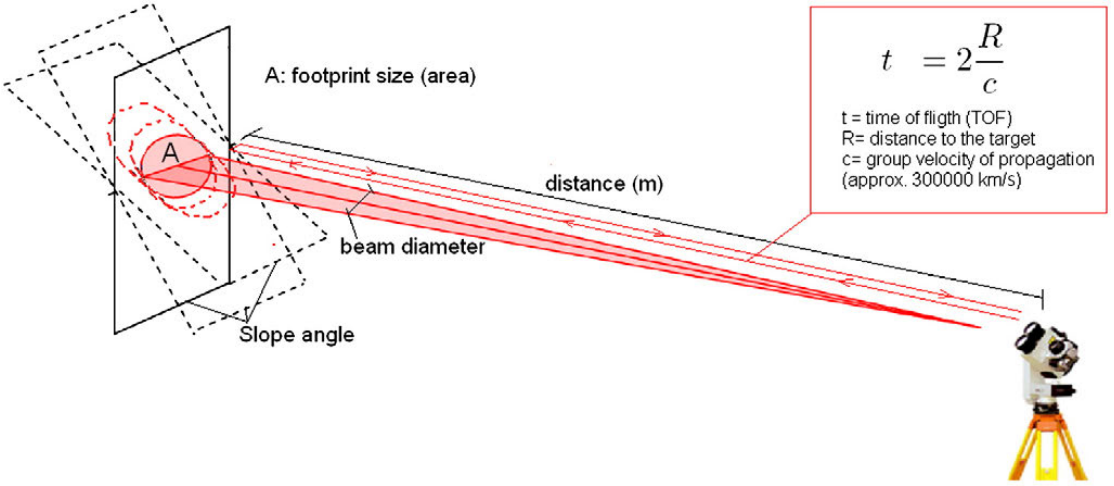

FIGURE 3.1: Measurement principle of laser scanning. Graphic from Prokop (2008).

The accuracy of the measurement depends on the technical specifications of the laser scanner. The two main factors are the beam width of the laser beam and the resolution (point density) of the laser scanner. Beam width and point density increase and, respectively decrease, with measurement distance to the target, thus leading to decreasing accuracy with larger measurement distances to the object. Measurement accuracy is further influenced by the incident angle defined by the angle between the axis of the laser beam and the normal vector of the target object. The highest accuracy is achieved when the laser beam hits the surface perpendicularly.

Furthermore, measurement quality is affected by several external factors, such as through the atmospheric effects on the speed of light. The propagation speed of the laser wave

and thus the time of flight is influenced by air temperature, air pressure and humidity. The effects have to be corrected, where the magnitude of the correction is as follows:

- A change of +1° C results in a correction factor of -1 ppm (parts per million, e.g. 1 mm for a measurement distance of 100 m).
- A change of +10 mbar requires a correction factor of -2.7 ppm.
- A change of humidity from 0% to 100% requires a correction of +0.5 ppm.

Measurement accuracy further depends on the nature of the scanned object and its reflectance properties with the laser beam. Figure 3.2 shows the reflectance characteristics of snow and clouds. It is observed that the reflectance of snow is strongly reduced for wavelengths above 1000 nm. Further, reflectance varies with grain size of the snow particles. Optically thick clouds also inhibit the passage of the near infrared waves; therefore, laser scanning is restricted to conditions of good visibility.

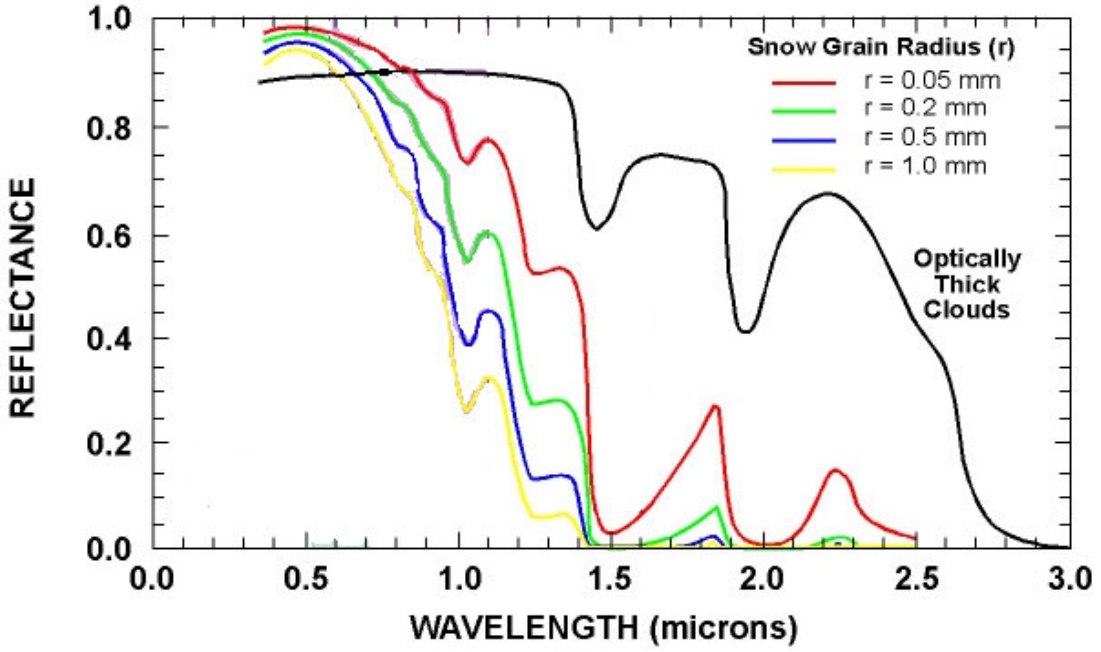

FIGURE 3.2: Reflectance properties of snow and clouds. Graphic adapted from NOHRSC (www.nohrsc.noaa.gov).

3.2 Measurements in the Vallée de la Sionne fieldsite

The site of Vallée de la Sionne (VdlS) is located in the south-western part of Switzerland in the canton of Valais, near Sion (Fig. 3.3).

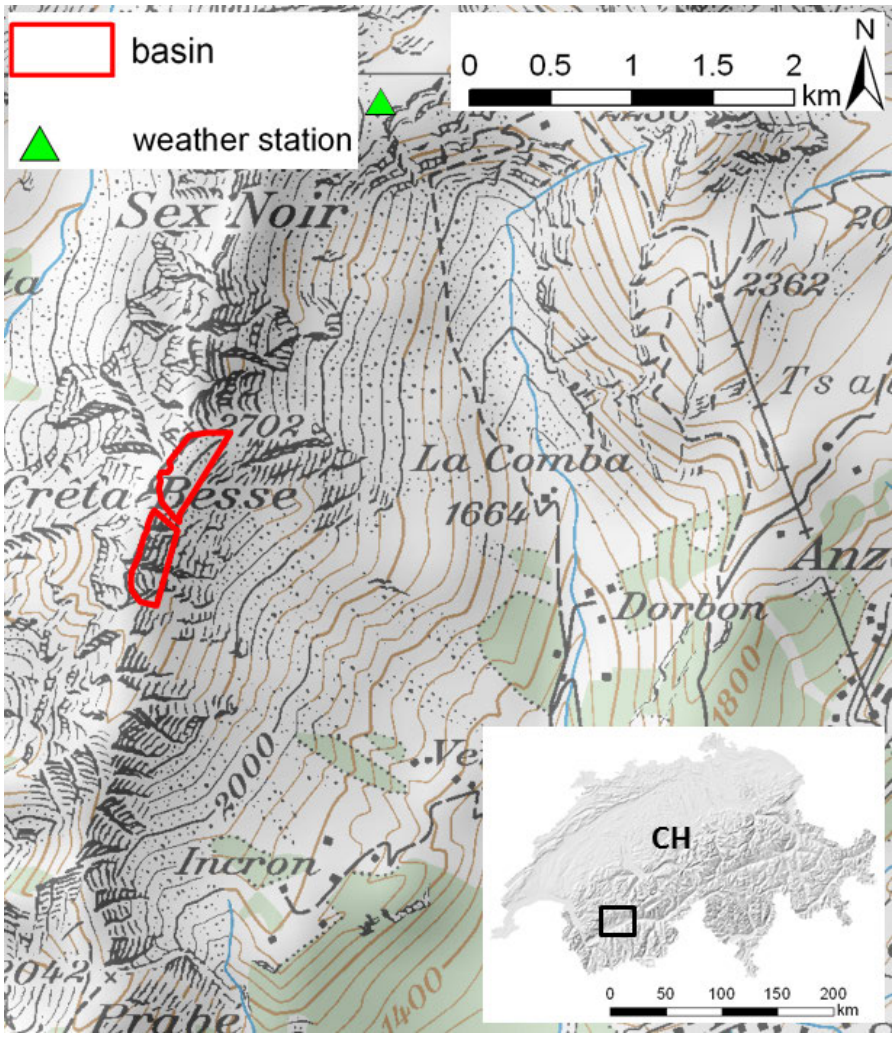

FIGURE 3.3: Field site Vallée de la Sionne near Sion. In red are marked the exact location of the analysed basins, CB1 and CB2, and in green is marked the location of the weather station. Pixmaps 2013 swisstopo (5704 000 000).

The area upon which we focus corresponds to typical release zones, and is characterised by elevations between 2460 m a.s.l. and 2679 m a.s.l., whilst orientation ranges from E to SE. The VdlS field site is divided into two different basins characterized by distinct topography: Crêta Besse 1 (CB1) is steeper and rougher, whereas Crêta Besse 2 (CB2) is less steep and shows a very homogeneous terrain surface without major ridges or cliffs (Fig. 3.4). The area of the basin CB1 is 52 600 m^2, its mean slope is 42.4° with a standard deviation of 6.0°. The area of the basin CB2 is 60 700 m^2 and it has a mean slope of 36.2° with a standard deviation of 3.9°. At the Vallée de la Sionne airborne laser scanning (ALS) measurements are performed before and after avalanche events using a

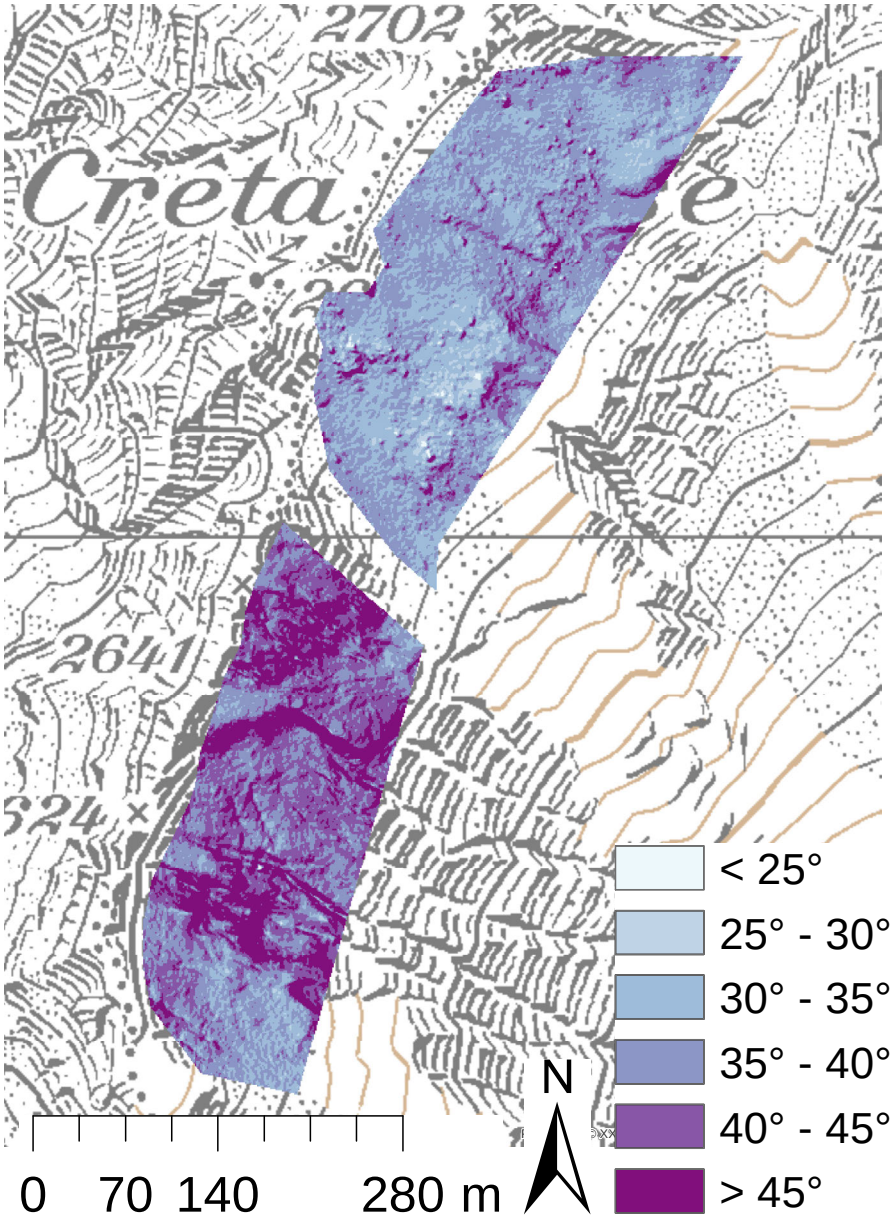

FIGURE 3.4: Field site Vallée de la Sionne near Sion. Slope in the basins CB1 and CB2 derived from a DTM with 1 m resolution. Pixmaps 2013 swisstopo (5704 000 000).

helicopter based system and a detailed description of the method and the precision of the measurements can be found in Sovilla et al. (2010). The vertical accuracy of the data is 0.10 m.

3.2.1 Snow cover distribution in the VdlS

At the Vallée de la Sionne test site, three ALS measurements were performed in three different winter seasons (Fig. A.8). The original grid was resampled from a resolution of 0.5 m to 1 m using cubic interpolation in order to have the same spatial resolution as

TABLE 3.1: Mean $\overline{\mathrm{HS}}$, standard deviation $\sigma(\mathrm{HS})$ and coefficient of variation C_v of snow depth distribution for every laser scan acquisition in the CB1 and CB2 basins.

Date	$\overline{\mathrm{HS}}$	$\sigma(\mathrm{HS})$	C_v
Crêta Besse 1			
(1) 8 Mar 2006	2.71	0.78	0.29
(2) 25 Jan 2009	1.36	0.64	0.47
(3) 8 Dec 2011	1.39	0.30	0.22
Crêta Besse 2			
(1) 8 Mar 2006	3.68	0.61	0.17
(2) 25 Jan 2009	2.13	0.62	0.29
(3) 8 Dec 2011	1.36	0.23	0.17

in the other experimental fieldsite of Steintälli (section 3.3). To calculate snow depth HS in every grid cell, a ALS summer terrain was subtracted from the winter terrain and negative snow depth values were excluded. Simple statistics were used to describe the snow depth distribution: Mean snow depth, $\overline{\mathrm{HS}}$, and its standard deviation, $\sigma(\mathrm{HS})$, as well as the coefficient of variation. The coefficient of variation, C_v, is a normalized measure of the variability of the snowpack defined by the standard deviation divided by the mean snow depth:

$$C_\mathrm{v} = \frac{\sigma(\mathrm{HS})}{\overline{\mathrm{HS}}}. \tag{3.1}$$

Figure 3.6 shows the evolution of snow depth for the winters 2005/2006, 2008/2009 and 2011/2012 at the weather station Donin du Jour, which is situated approximately 2 km away from the basins.

Table 3.1 shows the snow cover characteristics of all acquisitions for the basins CB1 and CB2. The three scans were taken at significantly different stages in the accumulation season. The scan acquired on 8 March 2006 can be considered close to the peak accumulation of the winter. The scan of 25 January 2009 is the result of several snowfalls within the winter season. Both scans show a significantly larger standard deviation. Finally, the scan of 8 December 2011 was performed following the first significant snowfall of the winter season, and represents a very homogeneous snowpack where little redistribution has taken place.

We observe that snow depth at the weather stations (Fig. 3.6) can significantly deviate from the mean snow depth observed in the basins (Tab. 3.1). Snow depth at the weather station therefore is only used for visualisation purposes of the winter history.

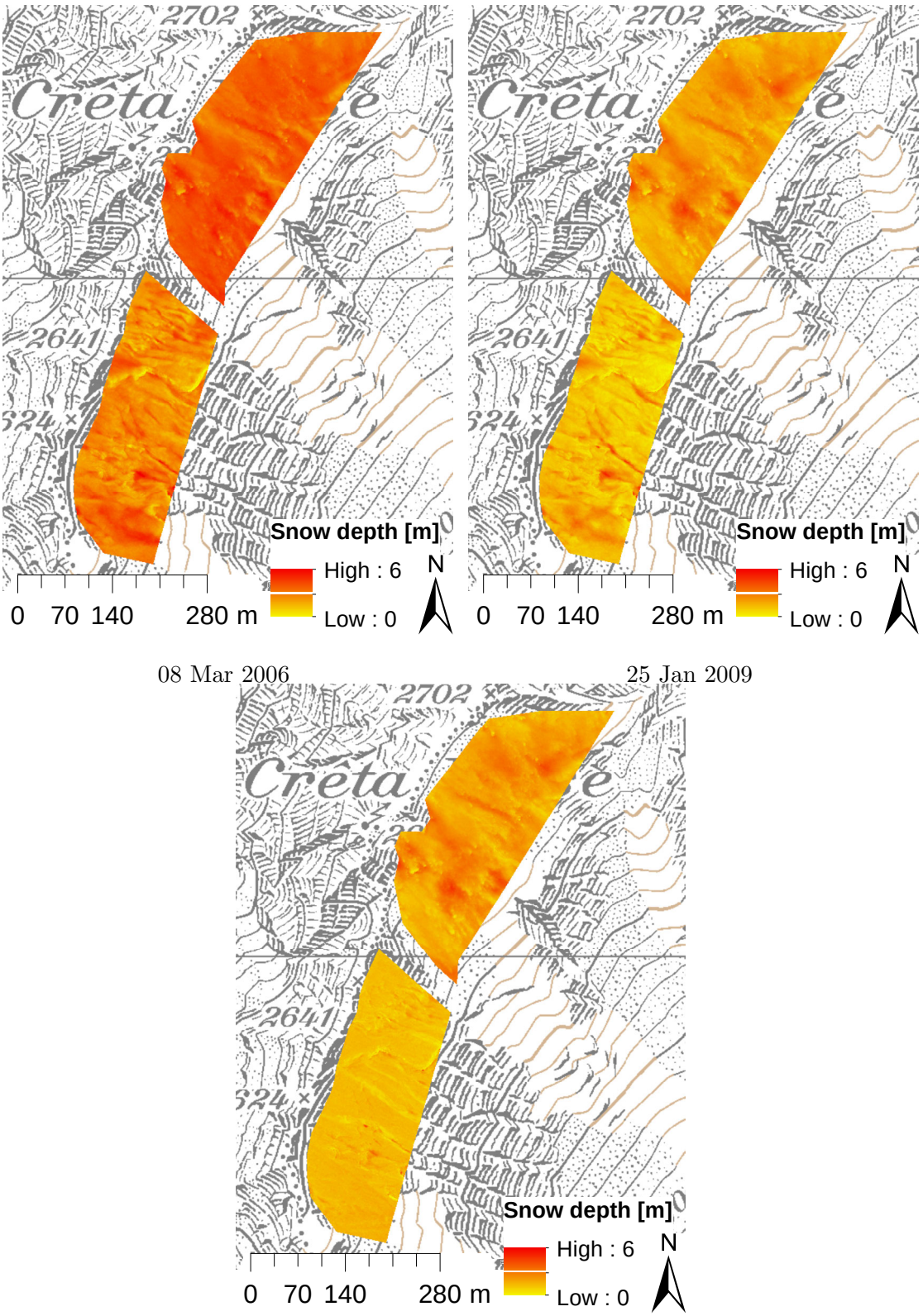

FIGURE 3.5: Snow depth distributions in the basins CB1 and CB2. Pixmaps 2013 swisstopo (5704 000 000).

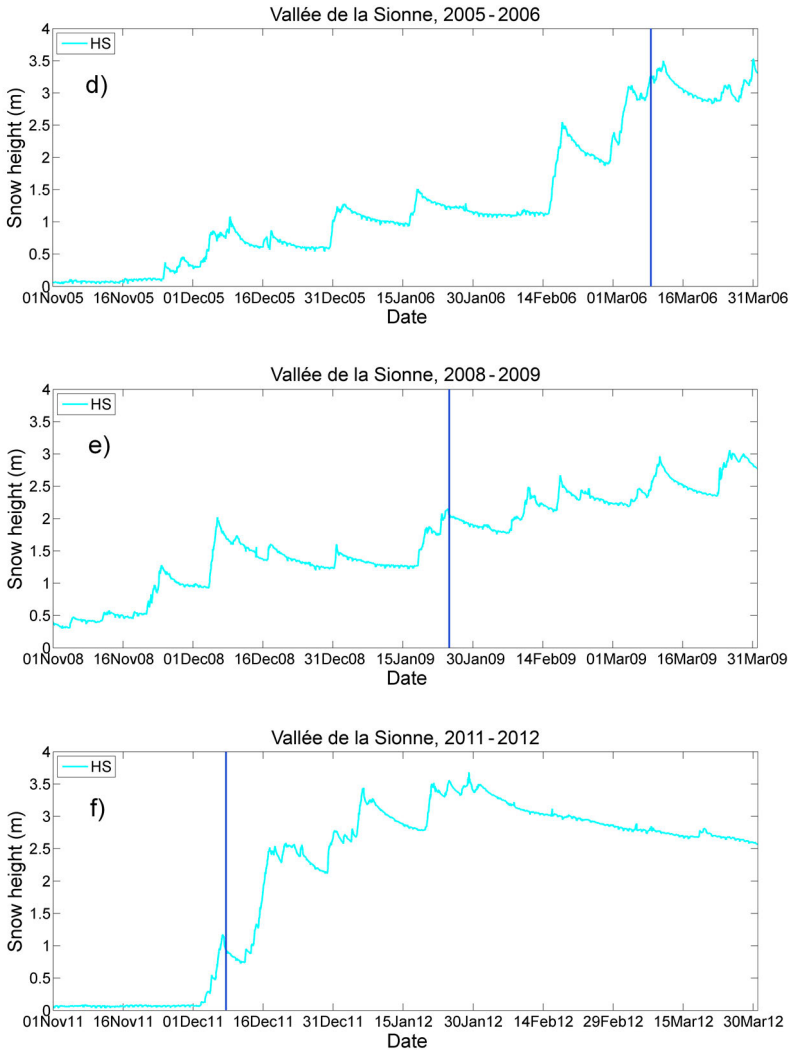

FIGURE 3.6: Evolution of snow depth from 1 November until 31 March measured at the weather station Donin du Jour in the Vallée de la Sionne for the winter seasons 2005/2006, 2008/2009 and 2011/2012. The vertical blue lines correspond to the acquisition times of the laser scans.

3.2.2 Characterization of slab avalanche properties

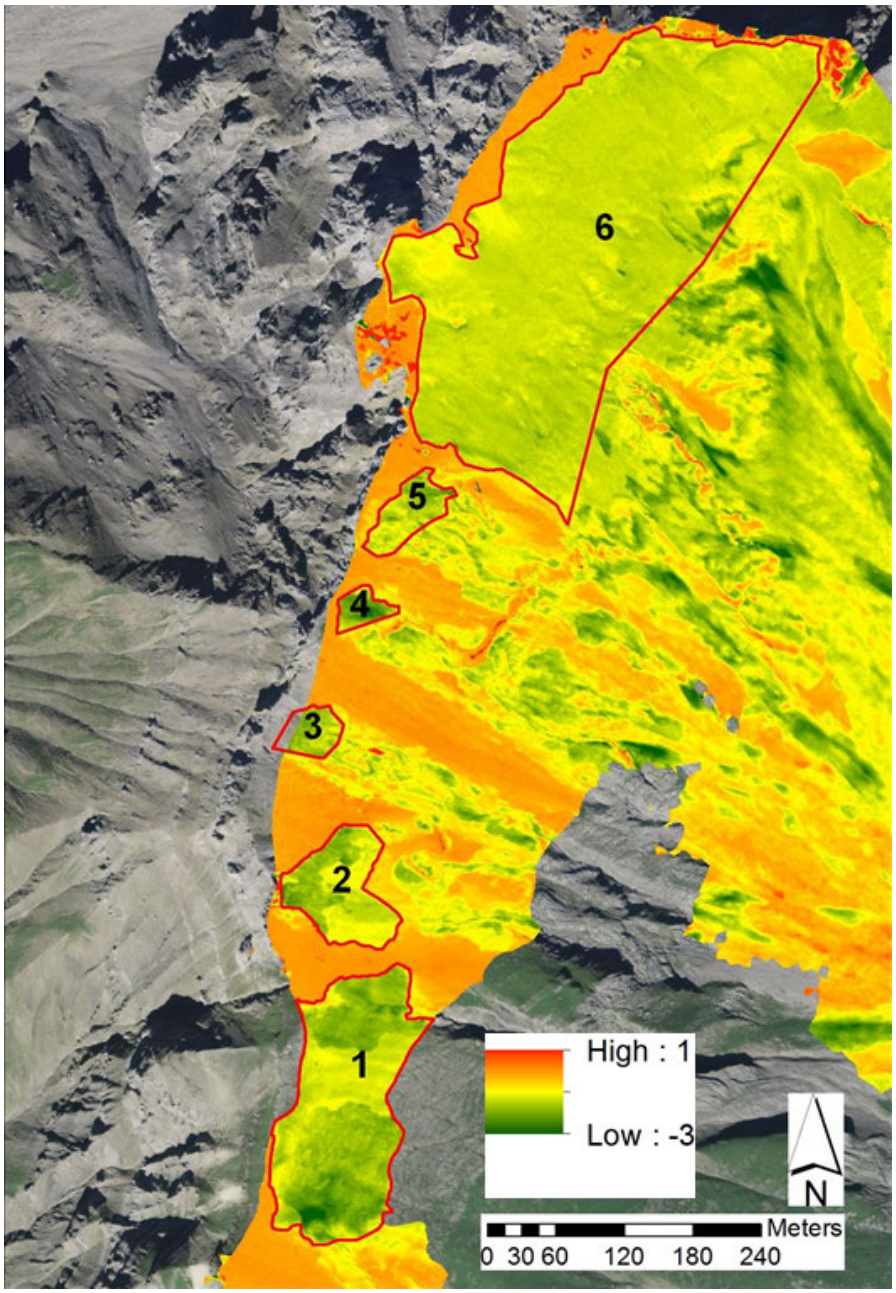

FIGURE 3.7: Difference of snow depth [m] before and after artificial avalanche release obtained from the scans of 8 March 2006. The six release zones and their avalanche tracks are clearly visible.

Six dry slab avalanches were artificially triggered on 8 March 2006, and an additional laser scan was performed after the releases. The difference in snow depth before and after avalanche release can be seen in Fig. 3.7. The triggered slabs comprised the new snow layer of the previous snowfall period and the slabs were running on the winter terrain previous to the snowfall period. Two large slabs were observed where the fracture

propagated over a larger distance within the very smooth parts of CB2 and south of CB1 (#1 and #6 in Fig. 3.7). The slab on the southern end of CB1, despite being small, nevertheless shows clear fracture propagation (#2 in Fig. 3.7), whereas the other slabs within CB1 were quite small with only very little fracture propagation (#3, #4, #5 in Fig. 3.7). Avalanche #1 and #2 also triggered deeper layers of the snowpack. Interestingly, avalanche #2 released due to the detonation, whereas avalanche#1 was triggered remotely by avalanche #2. Table 3.2 shows the mean and the standard deviation of the slab thickness of the triggered avalanches.

TABLE 3.2: Mean $\overline{\text{HS}}$ and standard deviation σ(HS) of slab thickness for avalanche release areas of March 6, 2006 in VdlS.

Aval Nr.	$\overline{\text{HS}}[m]$	$\sigma(\text{HS})[m]$
Avalanche 1	1.65	0.40
Avalanche 2	1.44	0.37
Avalanche 3	1.62	0.27
Avalanche 4	1.95	0.48
Avalanche 5	1.49	0.32
Avalanche 6	1.37	0.17

3.3 Measurements in the Steintälli fieldsite

The Steintälli site (ST) is situated in the eastern part of Switzerland near Davos (Fig. 3.8).

The area of the basin is 73 500 m^2. The terrain of the basin is characterised by elevations between 2418 m a.s.l. and 2600 m a.s.l., and the orientation ranges from NE through E to SE. Steep slopes are located near the ridge, flattening out in the lower part of the basin (Fig. 3.9). The terrain surface is less rugged and irregular when compared with CB1, but still contains more topographical variety, such as gullies and rocky outcrops than CB2. The mean slope of the basin is 35.6° with a standard deviation of 7.3°.

Snow distribution in the Steintälli basin was determined by terrestrial laser scanning (TLS) using the Riegl LPM-321 device operating at 905 nm. This device has proven its ability to work in harsh alpine environment with sufficient accuracy (Prokop, 2008; Prokop et al., 2008). Grünewald et al. (2010) compared TLS with Tachymeter measurements and established a mean deviation of 4 cm with a standard deviation of 5 cm at distances up to 250 m. Our measurement distances ranged from 200 m up to 600 m. In order to georeference the scans, we installed 6 reflector plates at different distances and angles from the scanner position. The plates were attached to existing weather stations or drilled into rockwalls; this assured stable positions over the three –year measurement period.

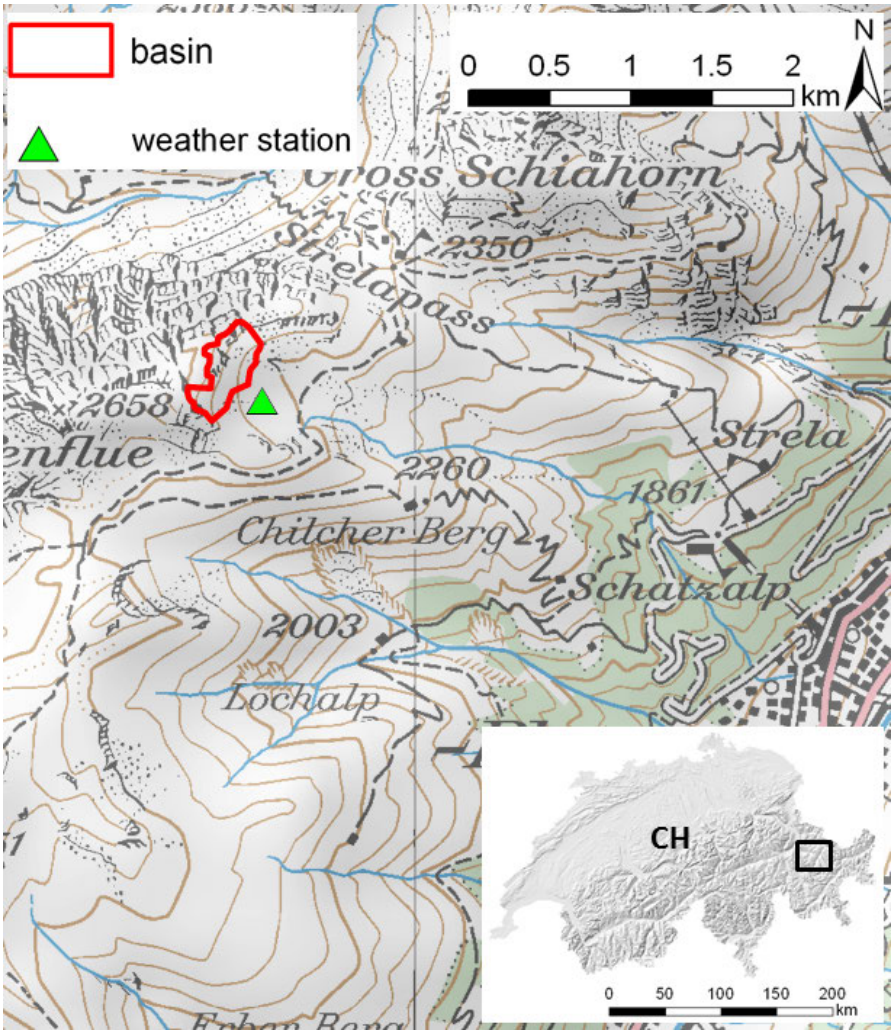

FIGURE 3.8: Field site Steintälli, in the area of Davos. In red is marked the exact location of the analysed basin ST and in green is marked the location of the weather station. Pixmaps 2013 swisstopo (5704 000 000).

In order to ensure scan quality, reproducibility tests were performed. A laser scan performed in coarse resolution at the beginning of the measurement campaign was compared with the normal laser scan acquisition, which permitted us, during the post– processing stage, to detect misalignments between the two, indicating possible errors due to an unstable scanner setup (stability of tripod, wind influence, etc.). Only scans with a mean deviation of less than 10 cm from the coarse scan were considered. Following the correction of meteorological influences, the laser point cloud was interpolated to raster maps with a spatial resolution of 1 m. In total, 8 scans of the winter terrain were performed between the months of January and March, within the winter seasons of 2010/2011, 2011/2012 and 2012/2013 (Fig. A.4). An additional scan of the summer terrain was acquired on 18 September 2011, and serves as reference for the snow depth calculations. To calculate snow depth HS, the summer terrain was subtracted from the winter terrain and negative snow depth values were excluded.

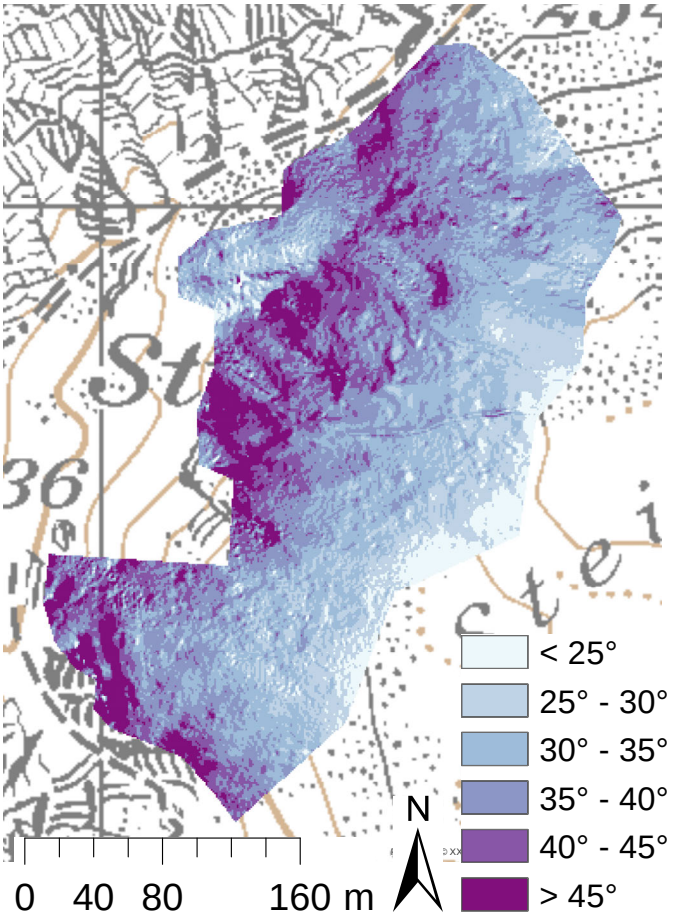

FIGURE 3.9: Field site Steintälli, in the area of Davos. Slope in the basin ST derived from a DTM with 1 m resolution. Pixmaps 2013 swisstopo (5704 000 000).

Table 3.3 details the snow cover characteristics of all acquisitions for the basin ST.

TABLE 3.3: Mean $\overline{\text{HS}}$, standard deviation $\sigma(\text{HS})$ and coefficient of variation C_v of snow depth distribution for every laser scan acquisition in the ST basin.

	Steintälli			
Date	$\overline{\text{HS}}[m]$	$\sigma(\text{HS})[m]$	C_v	winter season
2 Feb 2011	1.33	0.48	0.36	2010/2011
1 Mar 2011	1.43	0.53	0.37	2010/2011
11 Jan 2012	2.75	0.54	0.20	2011/2012
13 Feb 2012	1.91	0.60	0.32	2011/2012
4 Mar 2012	1.99	0.73	0.36	2011/2012
9 Mar 2012	2.31	0.70	0.30	2011/2012
20 Mar 2012	2.01	0.75	0.37	2011/2012
10 Jan 2013	1.36	0.35	0.26	2012/2013

Snow depths in 2010/2011 and 2012/2013 were lower (between 1.33 m and 1.43 m) than in 2011/2012 where snow depth varied between 1.91 m and 2.75 m. The coefficient of variation ranged from 0.2 to 0.37, with generally increasing values towards the end of the accumulation period. Thus, we believe it is a potentially good indicator for the increasing

FIGURE 3.10: The Steintälli basin and position of the laser scanner. Installation of reflector plates in rockwalls.

redistribution of the snow cover during the accumulation season. Figure 3.12 shows the evolution of snow depth for the three winter seasons of 2010/2011, 2011/2012 and 2012/2013 at the weather station WAN7 in close vicinity to the basin ST. Interestingly, the maximum snow depth was reached very early on in the winter season 2011/2012, in January, and is basically the result of one long period of intermittent snowfalls. Normally, peak accumulations at such altitudes are reached later on in the season, e.g. March or April.

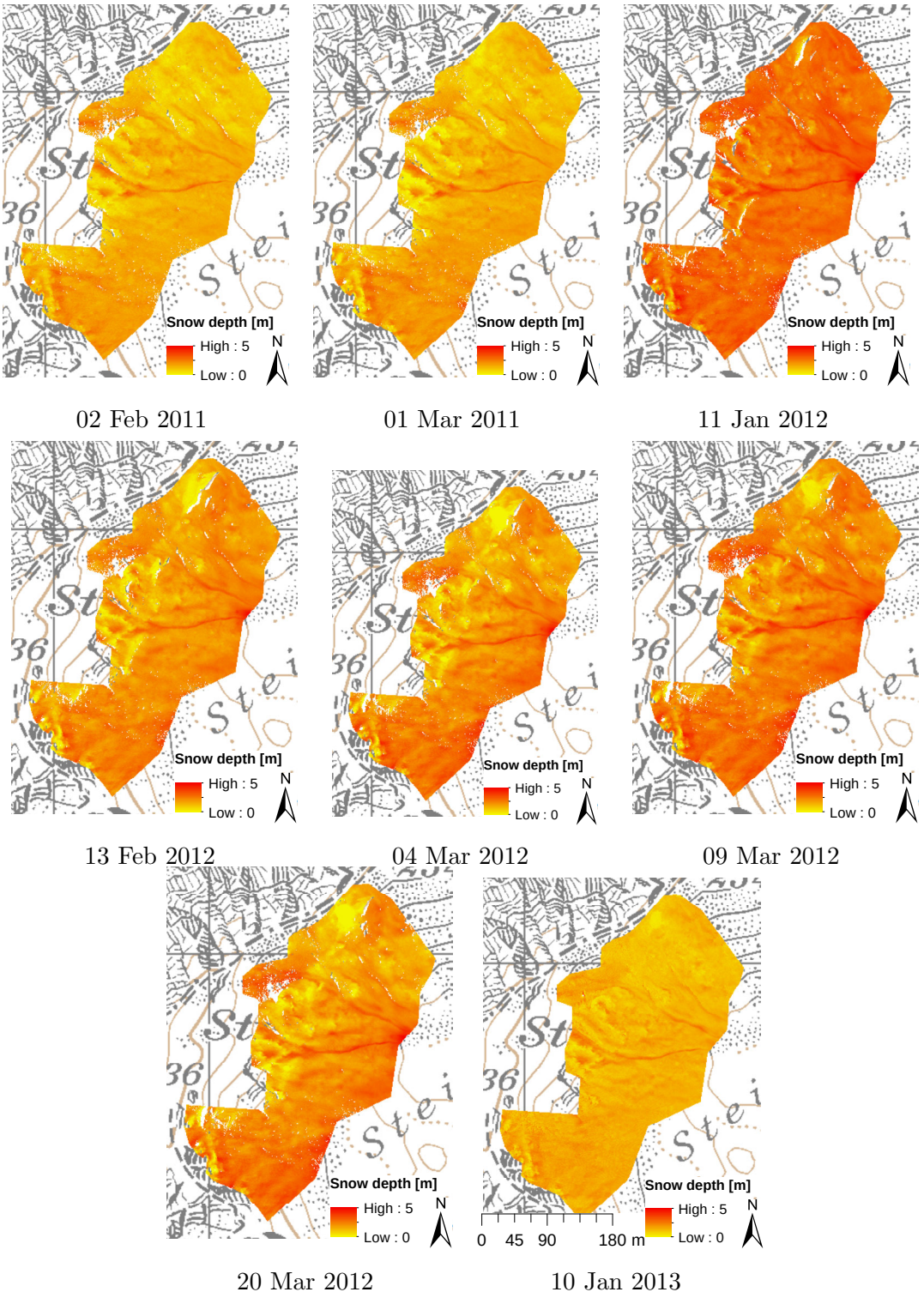

FIGURE 3.11: Snow depth distributions in the basin ST. Pixmaps 2013 swisstopo (5704 000 000).

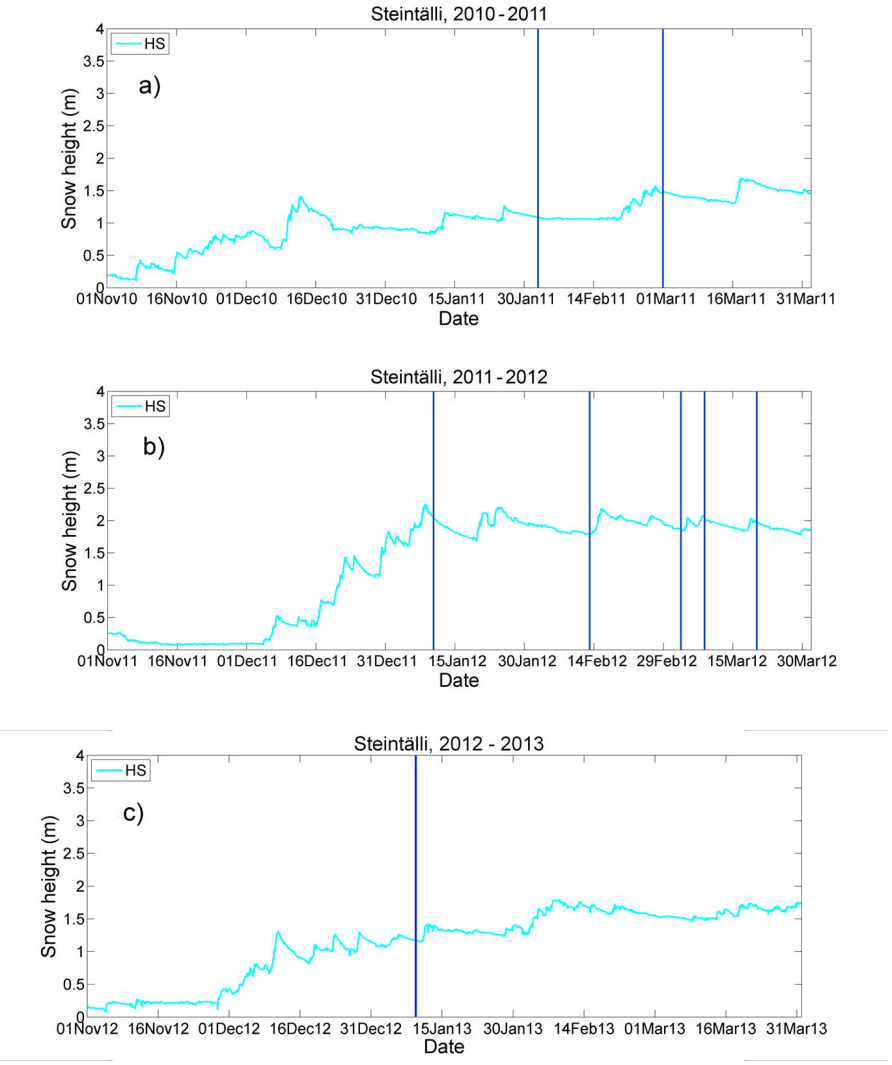

FIGURE 3.12: Evolution of snow depth from 1 November until 31 March measured **(a–c)** at the weather station WAN7 in Steintälli for the winter season 2005/2006, 2008/2009 and 2011/2012. The vertical blue lines correspond to the acquisition times of the laser scans.

3.4 Local avalanche observations in Zuoz

Since the winter 1982/1983, avalanches are continuously observed and documented in the region Zuoz (1716 m.a.s.l.), a village in the Engadine valley in southeast Switzerland (Fig. 3.13). The area is characterised by a continental climate with a mean winter precipitation of 270 mm and a mean winter temperature of -8^{o}C (Stoffel et al., 1998).

Overall, more than 2200 avalanches were manually documented by the local snow and avalanche observer of the village of Zuoz. The overlay of all observed avalanches is shown in Fig. 3.13. From the valley bottom, he draws observed avalanches on a map, together with a transparent sheet on top of it. Every avalanche is then digitised from a transparent sheet, checked for errors, and stored in a GIS database. Further, the observer also provides information relating to the type of avalanche (loose snow, slab avalanche,etc.) and the sliding surface of the avalanche (such as the ground, only new snow, etc.). Both, naturally and artificially triggered avalanches are documented. In addition, daily measurements from a snow observation field situated in the valley bottom are available. This data contains measurements of new-snow depth, snow depth, weather type and intensity, wind direction and speed, air and snow temperature, snow-surface condition, ram-penetration depth and water equivalent of new snow. Further, snow profiles have been taken twice a month.

The fact that the observer maps the avalanches from the valley bottom induces various limitations in the dataset. In cases of bad visibility or during snowfalls, for example, avalanches cannot be mapped. If they are still visible after a snowfall event, they are mapped; however, as the time of release is unknown, only the observation day is archived. Moreover, as avalanches occur at large distances from the observation point, the spatial location of the mapped avalanches contains some imprecisions. In particular the release areas, furthest away from the observation point may be displaced by up to several tens of metres from the original position. Still, this database is one of the most complete datasets of continuous avalanche observations in combination with snow depth measurements.

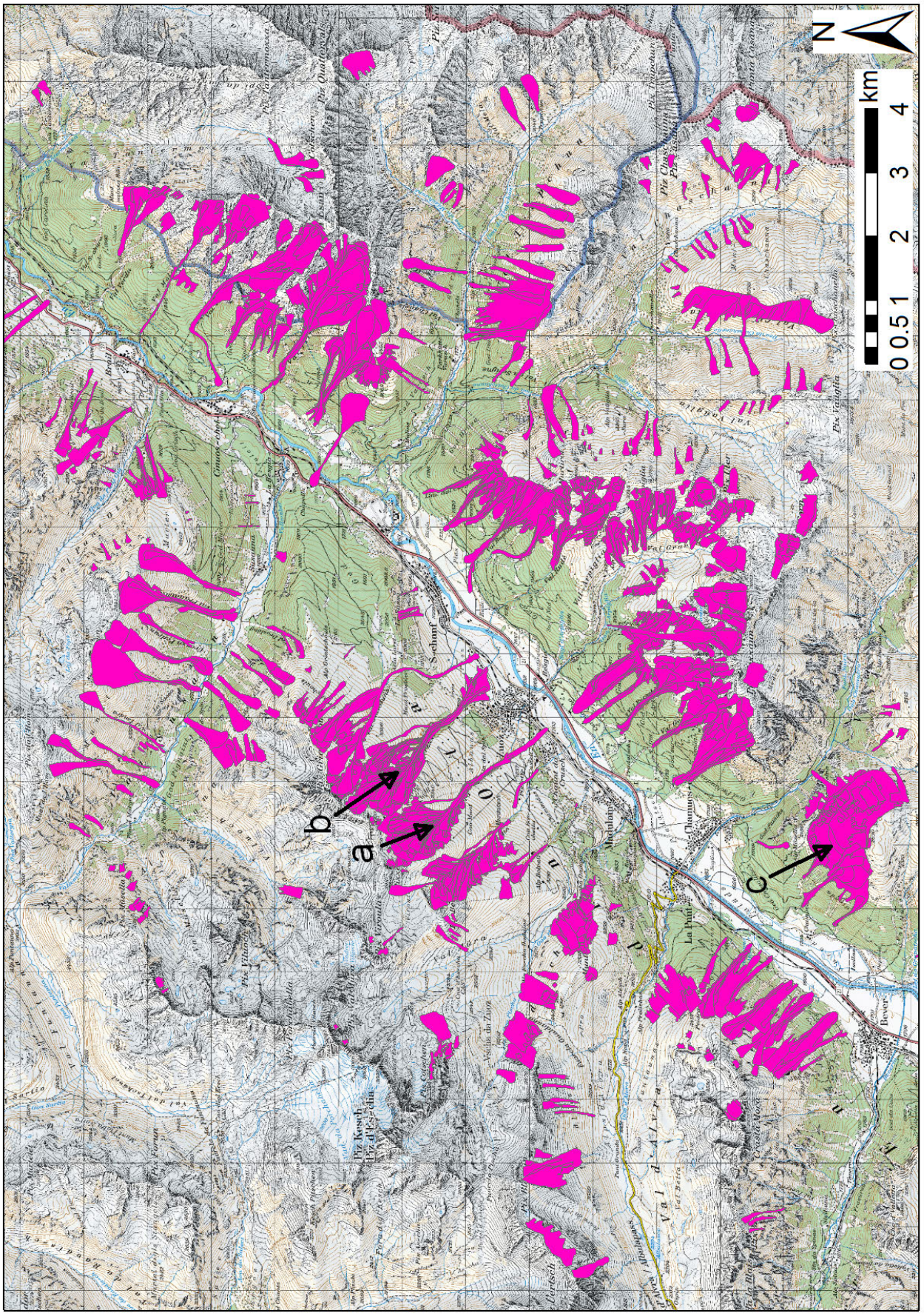

FIGURE 3.13: Fieldsite of Zuoz. Outlines of all avalanches mapped between 1982 and 2012 are shown. The avalanche paths used for more detailed investigation are a) Val Buera, b) Bal d'Urezza and c) Munt Müsella. Pixmaps 2013 swisstopo (5704 000 000).

Chapter 4

Influence of snow depth distribution on surface roughness in alpine terrain

In alpine terrain, the snow-covered winter surface deviates from its underlying summer terrain owing to the progressive smoothing caused by snow accumulation. As shown in section 2.3.4, the influence of snow depth on terrain morphology has not been quantified, despite the increasing availability of high-resolution snow depth measurements. The main aim of this chapter therefore is to develop a method to quantify terrain smoothing by combining roughness calculations of snow surfaces and their corresponding underlying terrain with snow depth measurements. To this end, elevation models of winter and summer terrain, from three basins of the fieldsites of Steintälli and Vallée de la Sionne, characterised by low, medium and high terrain roughness, are used. We evaluate terrain smoothing at pixel, local and basin level. Finally, we assess and quantify the persistence of snow depth and its corresponding terrain smoothing effects. This chapter is based on a journal publication in The Cryosphere.

Veitinger, J., Sovilla, B., and Purves, R. S.: Influence of snow depth distribution on surface roughness in alpine terrain: a multi-scale approach, The Cryosphere, 8, 547-569, doi:10.5194/tc-8-547-2014, 2014.

4.1 Methodology

Snow modifies the underlying terrain by filling gullies and covering rocks; it also creates drift features, such as dunes and cornices, which may be uncorrelated with the

underlying terrain. Therefore, in an effort to evaluate terrain smoothing, it is necessary to both calculate the degree of attenuation of terrain features produced by snow and accordingly estimate the degree of similarity between winter and summer surface. In order to assess terrain smoothing, we use the roughness measure of (Sappington et al., 2007), as presented in section 2.4.3.

We calculated the roughness for every 1 m grid cell of all measured winter surfaces, R_{S}, and the corresponding summer terrain, R_{T}. By varying the neighbourhood size from 3×3 pixels (3 m scale) up to 25×25 pixels (25 m scale), we aimed to account for different scales. Scale in our context therefore corresponds to the size of the moving window.

In an effort, to quantify terrain smoothing at basin scale, we perform a linear regression analysis between all pixels of a winter and the corresponding summer surface of the form

$$R_{\mathrm{S}} = b \times R_{\mathrm{T}}, \tag{4.1}$$

where b is the slope of the regression fit. We then denote the smoothing factor F:

$$F = 1 - b. \tag{4.2}$$

F ranges between 0, when surface roughness is equal to terrain roughness and no smoothing is observed, and 1 for a complete even snow surface. Theoretically, F can be negative for snow surfaces that are rougher than the terrain surface.

Further, we calculate the coefficient of determination, R^2, of the regression fit, which determines the degree of similarity between the snow surface and terrain surface. High values, of up to 1, indicate that the underlying terrain is still dominating and the influence of snow is low. Low values indicate that snow influence is dominant, creating significant changes of the surface structure. Thus, these measures, F and R^2 define terrain smoothing at basin scale.

At pixel scale, terrain smoothing is analysed as a function of the roughness of the summer terrain, as well as the snow depth at this position. We assume that terrain smoothing is dependent on the value of the terrain roughness under consideration. We binned terrain roughness values into classes, separated by intervals of 0.002. For each class with a similar terrain roughness, snow surface roughness is analysed as a function of snow depth.

In order to quantify intra- and interannual persistence of snow depth and surface roughness, the degree of correlation is calculated between two distinct winter snow covers using the coefficient of determination, R^2.

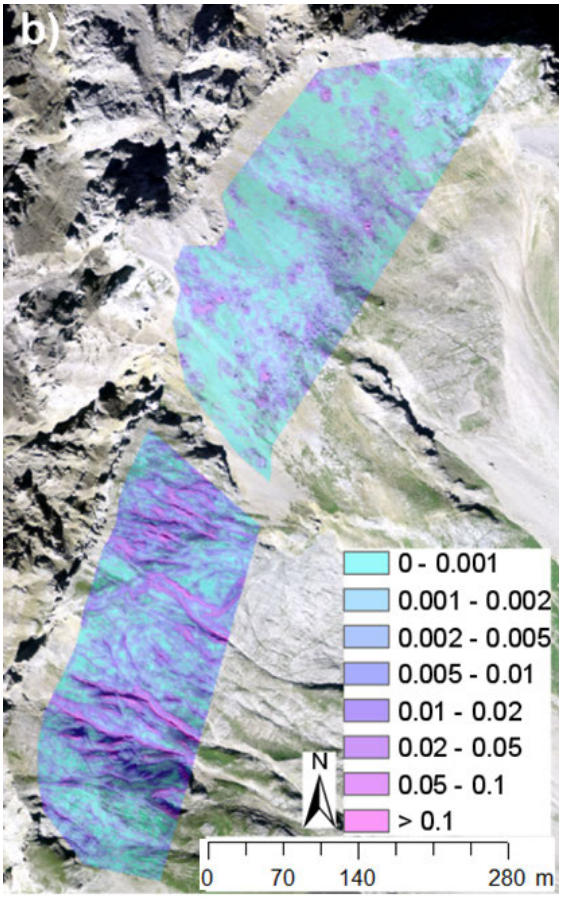

FIGURE 4.1: Terrain roughness derived from a DTM with 1 m resolution, for a 5 m scale in **(a)** the ST basin and **(b)** the VdlS basin. Swissimage 2013 swisstopo (5704 000 000).

4.2 Results and interpretation

4.2.1 Terrain smoothing at basin scale

Figure 4.1 shows terrain roughness of the three basins CB1, CB2 and ST. We observe that the vector ruggedness measure R captures terrain features such as rocky outcrops, boulders and small channels and gullies. It further confirms our selection criteria with increasing roughness from CB2 to ST to CB1. Mean roughness in CB2 is 0.0028 with a standard deviation of 0.0044, mean roughness in ST is 0.0050 with a standard deviation of 0.0089, and mean roughness in CB1 is 0.0084 with a standard deviation of 0.133 (all values calculated at a scale of 5 m).

Figure 4.2 shows an example of the correlation between terrain roughness, R_T, and snow surface roughness, R_S, for the CB1 basin and for scales of 5 m and 25 m. We observe a linear relationship between R_S and R_T. Although the correlation is very strong at larger

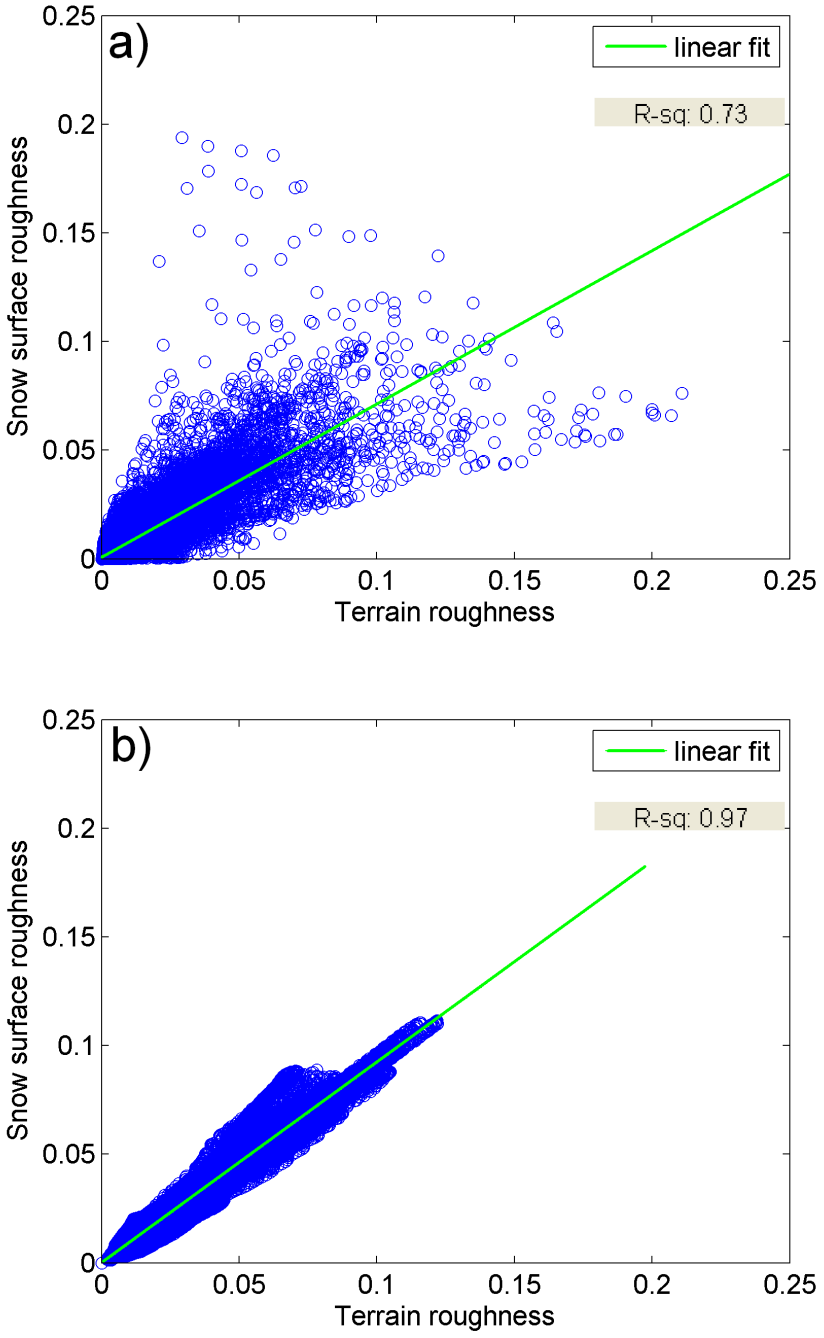

FIGURE 4.2: Snow surface roughness as a function of terrain roughness for every pixel in CB1 in the year 2011 for scales of **(a)** 5 m and **(b)** 25 m. In green the linear regression line.

scales (R^2 of 0.97 at a scale of 25 m), more deviation from the linear fit is observed on smaller scales (R^2 of 0.73 at a scale of 5 m).

Figure 4.3 provides an overview across all basins and shows F and the coefficient of determination, R^2, of terrain roughness and snow surface roughness as a function of different scales for the basins ST, CB1 and CB2. It confirms that the correlation between terrain and surface roughness increases with scale across all basins. Furthermore, all basins show a decreasing smoothing factor F with increasing scales. We observe an inversely proportional behaviour of R^2 and F, indicating that, the more terrain roughness is attenuated (high F), the more snow surface roughness can deviate from its underlying terrain, subsequently forming a distinct winter terrain (low R^2). This confirms quantitatively our intuitive understanding of terrain smoothing. We further observe that terrain smoothing is generally greater (higher F, lower R^2) in sampled basins with low terrain roughness (for example, CB2, Fig. 4.1). Smoothing is strongest in CB2 where fine-scale terrain roughness can be almost completely eliminated (F close to 1, R^2 almost 0). With increasing terrain roughness (ST, CB1) terrain smoothing is less pronounced. This behaviour can be best illustrated with the example of 8 December 2011 in CB1 and CB2, where the first significant snowfall of the winter season resulted in a very similar mean snow depth (1.39 m and 1.36 m in CB1 and CB2, respectively) in both basins. However, terrain smoothing is significantly greater (higher F, lower R^2) in CB2 than in CB1. This emphasises that every basin has a unique imprint and shows a different smoothing behaviour – even when there are almost identical snow depth distribution parameters such as mean snow depth.

Beside the basin characteristics, it is clear that the differences of the smoothing behaviour observed within every individual basin are due to varying snow cover distribution.

Figure 4.3 shows qualitatively that terrain smoothing increases with increasing snow depth. In the basin ST for example, we clearly identify two different smoothing behaviours between the two winters of 2010/2011 and 2012/2013 and the winter of 2011/2012, which were characterized by snow depths in the range of 1.33–1.43 m and 1.91–2.75 m, respectively. This pronounced difference in snow depth of the winter season 2011/2012 compared to the other two, results in more pronounced smoothing at scales up to 15 m. At larger scales, F of all winter seasons converges to values of around 0.45. However, this behaviour is not unequivocal, and mean snow depth alone cannot always explain terrain smoothing. For example, the scans of 11 January 2012 and 4 March 2012 show almost the same smoothing behaviour, despite a significantly larger mean snow depth on 11 January 2012 (2.75 m compared to 1.99 m on 4 March). In this case, the coefficient of variation, C_v, is significantly lower for the scan of 11 January 2012, indicating that the snow cover is less distributed than for 4 March 2012. This is confirmed in other basins.

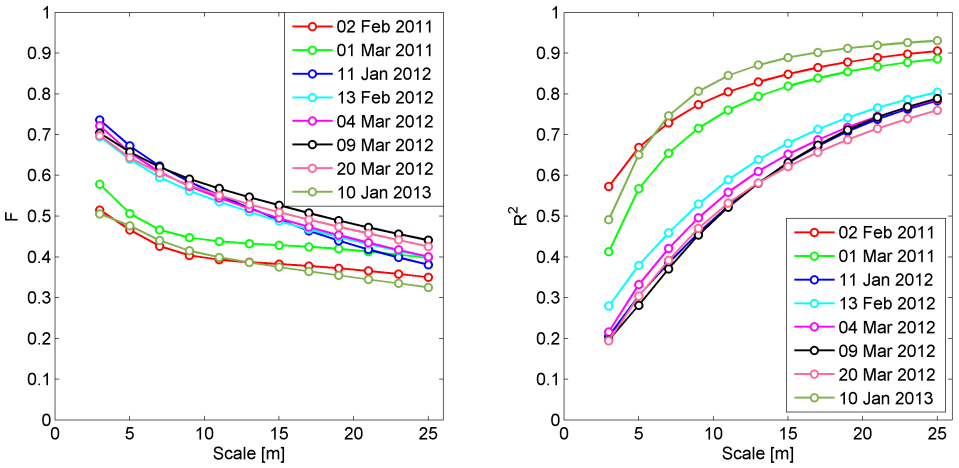

(a) F in ST **(d)** R^2 in ST

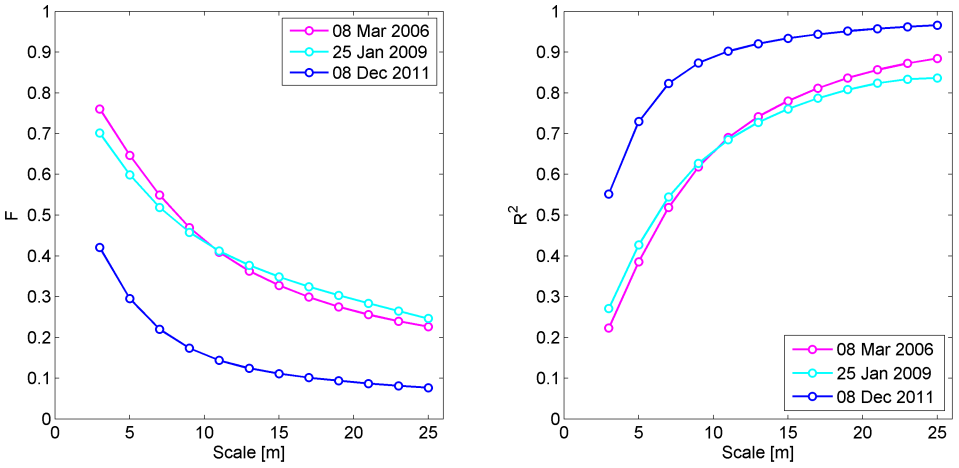

(b) F in CB2 **(e)** R^2 in CB2

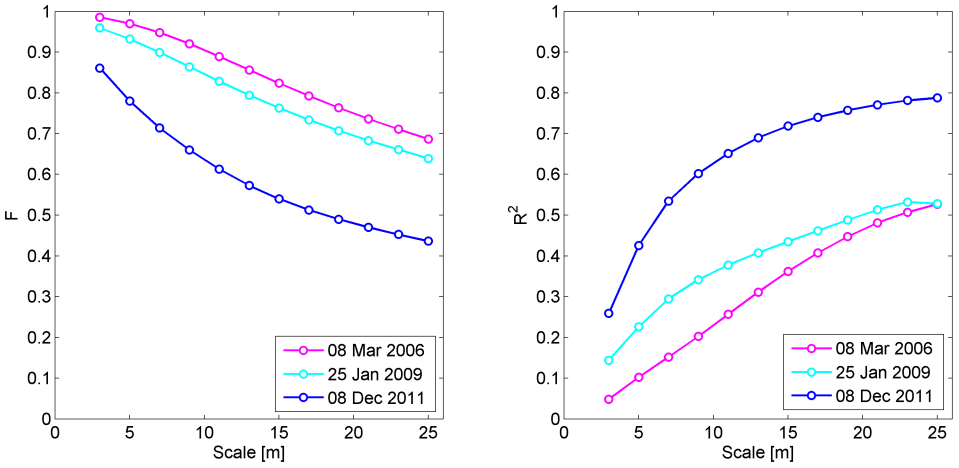

(c) F in CB1 **(f)** R^2 in CB1

FIGURE 4.3: **(a–c)** Smoothing factor F and **(d–f)** coefficient of determination R^2 ($p < 0.0001$) between snow surface roughness and terrain roughness as a function of scale for the basins ST, CB1 and CB2.

In CB2, we observe that the smoothing in the year 2006 is only slightly greater than in 2009 – despite a significantly thicker snowpack (3.68 m in 2006 compared to 2.13 m in 2009). Also, in this case, C_v is almost twice as large in 2009, indicating that relatively more snow has been redistributed. In CB1, we observe that both years 2006 and 2009 show a very similar smoothing behaviour, despite higher mean snow depth in 2006. Again, C_v is larger in 2009; thus, the snow cover was more affected by redistribution processes.

The above observations suggest that terrain smoothing may be dependent on the mean snow depth, $\overline{\mathrm{HS}}$, as well as its variability, $\sigma(\mathrm{HS})$. In an effort to examine this relationship, the data of the ST basin, where eight laser scans are available, was used. With only three scans in VdlS, this would not be possible. We define:

$$\widetilde{\mathrm{HS}} = \overline{\mathrm{HS}} \times \sigma(\mathrm{HS}) \ [\mathrm{m}^2]. \tag{4.3}$$

Figure 4.4 shows F with $\widetilde{\mathrm{HS}}$ for the scales of 5 m, 15 m and 25 m and as a comparison only with $\overline{\mathrm{HS}}$. In both cases, we can see that increasing scales lead to a decreasing smoothing behaviour and that a linear increase in $\overline{\mathrm{HS}}$ and $\widetilde{\mathrm{HS}}$ does not result in a linear increase of the smoothing factor. Therefore, a power function of the form

$$\widetilde{\mathrm{HS}} = c \times F^r, \tag{4.4}$$

where c and r are coefficients depending on terrain characteristics and scale, better describes the exponential increase of $\widetilde{\mathrm{HS}}$ with F. Further, through visual inspection, it can be seen that there is better agreement with the fit when the variability of snow depth is integrated.

If we solve Eq. (4.4) for F we obtain

$$F = \left(\frac{\widetilde{\mathrm{HS}}}{c} \right)^{\frac{1}{r}}, \tag{4.5}$$

where Table 4.1 shows the characteristic values of c and r for the basin ST.

TABLE 4.1: Coefficients c and r of the power function modelling terrain smoothing in the basin of ST.

	Steintälli	
Scale	c	r
5 m	2.8	2.2
15 m	10.6	3.2
25 m	24.9	3.5

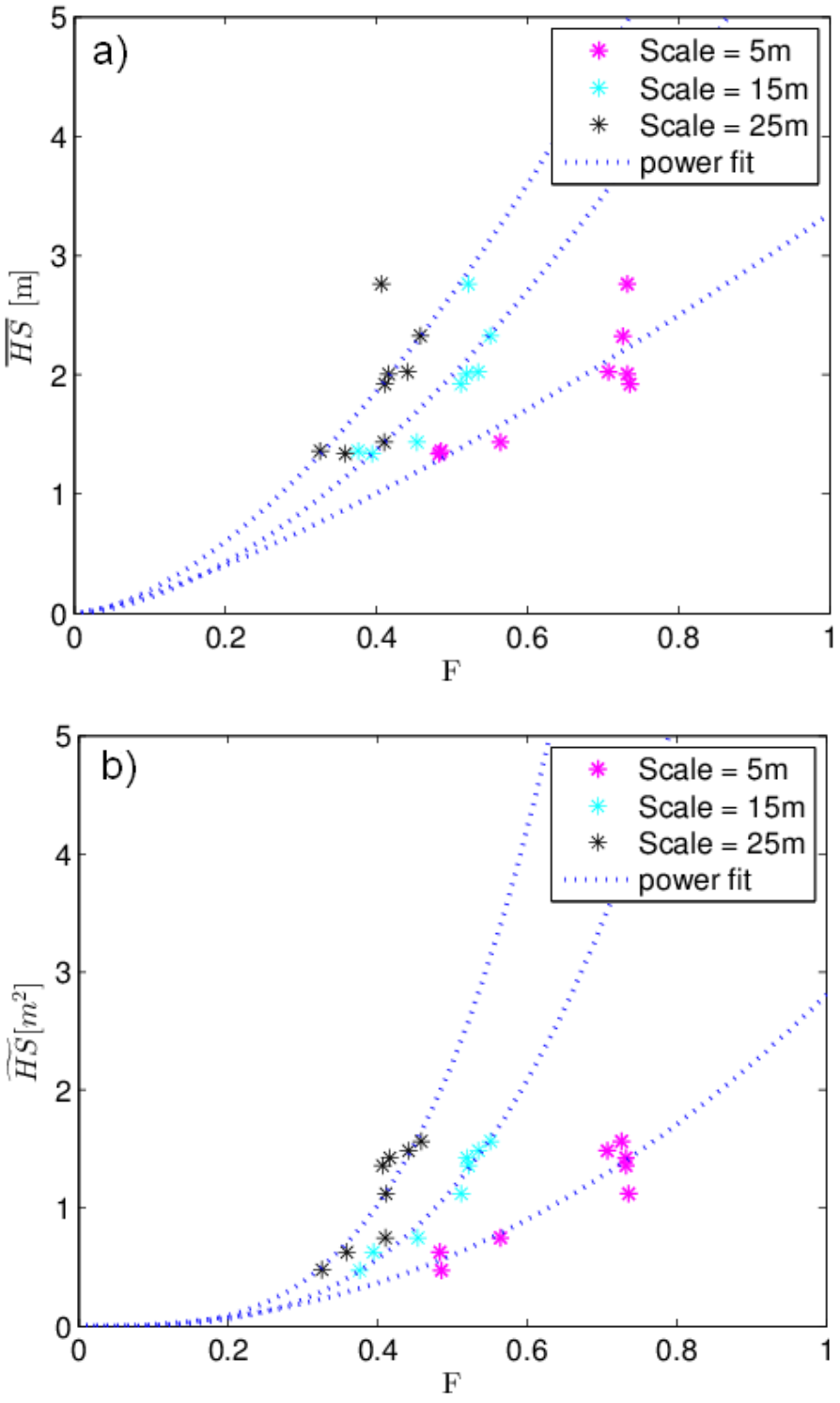

FIGURE 4.4: **(a)** F as a function of mean snow depth and **(b)** F as a function of mean snow depth multiplied by its standard deviation for scales of 5 m, 15 m and 25 m.

The observed smoothing behaviour indicates that the snow that fell at the beginning of the winter season is more efficient in cancelling out roughness than larger snowfalls occurring later on in the season, when the snow cover is already relatively deep. Furthermore, it shows how a simple standard deviation can capture complex redistribution processes, such as a wind transport–at least at basin scale.

We believe that the obtained relation in this basin captures well the essence of terrain smoothing. Basins with different terrain characteristics may show different behaviours with stronger or weaker increases of F in relation to snow depth and its variability.

Assuming that snow influence on terrain morphology is significant for values of $R^2 < 0.5$ between snow surface roughness and terrain roughness, we find critical scales mostly between 5 m and 10 m for snow depth roughly ranging between 1 m and 3 m. Larger critical scales were found in the smoother terrain of CB2 with values around 25 m. This finding is very useful in selecting the appropriate resolution of the DTM for modelling purposes in a winter terrain.

4.2.2 Terrain smoothing at local scale

As discussed above, terrain smoothing at basin scale is directly proportional to the average snow depth and its standard deviation; however, in order to understand the smoothing behaviour of single terrain features, it is necessary to assess the link between snow depth and surface roughness at a local scale. Accordingly, the correlation between snow depth and terrain smoothing was analysed at pixel scale (Fig. 4.5). This example shows that, in contrast to what was observed at basin level, it is not possible to establish a general relationship between the two variables. No relationship was found in any basin or at any scale.

In order to develop a deeper understanding of this behaviour, gridded maps with a spatial resolution of 1 m of snow depth and surface roughness were produced, and the spatial distribution of snow depth and surface roughness was assessed. Figures 4.6 and 4.7 show two selected snow depth distributions and the corresponding surface roughness and underlying terrain roughness at a scale of 5 m and 25 m in the basins ST and VdlS, respectively. Maps of all snow depth and roughness distributions can be consulted in the Appendices. Even if a correlation between snow depth and smoothing at the pixel level could not be identified, through visual inspection it can be observed that snow can influence the smoothing processes at feature level –both– systematically and persistently. This can be observed in Fig. 4.6, for example, where channels (marked with black circles) are systematically filled with snow and which completely disappear on the surface roughness maps in all observed scans. Another example is surface roughness

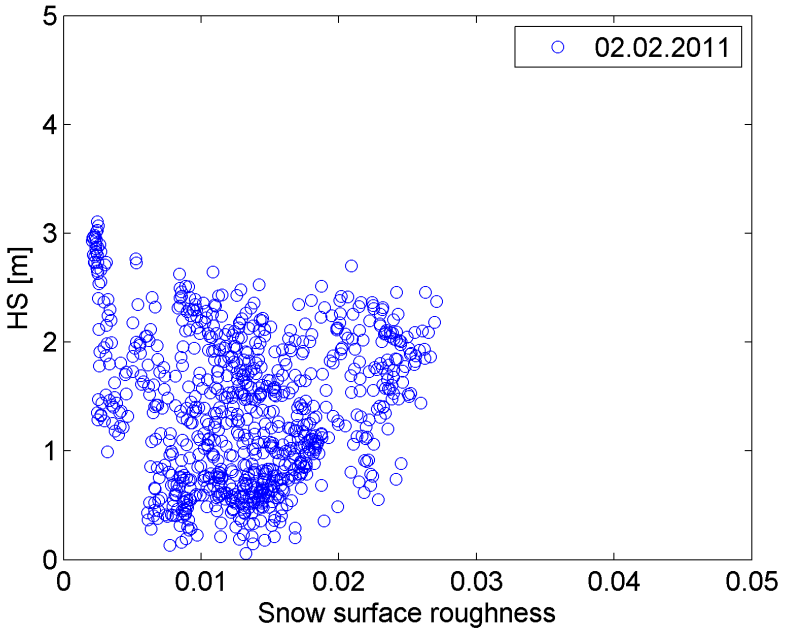

FIGURE 4.5: Snow surface roughness as a function of snow depth for pixels with terrain roughness of 0.025 ± 0.001. Example for acquisition of 2 February 2011 and a scale of 15 m in the basin ST.

due to small rocks (marked with yellow circles), which persist in all given snow cover distributions. This illustrates that smoothing processes are strongly driven by single features, and explains why a local gridded representation of terrain cannot capture the complex relationship between snow depth and terrain smoothing.

However we stress that, under snow influence, characteristic patterns of surface roughness appear to be persistent. In the following, we therefore analyse quantitatively the persistence of snow depth distribution and whether or not persistence is further transferred to surface roughness.

4.2.3 Intra- and interannual persistence of snow depth

Table 4.2 shows the correlations of the snow depth distribution for the Steintälli basin. We observe high intra-annual correlation of 0.81 between the two scans in the season 2010/2011 as well as the last four scans in 2011/2012, with values ranging from 0.73 to 0.93. Only the scan from 11 January 2012 is correlated to a lesser strong extent with all other scans from this winter season, with values ranging from 0.43 to 0.58. Thus, in general, the intra-annual correlation at this site is strong, with higher values towards the middle and end of the accumulation season.

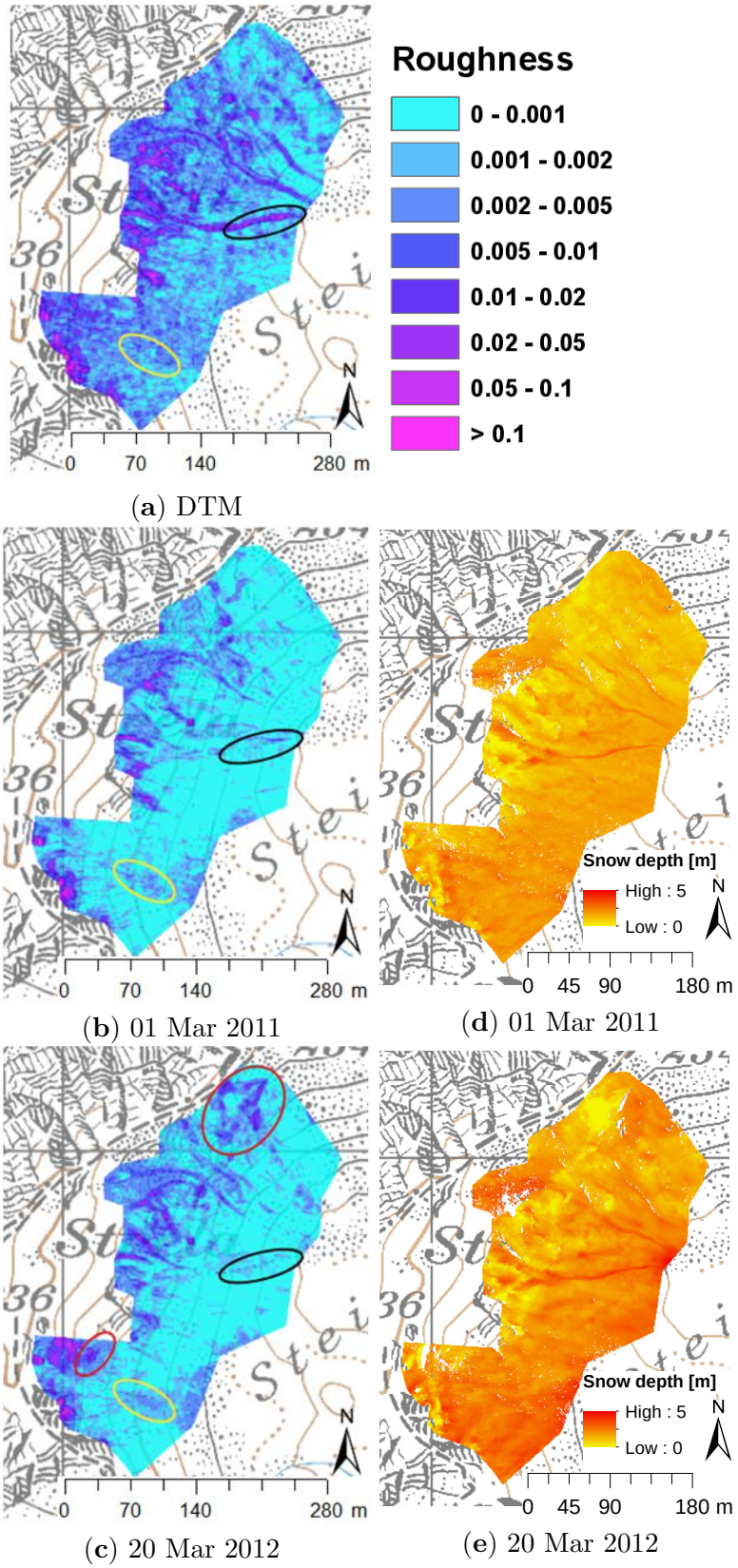

(**a**) DTM

(**b**) 01 Mar 2011

(**d**) 01 Mar 2011

(**c**) 20 Mar 2012

(**e**) 20 Mar 2012

FIGURE 4.6: **(a)** Surface roughness of summer terrain and **(b)**, **(c)** winter terrain at a scale of 5 m in the basin ST. **(d)**, **(e)** show the corresponding snow depth distributions. The black and yellow circles show persistent smoothing features. Red circles show the location of glide cracks. Pixmaps 2013 swisstopo (5704 000 000).

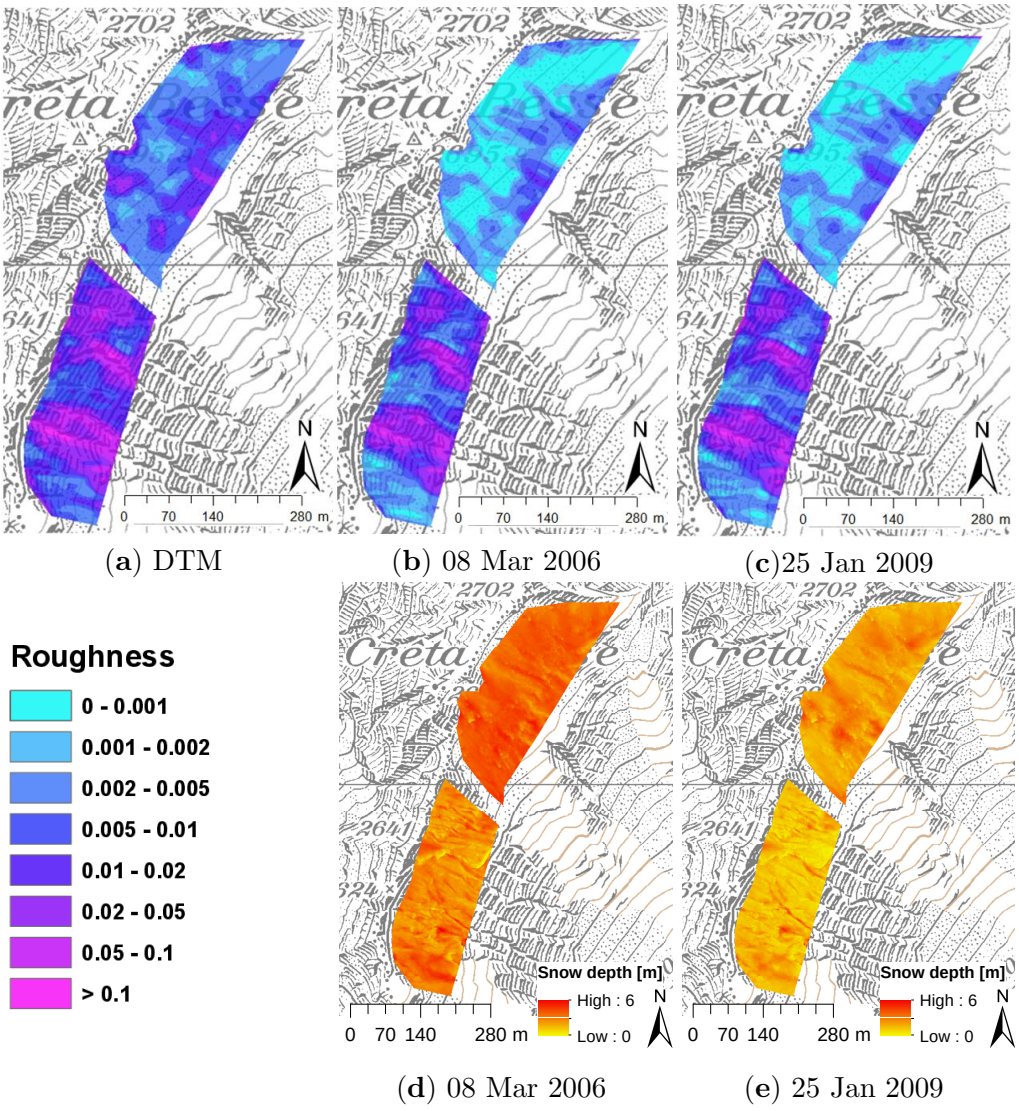

(**a**) DTM (**b**) 08 Mar 2006 (**c**)25 Jan 2009

(**d**) 08 Mar 2006 (**e**) 25 Jan 2009

FIGURE 4.7: **(a)** Surface roughness of summer terrain and **(b)**, **(c)** winter terrain at a scale of 25 m in the basins CB1 and CB2. **(d)**, **(e)** show the corresponding snow depth distributions. Pixmaps 2013 swisstopo (5704 000 000).

The same holds for the interannual comparison. The correlation between scans performed at the beginning of the winter season is generally lower as in the case of the scan from 11 January 2012 compared with the scan from 2 February 2011 ($R^2 = 0.25$) and with that of 10 January 2013 ($R^2 = 0.28$). The correlation increases for scans performed towards the end of the winter season as in the case of scans from 1 March 2011 and 20 March 2012 ($R^2 = 0.65$). Still, we observe that strong correlations exist also between scans acquired substantially before the peak of the accumulation season (such as those from 10 January 2013 and 2 February 2011 with a correlation of $R^2 = 0.69$).

Table 4.3 shows correlations of the snow depth distribution for the basins CB1 and CB2. In this case, we can only perform an interannual comparison, and in agreement with the

TABLE 4.2: Coefficient of determination (R^2) of correlations between snow depth distributions in the ST basin ($p < 0.0001$).

	Steintälli							
Date	(1)	(2)	(3)	(4)	(5)	(6)	(7)	(8)
(1) 02 Feb 2011	1							
(2) 01 Mar 2011	0.81	1						
(3) 11 Jan 2012	0.25	0.30	1					
(4) 13 Feb 2012	0.37	0.51	0.58	1				
(5) 04 Mar 2012	0.53	0.64	0.44	0.81				
(6) 09 Mar 2012	0.54	0.57	0.52	0.79	0.86	1		
(7) 20 Mar 2012	0.61	0.63	0.43	0.73	0.91	0.93	1	
(8) 10 Jan 2013	0.69	0.59	0.28	0.34	0.41	0.50	0.49	1

results from the Steintälli basin the correlation increases for scans that correspond to the end of the accumulation season. In fact, we can observe that, in basin CB1, the years 2006 and 2009 are more highly correlated ($R^2 = 0.73$) than 2006 and 2009 with 2011 ($R^2 = 0.41$ and $R^2 = 0.34$, respectively). In CB2 this effect is less pronounced, which can be explained by the fact that smooth terrain generally shows lower interannual persistence ($R^2 = 0.58$ between 2006 and 2009).

TABLE 4.3: Coefficient of determination (R^2) of correlations between snow depth distributions in the CB1 and CB2 basins ($p < 0.0001$).

Date	8 Mar 2006	25 Jan 2009	8 Dec 2011
	Crêta Besse 1		
8 Mar 2006	1		
25 Jan 2009	0.73	1	
8 Dec 2011	0.41	0.34	1
	Crêta Besse 2		
8 Mar 2006	1		
25 Jan 2009	0.58	1	
8 Dec 2011	0.54	0.29	1

To summarise, generally, we observe larger intra- and interannual persistence for snow depth distributions acquired closer to the end of the accumulation period, which have been exposed to settling and redistribution processes over a whole winter. Nonetheless, large persistence is possible early on in the accumulation season, under the condition that a certain settling and redistribution has occurred (e.g. scans of 10 January 2013 and 2 February 2011 in ST). A significantly weaker intra- and interannual consistency was observed for snow depth distributions which resulted basically from the first snowfall or snowfall period in the winter season, like the scans from 11 January 2012 in ST or the scan from 8 December 2011 in VdlS. Thus, a single snowfall (period) at the beginning of the accumulation season can considerably vary from the characteristic accumulation pattern.

The results support the hypothesis that snow distribution converges towards a site-specific, characteristic pattern.

4.2.4 Intra- and interannual persistence of surface roughness

Tables 4.4 and 4.5 show the correlation of surface roughness of all winter surfaces with each other and with terrain roughness at scales of 5 m, 15 m and 25 m for the basins ST, CB1 and CB2 respectively.

Generally, correlations between summer and winter terrain roughness and between the different winter surfaces can be seen to increase with larger scales. Further, winter surfaces with a thinner snowpack are more strongly correlated with the terrain than winter surfaces consisting of a thick snowpack (as in the scans of 2010/2011 and 2012/2013 compared to 2011/2012 in ST).

We observe that the persistence of snow surface roughness follows similar patterns to those observed for the snow depth distribution: for example, the intra-annual persistence at a scale of 5 m in ST in 2010/2011 is slightly larger than those of the corresponding snow depth distribution ($R^2 = 0.89$ compared to 0.81 for snow depth), whereas in 2011/2012 the persistence is slightly weaker. The same is observed for the interannual persistence. If we take as a reference the scan of 10 January 2013, interannual persistence is greater when compared with the scans of 2010/2011 and lower when compared with scans towards the end of the winter season of 2011/2012. This can be explained with the increasing formation of glide snow cracks, leading to substantial alterations of the snow surface (marked with red circles in Fig. 4.6). Whereas persistence of snow surface roughness is similar to those of the snow depth distribution at a scale of 5 m, it is significantly higher for the larger scales of 15 m and 25 m; even more important, winter terrain roughness is correlated to a significantly larger degree with all other winter surfaces with similar or larger snow depth than each of the winter surfaces with the terrain. For example, at a scale of 5 m in ST, an increase of R^2 between 0.09 and 0.16 for all winter surfaces is observed using the winter terrain of 10 January 2013 as a reference rather than the summer terrain. This is noteworthy as several glide cracks in winter 2011/2012 introduced considerable alteration in the surfaces. At larger scales of 15 m and 25 m, the increase is also observed but to a slightly lesser extent. This is mainly due to the already very strong correlation with the terrain at larger scales, reducing the potential gain in correlation.

The same behaviour can be observed in the basins CB1 and CB2: for example, the scan of the first snowfall of the winter season of 8 December 2011 rather than the summer terrain, increases the correlation with the surfaces of 8 March 2006 and 25 January 2009,

amounting to 0.1 and 0.23, respectively, in CB1 (0.21 and 0.1 in CB2, respectively). In the case of CB2, the increase of correlation is even more pronounced on larger scales (15 m and 25 m) rather than at the 5 m scale, with an increase of R^2 up to 0.31. This confirms the finding detailed in section 4.2.1, where snow influence in smooth terrain affects coarser scales than in rough terrain.

Overall, this finding is important in the sense that, at scales where snow has a significant influence on terrain morphology, a DSM of a snow surface explains to some extent the variance between snow surface roughness and terrain roughness. Therefore, it might be possible to capture the persistent characteristics of a winter terrain surface, including wind effects, without the extensive modelling of the snow cover; however, this is only true if the reference DSM is used to approximate winter surfaces with similar or deeper snowpack. A DSM representing a very thick snow cover situation might be less representative for a thin snow cover situation than the summer DTM.

Moreover, the patterns of homogeneous snow surface roughness, especially at larger scales (> 10 m), seem to be well suited to defining potential avalanche release areas. We recognise that these patterns are generally strongly persistent for different snow depth distributions; nonetheless they still diverge locally in some regions. The persistent parts may represent the zone where an avalanche most often releases, the changes (such as connection of two areas with low surface roughness, Fig. 4.7), on the other hand, could explain, to some extent, the regularly observed differences in release area size and location.

However, it has to be mentioned that the relative paucity of data restricts the generality of the results. The three studied basins are not representative for the variety of snow climates, wind regimes and terrain types that can be found in different regions of the world. In this thesis, only high alpine, moderately steep and mostly leeward aspects were examined. Consequently, the results are only meaningful for this type of terrain and further investigations in other areas are needed to complement our findings in order to draw more general and robust conclusions.

TABLE 4.4: Coefficient of determination (R^2) of surface roughness correlations in the ST basin ($p < 0.0001$).

Steintälli										
Scale	Date	2 Feb 2011	1 Mar 2011	11 Jan 2012	13 Feb 2012	4 Mar 2012	9 Mar 2012	20 Mar 2012	10 Jan 2013	DTM
5m	2 Feb 2011	1								
5m	1 Mar 2011	0.89	1.00							
5m	11 Jan 2012	0.43	0.42	1						
5m	13 Feb 2012	0.51	0.50	0.49	1					
5m	4 Mar 2012	0.48	0.50	0.51	0.69					
5m	9 Mar 2012	0.41	0.38	0.41	0.53	0.80	1			
5m	20 Mar 2012	0.45	0.47	0.40	0.52	0.79	0.77	1		
5m	10 Jan 2013	0.78	0.73	0.44	0.51	0.44	0.38	0.41	1	
5m	DTM	0.67	0.57	0.30	0.38	0.33	0.28	0.30	0.65	1
15m	2 Feb 2011	1								
15m	1 Mar 2011	0.98	1.00							
15m	11 Jan 2012	0.66	0.65	1						
15m	13 Feb 2012	0.70	0.68	0.77	1					
15m	4 Mar 2012	0.68	0.67	0.80	0.88					
15m	9 Mar 2012	0.68	0.67	0.74	0.80	0.96	1			
15m	20 Mar 2012	0.67	0.67	0.72	0.77	0.94	0.97	1		
15m	10 Jan 2013	0.94	0.93	0.75	0.75	0.74	0.72	0.70	1	
15m	DTM	0.85	0.82	0.63	0.68	0.65	0.63	0.62	0.89	1
25m	2 Feb 2011	1								
25m	1 Mar 2011	0.99	1.00							
25m	11 Jan 2012	0.81	0.80	1						
25m	13 Feb 2012	0.80	0.79	0.89	1					
25m	4 Mar 2012	0.80	0.79	0.91	0.94					
25m	9 Mar 2012	0.83	0.82	0.90	0.92	0.98	1			
25m	20 Mar 2012	0.79	0.79	0.86	0.88	0.97	0.99	1		
25m	10 Jan 2013	0.97	0.96	0.87	0.85	0.85	0.87	0.82	1	
25m	DTM	0.91	0.89	0.78	0.80	0.79	0.79	0.76	0.93	1

TABLE 4.5: Coefficient of determination (R^2) of surface roughness correlations in the CB1 and CB2 basins ($p < 0.0001$).

		Crêta Besse 1				Crêta Besse 2			
Scale	Date	8 Mar 2006	25 Jan 2009	8 Dec 2011	DTM	8 Mar 2006	25 Jan 2009	8 Dec 2011	DTM
5m	8 Mar 2006	1				1			
5m	25 Jan 2009	0.62	1			0.38	1		
5m	8 Dec 2011	0.49	0.65	1		0.31	0.33	1	
5m	DTM	0.39	0.43	0.73	1	0.10	0.23	0.43	1
15m	8 Mar 2006	1				1			
15m	25 Jan 2009	0.89	1			0.74	1		
15m	8 Dec 2011	0.84	0.84	1		0.67	0.64	1	
15m	DTM	0.78	0.76	0.93	1	0.36	0.43	0.72	1
25m	8 Mar 2006	1				1			
25m	25 Jan 2009	0.95	1			0.83	1		
25m	8 Dec 2011	0.92	0.89	1		0.81	0.74	1	
25m	DTM	0.88	0.84	0.97	1	0.53	0.53	0.79	1

4.3 Key findings

In this chapter, we have presented a method to quantify terrain smoothing based on a multi-scale roughness approach. This method allows us to link terrain smoothing to geomorphological parameters as the roughness estimates used in our study are based on changes in slope and aspect.

The analysis of three selected alpine basins suggests that, at basin scale, not only mean snow depth but also its variability drive the process of terrain smoothing. The multitemporal analysis in one basin reveals that the relation between terrain smoothing and snow depth parameters follows a power law, indicating that snowfalls at the beginning of the winter season are more efficient in eliminating terrain roughness than the snowfalls occurring later on in the season. On the other hand, however, a relationship between terrain smoothing and snow depth was not found at pixel level as geomorphology and snow depth of neighbouring pixels strongly influence surface roughness at a given point. Nonetheless, at coarser scales, winter terrain roughness can be derived, even at pixel level, from a summer DTM, utilising a simple smoothing factor as the relationship between terrain and snow surface roughness is strongly linear. At finer scales, snow surface roughness decorrelates stronger from terrain roughness and the summer DTM is no longer representative for the winter surface. In this case, the representation of a winter terrain can be significantly improved by the acquisition of a winter DSM with similar or less snow depth as it captures site-specific and persistent effects of wind–terrain interaction on snow depth distribution.

The persistent patterns of winter surface roughness appear to be well suited to defining potential avalanche release areas. In chapter 5, therefore, we will evaluate the influence of surface roughness– more specifically, that of the winter terrain – on avalanche release area size and location.

Chapter 5

Terrain smoothing and its relation to avalanche release area size and location

In chapter 4 we showed that the surface roughness of a winter terrain, besides being significantly smoother than its underlying summer terrain, is, to some degree, persistent in between winter seasons for scales larger than the size of drift features, such as dunes or cornices. This finding allows us to systematically integrate this effect into release area definition procedures; however in order to make this approach amenable, the significance of surface roughness for release area size and location must first be explored. The literature (e.g. Mott et al. (2010); Simenhois and Birkeland (2008); Schweizer et al. (2003)) clearly pointed out that increasingly homogeneous snow deposition patterns, due to terrain smoothing, favour weak layer and slab homogeneity, which might ultimately increase potential size of slab avalanches. This raises the question as to whether a homogeneous terrain surface is more favourable in terms of producing larger avalanche release areas than an irregular one. In order to test this hypothesis, the relation between surface roughness of summer and winter terrain and release area properties is investigated using a set of artificially triggered avalanches at the Vallée de la Sionne fieldsite. We further evaluate the potential of surface roughness to define the observed release area sizes in the experiments.

Finally, the effect of a smoothed winter terrain on potential release area size is assessed using 30 years of observation resulting in more than 2200 recorded avalanches in the region of Zuoz, Switzerland. This chapter is partly based on a conference contribution to the International Snow Science Workshop in Grenoble, France, October 7- 11, 2013.

Veitinger, J.; Sovilla, B.; Purves, R.S., 2013: Winter terrain roughness as a new parameter to define size and location of avalanche release areas. In: Naaim-Bouvet, F.; Durand, Y. ; Lambert, R. (eds) International Snow Science Workshop 2013, October, 2013 7th-11th. Proceedings. ISSW 2013. Grenoble - Chamonix Mont Blanc. Grenoble, ANENA. 703-706.

5.1 Surface roughness and avalanche release areas: Case study Vallée de la Sionne

In this section we analyse the roughness of terrain, bed surface and snow surface of the artificially triggered avalanches in the Vallée de la Sionne. We further compare surface roughness with measured slab properties, such as slab thickness and its variability. We use the original 0.5 m resolution to analyse the very fine scale roughness.

5.1.1 Relating surface roughness to release area properties

In order to analyse the relation between release area properties (size, slab thickness, slab variability) and surface roughness, the set of artificially triggered avalanches in the Vallée de la Sionne (section 3.2.1) is used. In a first step, the relation between slab thickness, slab variability (standard deviation of slab thickness) and release area size (Fig. 5.1) was explored.

Slab thickness is approximately 1.5 m, except for avalanches #1 and #4, which show slightly greater mean slab thickness. With regard to the slab variability, at first view we recognise only little relation between slab variability and release area size: the largest avalanche has a more homogeneous slab than all others, whilst the smallest slab release is characterised by the highest slab variability. However, as mentioned in section 3.2.1, avalanches #1 and #2 eroded in deeper layers of the snowpack, therefore increasing slab variability. This could explain the increasing slab variability compared with the smaller release areas #3 and #5.

In a second step, the release area size was analysed as a function of roughness of the summer terrain, roughness of the bed surface, and roughness of the snow surface prior to avalanche release (Fig. 5.2). Two different scales are shown– 1.5 m and 6.5 m. We observe that the roughness of the bed surface is generally less rough when compared with the underlying terrain. At the same time, the snow surface prior to avalanche release is always smoother than the underlying bed surface (and the terrain). This nicely illustrates the progressive terrain smoothing within avalanche release areas. The results

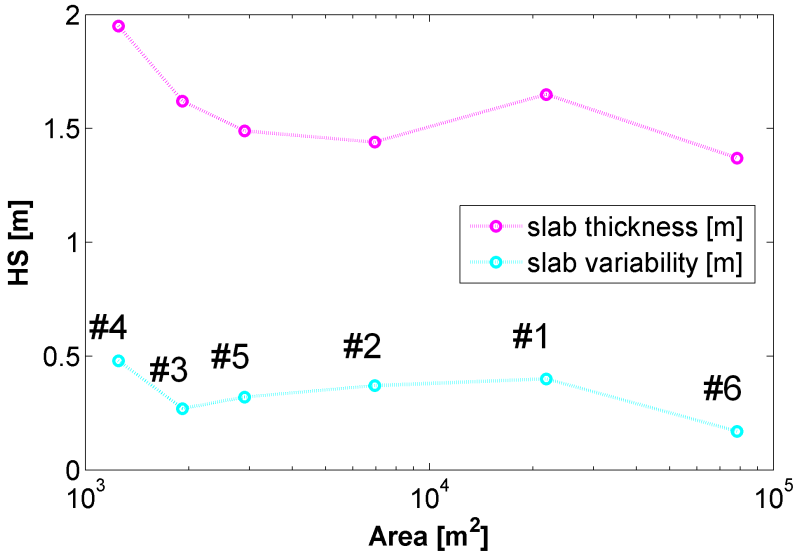

FIGURE 5.1: Release area size as a function of slab thickness and slab variability. Numbers of avalanches are marked according to Fig. 3.7.

further show a clear trend of decreasing roughness with increasing release area size. One exception is terrain roughness at the 1.5 m scale, where no clear trend is observed. The comparison with snow surface roughness shows that, at fine scales, strong deviations from the summer terrain are possible, thus indicating that bed surface roughness is independent from those of its underlying terrain. This suggests that fine scale terrain features are not relevant in this snow situation; However, it might be highly relevant for early winter situations or ground avalanches.

We further observe that snow surface roughness prior to avalanche release is almost equal for the three largest avalanches, suggesting that terrain smoothing is limited to a certain minimum value where no more smoothing occurs– even with additional snow. Further, if the difference of surface roughness between snow surface and sliding surface is relatively small, it can be assumed that maximum smoothing has already been reached prior to the last snowfall. This can be effectively seen when compared with the corresponding slab variability. For example, avalanche #6, with the smallest difference between roughness (at a 1.5 m scale) of the bed surface and the snow surface also reveals the most homogeneous slab thickness. This suggests that smooth terrain surfaces (or smoothed-out winter terrain surfaces) more likely form homogeneous slabs, which are more prone to producing large avalanche releases.

It is evident that the limited number of avalanches observed at only one given day at a single fieldsite is far from being generally conclusive; further studies are needed, involving different terrain types or snow climates. Further, the results are only representative for

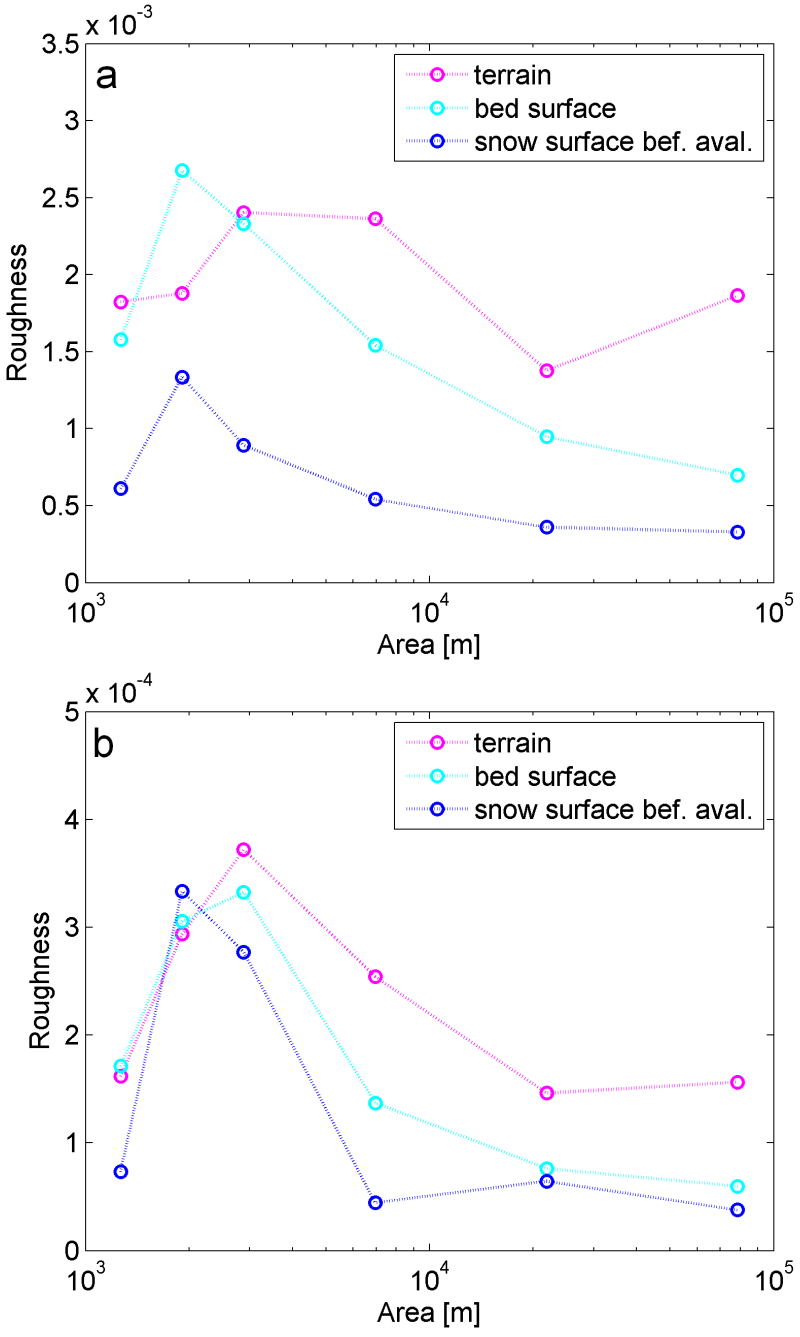

FIGURE 5.2: Release area size as a function of summer and winter terrain roughness for a scale of (**a**) 1.5 m and (**b**) 6.5 m.

artificially released avalanches. Nonetheless, they clearly support the link between slab homogeneity and the underlying (winter) terrain and, as a consequence, the size of avalanche release areas.

5.1.2 Surface roughness as a new parameter to define size and location of avalanche release areas

The previous section revealed the potential link between surface roughness and the size of a release area. However, the previous analysis was only based on statistical values of release area properties, such as mean surface roughness; however the spatial distribution of the single parameters was not considered. Accordingly, in this section, the spatial organisation of winter terrain roughness is compared to the summer terrain. The hypothesis we want to put forward is that the areas of low surface roughness may be generally more favourable for avalanche release of larger avalanches than regions with high surface roughness. With increasing snow depth, we expect clusters with low surface roughness to connect, thus allowing the formation of potentially larger release areas.

Methodological approach

The elevation models of winter and summer terrain, performed by airborne LIDAR at the Vallée de la Sionne test site, are again utilised. As we have seen in the previous section, the very fine scale roughness (0.5 m resolution) may not be very representative for the snow cover scenario of 8 March 2006; therefore, we chose a resolution of 2 m and calculated roughness at a scale of 6 m (3x3 kernel window for slope and aspect). We evaluate the ability of winter terrain roughness to define size and location of avalanche release areas by comparing clusters of low surface roughness to the measured release zones of 8 March 2006. As artificial avalanche release was performed near the main ridge of the slope, we restrict our analysis to the upper part of the slope. Lower release areas within the same slope can be neglected, as they were part of the avalanche track from the avalanches releasing above.

When analysing whether clusters of low surface roughness are suitable in terms of defining potential release areas, we need to have an idea of typical roughness values of a bed surface from real slab avalanches; therefore the mean bed surface roughness of all observed avalanches was calculated. The mean roughness of the bed surfaces ranged from 0.00025 up to 0.0015. The higher values were generally observed in the smaller release zones. In a next step, both summer and winter terrains were classified into Potential Release Area (PRA) and No Potential Release Area (nPRA). In order to discriminate between the two, a threshold of 0.001 was selected, corresponding roughly to the average upper limit for bed surface roughness in our field data. We assigned all pixels exceeding the threshold of 0.001 to the class nPRA, whilst values equal to or smaller than the threshold were assigned to the class PRA.

Results

Figure 5.3 shows roughness at a scale of 6 m for a winter and a summer terrain. In agreement with the results of chapter 4, we observe that the winter terrain is generally smoother. Roughness due to single rocks is smoothed out, whilst the larger structures persist. We further observe that larger areas of low roughness evolve.

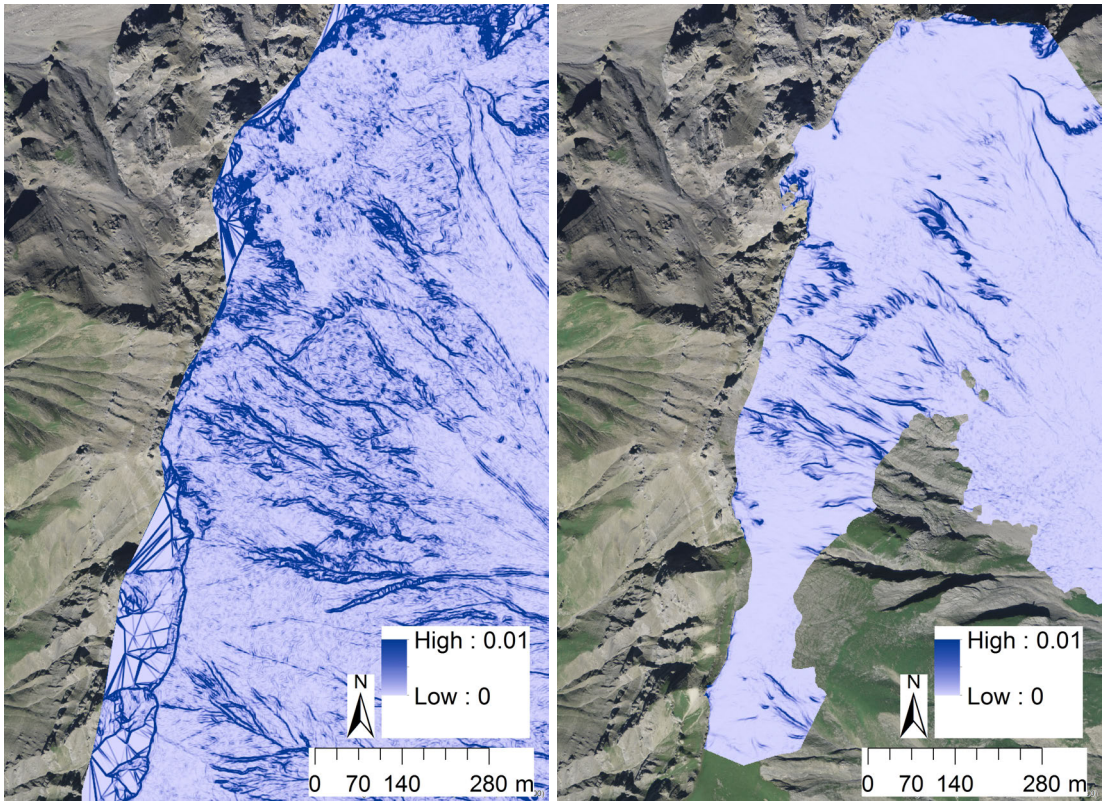

FIGURE 5.3: Surface roughness at a scale of 6 m of (**a**) the summer terrain and (**b**) the winter terrain for the snow distribution of 8 March 2006.

Figure 5.4 provides an example of the PRA classification for the winter terrain surface of 8 March 2006 and the summer terrain. We clearly identify significant differences between winter and summer terrain. The area classified as PRA is significantly larger in the winter terrain than in the summer terrain.

We further observe that numerous clusters of small patches of low terrain roughness are connected and form larger, continuous areas in the winter terrain. These larger areas correspond qualitatively well to the avalanche release zones observed. The majority of the observed release zones are classified as potential release areas– especially for the area in the vicinity of the crown. Lateral boundaries of the slab are often well reproduced, therefore suggesting that changes of morphology might play an important role in the definition of release area size; however, in the case of avalanches #1 and #2, surface roughness cannot explain the separation into two different release areas; rather,

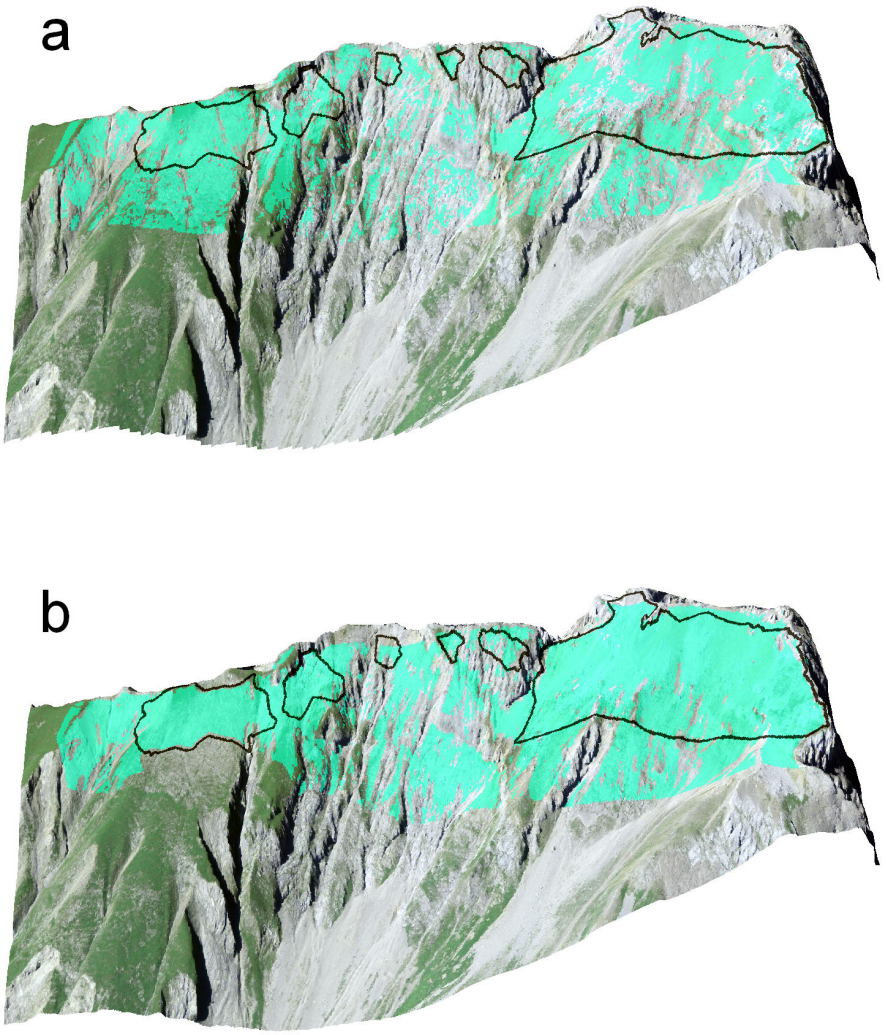

FIGURE 5.4: PRA derived from (**a**) a summer and (**b**) a winter terrain. PRA was derived from 2 m resolution grids at a scale of 6 m. A threshold of 0.001 was applied to separate the class PRA from the class nPRA. In black the boundaries of the slab releases of the artificially triggered avalanches on 08 March 2006.

it would suggest one continuous release area. As shown in section 3.2.1, avalanche #1 was remotely triggered by avalanche #2. This indicates that the fracture could propagate between #1 and #2, but did not lead to a release of the area in between, suggesting that the snowpack was partly more stable in this area. This underlines the fact that snow cover properties play a major role in the actual size and location of avalanche release areas, which may strongly differ from the potential release area size. Nevertheless, the fact that avalanches #1 and #2 almost simultaneously released, ultimately supports the PRA results obtained from surface roughness, suggesting one single continuous avalanche.

Lower parts of the release area are less well reproduced, which may be partly explained by the difficulty in identifying the stauchwall – especially for the small avalanches with little fracture propagation; therefore, parts of the avalanche track might have been erroneously integrated in the release area; alternatively, parts of the release area might have been defined as avalanche track.

In order to quantitatively confirm the improved classification result using winter terrain roughness, the Jaccard Index was calculated, as defined in section 2.5.3.

TABLE 5.1: Jaccard index between the classified PRA area and the observed release areas.

Reference dataset	Jaccard index
Terrain roughness, scale = 6 m	0.47
Snow surface roughness, scale = 6 m	0.63

Table 6.1 shows the Jaccard index for summer and winter terrain roughness. The Jaccard index of winter terrain roughness increases from 0.47 to 0.63 if compared to summer terrain roughness calculated at a scale of 6 m. This clearly indicates that winter terrain can reproduce release area size and location to a much better extent than the summer terrain; however, as the same data is used for training (threshold determination) and for classification purposes, an independent validation will be provided within the framework of the release area algorithm detailed in chapter 6.

5.2 Terrain smoothing and release area size: Case study Zuoz

Despite the encouraging results from the analysed avalanches in the Vallée de la Sionne test site, highlighting the important effect that terrain smoothing could have on potential release area size, they do not give evidence as to whether the terrain (and its modified winter terrain) is effectively the determining factor for the avalanche sizes observed. Most often, only parts of the potential release area effectively release, depending on snowpack or meteorological parameters. Many more case studies with, comprising detailed snow data and observed avalanches, would be necessary in order to draw robust conclusions about the influence of single factors, such as terrain; however, such detailed data is generally not available, and other strategies have to be developed to address the effect of terrain smoothing on release area size.

However, long-term avalanche documentation exists in Switzerland, where avalanches are continuously mapped providing solid databases of often several thousand avalanches. Although detailed snow cover distribution (e.g. through laser scanning) is not available,

manual snow depth measurements or measurements from automatic weather stations still provide general information concerning the snow cover situation. This snow cover information can also be linked to avalanche release area size.

Therefore, in this section, the avalanche database of the area of Zuoz– notably containing more than 2200 documented avalanche events– is exploited, spanning across 30 years of observation (Stoffel et al., 1998).

5.2.1 Release area size and snow depth: A statistical analysis

In the database of Zuoz, the overall snow depth, as well as new snow depth, is available for every day of the 30 –year observation period. The possibility of a relationship between the size of the release area and the snow depth measurements in the area is examined. Hereby, we assume that a greater snow depth value is related to higher terrain smoothing. Snow depth at the day of avalanche release is compared with the release area size. Size, in this case, corresponds to the maximum width of the avalanche release area. In the case where the day of avalanche release was unknown, the day of observation was used. In an effort to link the degree of terrain smoothing to the observed avalanche size, the avalanches are divided into three groups depending on snow depth. As snow depth at the valley bottom over the 30 years varies between 0 and 120 cm, thresholds of 35 cm and 70 cm, respectively, are manually selected for the partitioning of the groups.

Figure 5.5 shows boxplots of the release area sizes as a function of snow depth at the day of avalanche occurrence. We observe that each class shows very large dispersion of observed release area widths. This corresponds with the behaviour we observe in reality, where only parts of the potential release area do effectively release. Further, we observe only a small increase of median avalanche size with snow depth. Nonetheless, due to the large number of avalanches, a statistically significant difference ($p < 0.001$, one way ANOVA) between the three classes is identified.

As new snow depth in Zuoz at times of avalanche release never exceeded 120 cm, new snow depth can potentially exceed old snow thickness in case of very intense snowfall events. In such cases, large overall snow depth would rather indicate important slab thickness than the degree of terrain smoothing of the bed surface prior to the loading of the slope. To ensure that important new snow depths do not bias the results, the snow depth classification was carried out using the snow depth 3 days prior to the avalanche event (Fig. 5.6). The three thresholds were adapted to < 25 cm, 25 cm - 50 cm and $>$ 50 cm. Likewise, the results show a statistically significant difference between the three classes ($p < 0.001$, one way ANOVA).

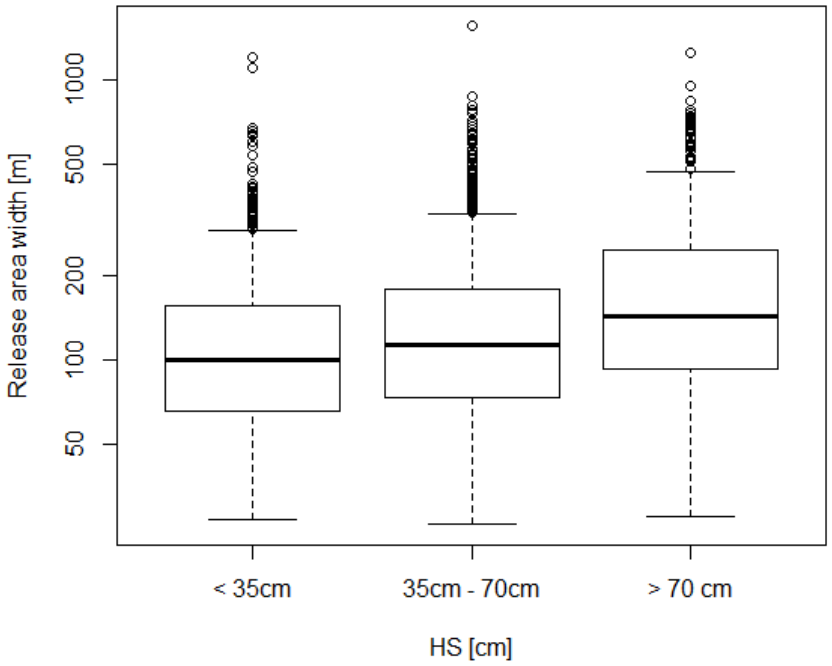

FIGURE 5.5: Release area width as a function of snow depth at the day of avalanche release in the region of Zuoz, Switzerland.

This shows that new snow depth, despite being the driving factor for avalanche release in many cases, cannot solely explain the differences in release area width. The results rather suggest that larger overall snow depths, prior to the loading of the slope, lead to an increasing amount of larger release zones. As a deeper snowpack generally produces more smoothing than a shallow one, this supports the hypothesis that a smoothed terrain is more favourable for larger release areas.

So far, the statistical analysis has been performed for all avalanches in the region of Zuoz, comprising different sized avalanche paths with different snow climatological conditions and terrain characteristics, such as exposition or slope. However, the distribution of avalanche release sizes is most meaningful when compared only within single avalanche paths, as release area width is strongly controlled by the terrain of the single avalanche path. In the next section, the relation between snow depth, new snow depth and release area size in selected avalanche paths is compared.

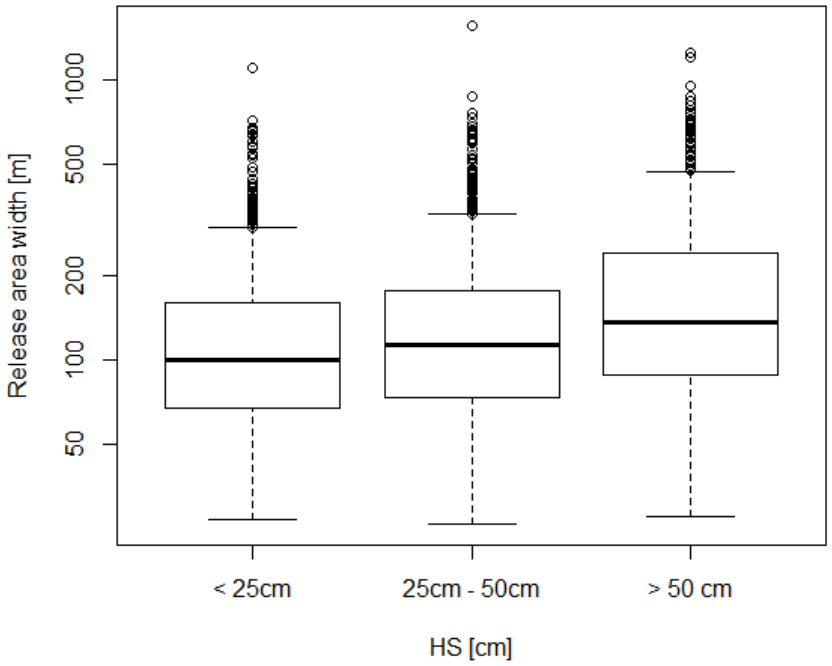

FIGURE 5.6: Release area width as a function of snow depth 3 days prior to avalanche release in the region of Zuoz, Switzerland.

5.2.2 Release area size as a function of snow depth and avalanche type within single avalanche paths

Three documented avalanche paths in the region of Zuoz, namely Val Buera and Val d'Urezza north of Zuoz (Fig. 5.7), were selected, all of which are controlled by artificial avalanche release and Munt Müsella south of Zuoz (Fig. 3.13).

The width of the release area was compared to snow depth, new snow depth and the 3– day new snow sum at the given avalanche day. Further, the avalanches were classified into different categories. First, we distinguish the release type, namely artificial release (explosives), skier or animal– triggered avalanches and natural release. Second, we distinguish between surface slabs (new snow, blown snow or persistent old snow layers) and slabs, which released near the ground (persistent weak layers close to ground or deep slabs).

Figure 5.8, Figure 5.9 and Figure 5.10 show release area width as a function of snow depth at the day of avalanche release, the 24-hour new snow depth and the 3– day new sum, prior to the day of avalanche release.

FIGURE 5.7: The two avalanche paths (**a**) Val Buera and (**b**) Val d'Urezza in the region of Zuoz, Switzerland.

In all three avalanche paths, a relation with snow depth and release area size can be observed. Whereas small release area widths (< 200 m) occurred within the whole range of overall snow depth, very large release areas (width > 600 m) mainly occured when snow depth in the valley was at least 50 cm. At the same time, 24-hour and 3–day new snow depth prior to new snow depth showed only little relation with observed avalanche size. It is rather the case that new snow, in combination with large overall snow depth, produced larger avalanches than with little overall snow depth. This finding is an indicator that terrain smoothing favours the formation of larger avalanche release areas.

However, some exceptions of this behaviour are observed, where large avalanches occurred with significant less overall snow depth. Interestingly, those avalanches did all naturally release (except one, which was remotely triggered by a skier) at weak layers near ground or very late in the season. Furthermore, 24-hour new snow depth is generally small (< 10 cm) for this type of avalanche, which might indicate that very unfavourable snowpack conditions, such as depth hoar layers, which are commonly observed in shallow snowpacks, are the reason for the large release areas. Moreover, deep slabs are, on average, larger than the surface slab avalanches –despite being less frequent. As an example, the largest avalanches in Val d'Urezza avalanche path were both deep slabs occurring at an only medium snow depth of 60 cm. This indicates that snowpack conditions are an equally important factor for avalanche release area size. In case of the late season

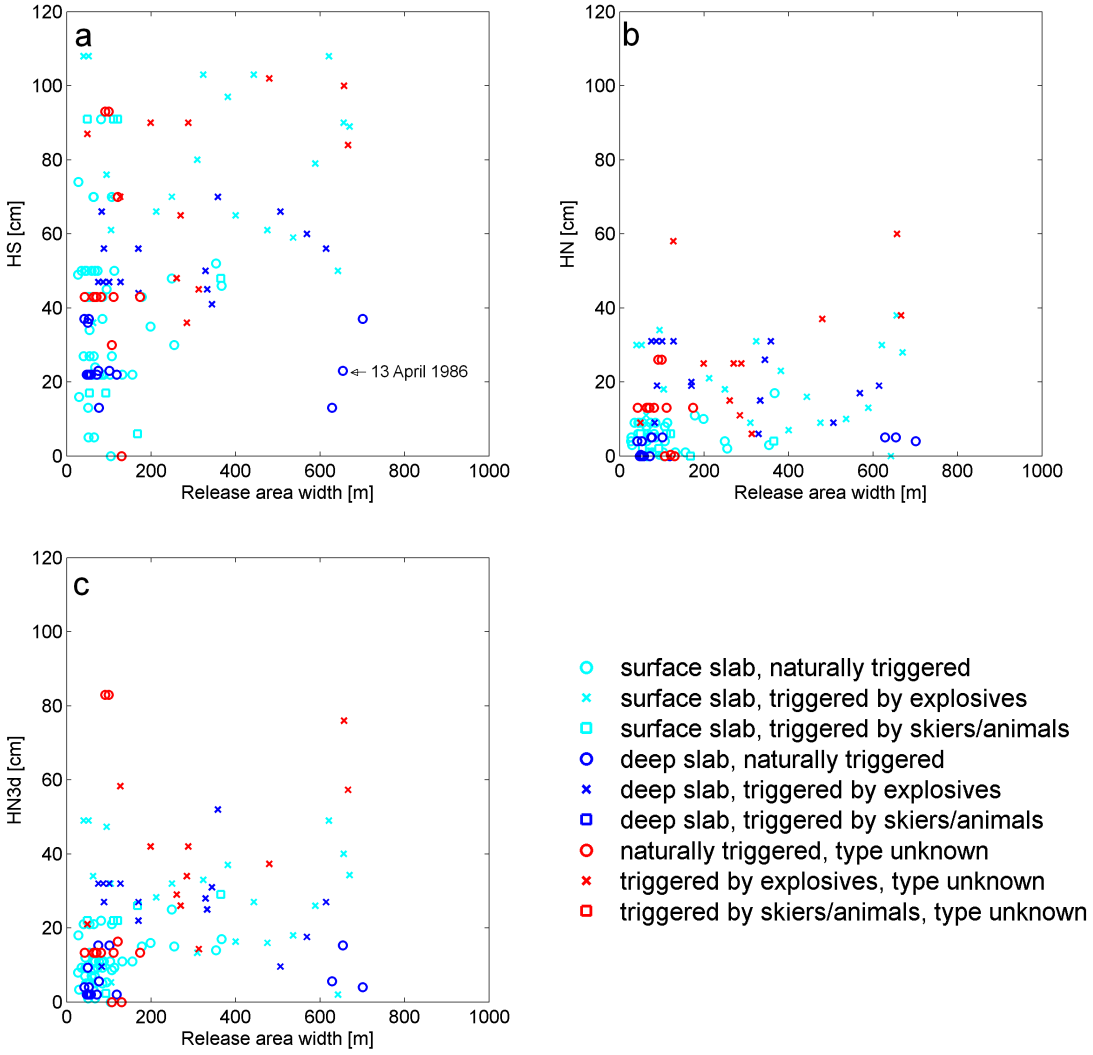

FIGURE 5.8: Release area width as a function of (**a**) snow depth at time of avalanche release, (**b**) the 24-hour new snow depth at the day of avalanche release and (**c**) the 3 –day new snow sum at the day of avalanche release in the Val Buera avalanche path.

avalanches (we marked the dates of avalanches occurring later than March), snow depth in the valley might underestimate the mountain snow cover, as the melting season had already started at lower elevations. Therefore, those avalanches probably occurred in a deeper snowpack than indicated by the measurement in the valley.

We further observe that artificially triggered avalanches are mostly surface slabs with a greater proportion of large release areas compared to naturally released ones. This finding reflects the fact that avalanche control is normally executed in critical situations, such as where large avalanches are expected. Although in some cases artificial avalanches where triggered without previous snowfall (snow drift or spring situation), a significant minimum new snowfall ($> 10\,\text{cm}$) was mostly observed at times of artificial avalanche

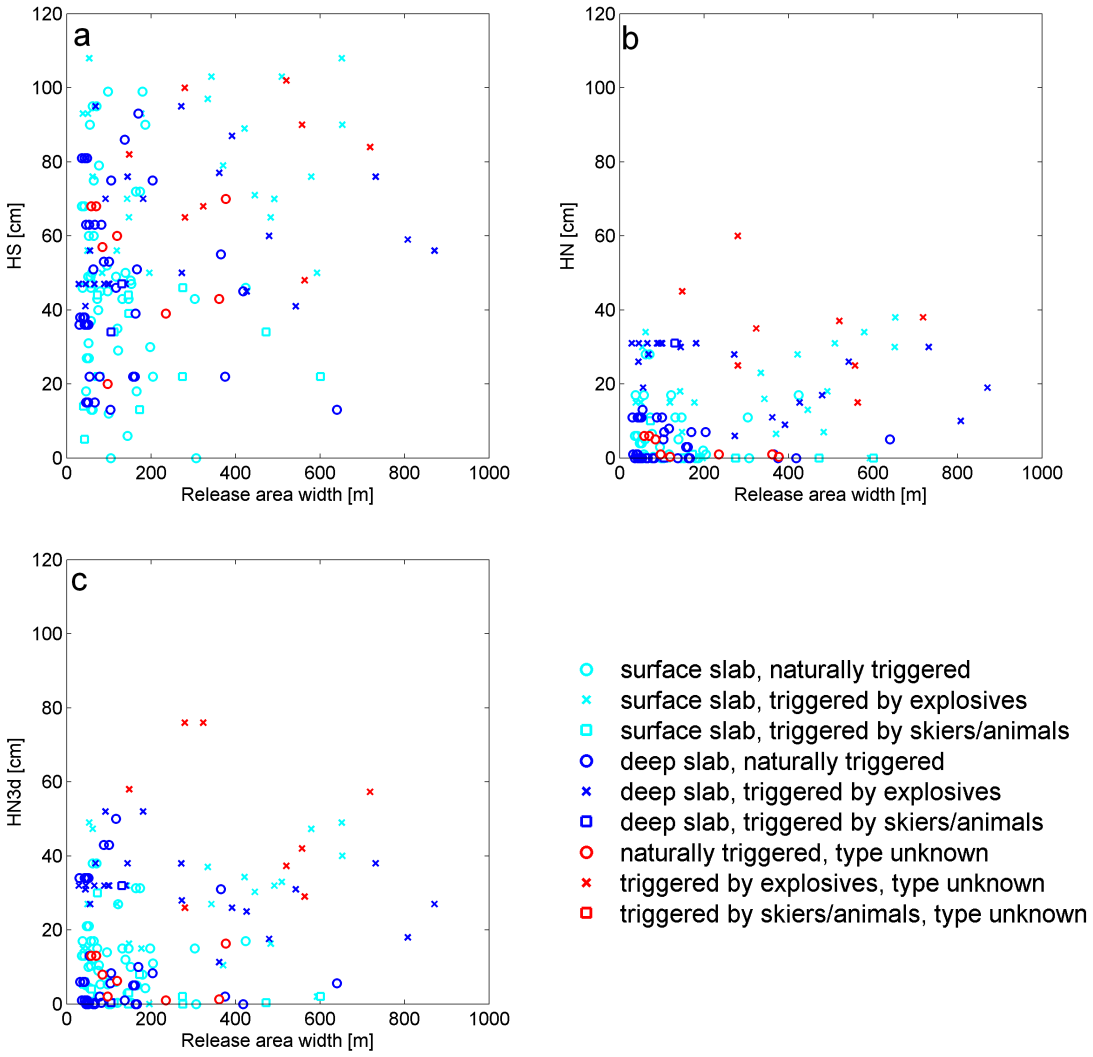

FIGURE 5.9: Release area width as a function of (**a**) snow depth at time of avalanche release, (**b**) the 24-hour new snow depth at the day of avalanche release and (**c**) the 3–day new snow sum at the day of avalanche release in the Val d'Urezza avalanche path.

release (most probably because new snow depth served as an important criterion to execute avalanche control). However, the amount of new snow did not show a relation to the observed avalanche release area size. Again, overall snow depth was more decisive in predetermining the potential release area size.

Finally, we stress that the snow depth values mentioned in this analysis should only be considered as rough indicators of the snow conditions in the avalanche paths. We are aware that point measurements at the valley bottom are not fully representative of snow conditions in a high altitude slope, where local conditions might strongly deviate from the valley. Nevertheless, due to the high elevation of the measurement station, normally, no extensive melting periods occur in high winter (December – March). Therefore, we

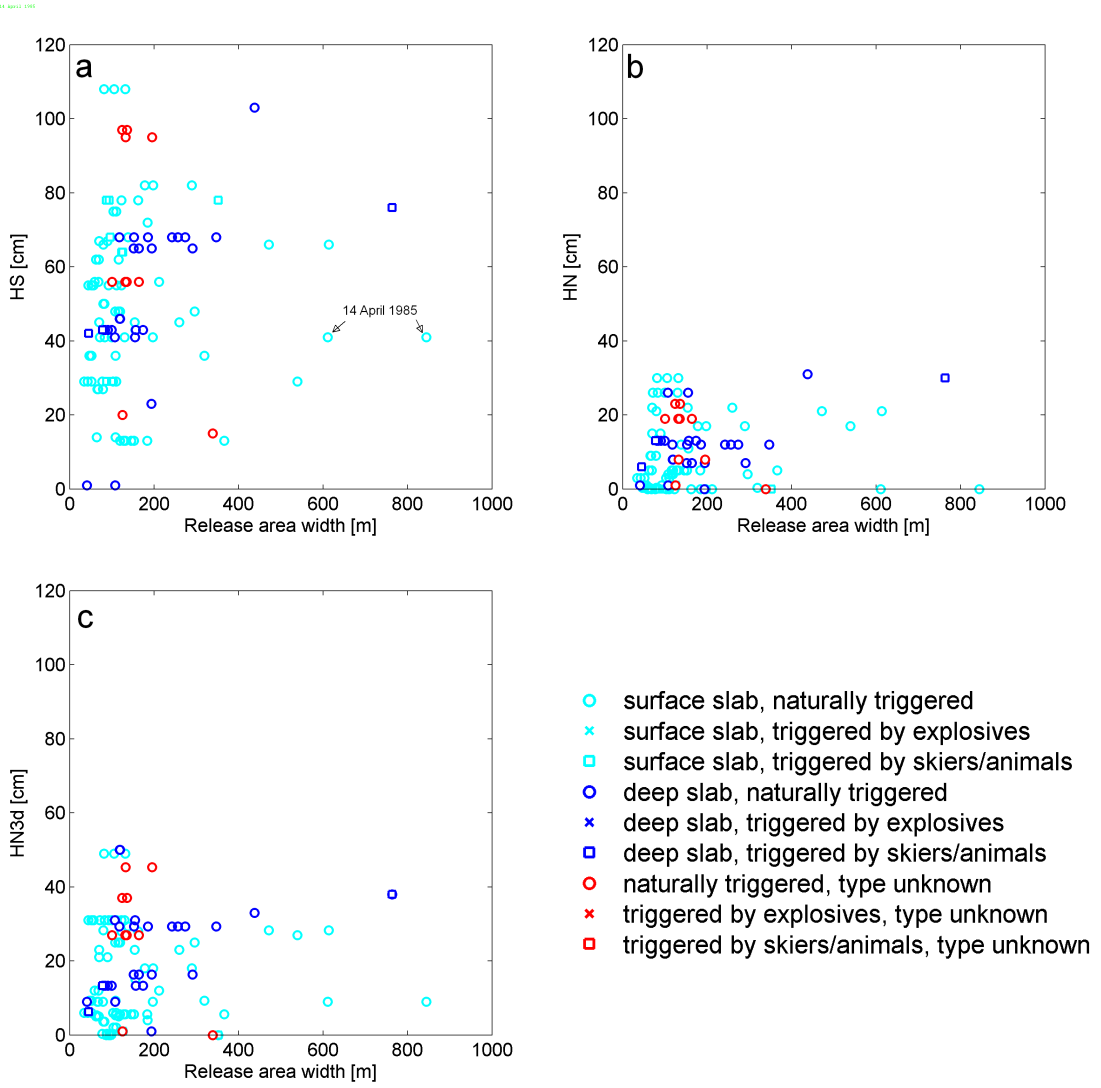

FIGURE 5.10: Release area width as a function of (**a**) snow depth at time of avalanche release, (**b**) the 24-hour new snow depth at the day of avalanche release and (**c**) the 3–day new snow sum at the day of avalanche release in the Munt Müsella avalanche path.

believe that measurements from the valley bottom remain a valid indicator of snow depth on the mountain. We further did not consider fracture depth in the analysis, which also influences potential release area size.

5.3 Key findings

The preliminary results from avalanche experiments in the Vallée de la Sionne highlight the potential relation between slab homogeneity, the underlying (winter) terrain and the size of an avalanche release area. They further show that the winter terrain surface can serve as a valuable input for the better definition of potential avalanche release areas.

Using a roughness parameter, we showed that the winter terrain can reproduce release area size and position to a much better extent than the summer terrain.

Comparing release area width with overall snow depth of more than 2200 avalanches in a 30– year observation period revealed statistically significant larger release area widths with greater snow depth for surface slab avalanches. Large release area sizes occurred mainly at a given minimum snow depth of approximately 50 cm, thus suggesting that greater terrain smoothing within deeper snowpacks may be an important factor for this behaviour.

However, large slabs were observed with significantly less overall snow depth in situations when persistent weak layers near the ground, such as depth hoar, were present. This suggests that the influence of terrain smoothing on release area size is not universal but rather is dependent on the type of avalanche. This is in accordance with observations in avalanche practice. Nevertheless, taking into account the morphological changes of the winter terrain into release area algorithms might be a significant step forwards in defining potential avalanche release zones as a function of the snow distribution.

Chapter 6

Slab avalanche release area estimation - a new GIS tool

In chapter 5, the potential of winter terrain roughness for the release area definition was highlighted. In this chapter, therefore, we present a new GIS tool for potential release area estimation, which integrates the surface morphology of a winter terrain. However, as the winter terrain in a given situation is rarely available, we develop in a first step a simple procedure centred on how to approximate snow surface roughness from a summer terrain. The resulting snow depth - dependent roughness parameter is then implemented into an algorithm for potential release area definition. We show, in detail, the design, modelling and the workflow of this algorithm and accordingly provide examples centred on how this tool could be used in practical applications.

This chapter is based on a conference contribution to the International Snow Science Workshop in Banff, Alberta, Canada, September 29 - October 3, 2014.

Veitinger, J.; Sovilla, B.; Purves, R.S., 2014: Slab avalanche release area estimation: A new GIS tool. Proceedings of the International Snow Science Workshop 2014, Banff, Alberta, Canada, September 29 - October 3

6.1 Roughness calculation based on quadratic modelling of the terrain surface

So far in this thesis, the ruggedness parameter of Sappington et al. (2007) was used to calculate roughness. The scale of roughness calculations was accounted for by varying the size of the kernel window. This method, although capturing the multi-scale behaviour of

terrain smoothing, has some limitations, as illustrated in the following figure. Figure 6.1 provides a comparison of terrain roughness and snow surface roughness at scales of 5 m 15 m and 25 m. It can be observed that very large window sizes produce significant blurring effects. As an example, the large gullies in the area of CB1 (black circles) are represented much larger at a 25 m scale than at a scale of 5 m. Second, fine-scale roughness, such as small rocks (red circles), still influence roughness calculations at larger scales in the case of terrain roughness. However, it can be observed that, in the winter terrain, these features are cancelled out by snow.
One possible explanation for this behaviour is that, even for coarser scales, estimates of slope and aspect are calculated in a 3x3 kernel window for every grid cell, thus calculating local changes of these variables. In order to realistically represent the effect of terrain smoothing, a roughness measure should take into account terrain features at a given scale whilst at the same time filter out smaller scale features.

One solution to overcome this limitation is adapting slope and aspect to scale. This can be achieved through the multi-scale definition of Wood (1996), as presented in section 2.4.2. This definition allows the derivation of slope and aspect estimates for different scales by fitting the trend surface over any arbitrarily sized neighbourhood window; therefore, we define a new enhanced multi-scale roughness (ERM) measure, which modifies the definition of scale used by Sappington et al. (2007).

Biquadratic polynomials of the form

$$z = ax^2 + by^2 + cxy + dx + ey + f, \tag{6.1}$$

where z corresponds to the elevation estimate at a point (x, y) and $a - -f$ are the coefficients that define the quadratic surface (Evans, 1980) are used as a basis for the computation of slope and aspect.

Direction (aspect) and magnitude (slope) of the steepest gradient at the central grid cell of the fitted surface is determined by calculating the rate of change in x and y direction:

$$\frac{\mathrm{d}z}{\mathrm{d}xy} = \left(\sqrt{\left(\frac{\mathrm{d}z}{\mathrm{d}x}\right)^2 + \left(\frac{\mathrm{d}z}{\mathrm{d}y}\right)^2} \right). \tag{6.2}$$

The partial derivatives for x and y are noted as:

$$\frac{\mathrm{d}z}{\mathrm{d}x} = 2ax + cy + d, \tag{6.3}$$

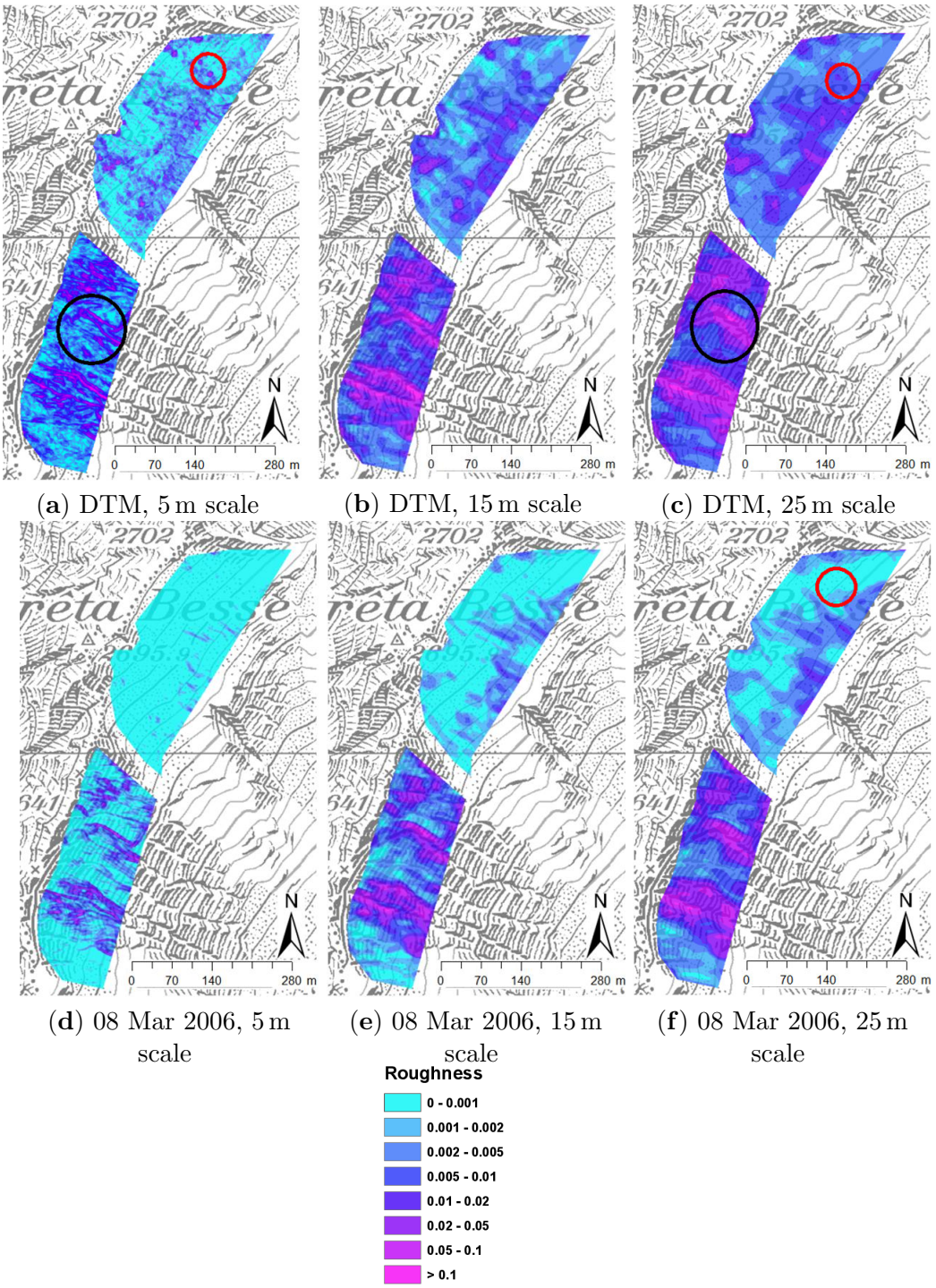

(**a**) DTM, 5 m scale (**b**) DTM, 15 m scale (**c**) DTM, 25 m scale

(**d**) 08 Mar 2006, 5 m scale (**e**) 08 Mar 2006, 15 m scale (**f**) 08 Mar 2006, 25 m scale

FIGURE 6.1: Surface roughness of (**a** – **c**) summer terrain and (**d** – **f**) winter terrain at a scale of 5 m, 15 m and 25 m in basins CB1 and CB2. Black circles show large gullies in CB1, red circles show single rock features in CB2. Pixmaps 2013 swisstopo (5704 000 000).

and

$$\frac{\mathrm{d}z}{\mathrm{d}y} = 2by + cx + e. \tag{6.4}$$

In order to obtain the parameter at the central point of the surface ($x = y = 0$), equations 6.3 and 6.4 are integrated into equation 6.2, and note:

$$\frac{\mathrm{d}z}{\mathrm{d}xy} = \sqrt{d^2 + e^2}. \tag{6.5}$$

Slope (α) is thus given as:

$$\alpha = \arctan\sqrt{d^2 + e^2}. \tag{6.6}$$

Likewise aspect is defined as

$$\beta = \arctan\frac{e}{d}.$$

Wood (1996), instead of taking into account only grid values within a 3x3 window, showed that one can fit the trend surface over any arbitrarily sized window. By this means, multi-scale slope and aspect calculations can be obtained. We use these new definitions of slope and aspect to derive multi-scale roughness. In contrast to the method of Sappington et al. (2007), we preserve a constant 3x3 kernel window to calculate roughness. Scale is accounted for by the size of the neighbourhood window used to compute slope and aspect. Scale is defined as the width of the kernel window.

Thus, the new roughness definition reads as follows:

Normal unit vectors of every grid cell of a digital elevation model (DEM) are decomposed into x, y and z components (Fig. 2.14):

$$z = 1 \cdot \cos(\alpha), \tag{6.8}$$

$$d_{xy} = 1 \cdot \sin(\alpha), \tag{6.9}$$

$$x = d_{xy} \cdot \cos(\beta), \tag{6.10}$$

$$y = d_{xy} \cdot \sin(\beta). \tag{6.11}$$

A resultant vector $|r|$ is then obtained for every pixel by summing up the single components of the centre pixel and its 8 neighbours using a moving window technique.

$$|r| = \sqrt{(\sum x)^2 + (\sum y)^2 + (\sum z)^2}, \tag{6.12}$$

as shown in Fig. 2.14b. The magnitude of the resultant vector is then normalised by the number of grid cells and subtracted from 1:

$$R = 1 - \frac{|r|}{9}, \tag{6.13}$$

where R is the vector ruggedness measure.

Figure 6.2 shows a comparison between the original method of Sappington et al. (2007) and the new enhanced multi-scale roughness (ERM) measure.

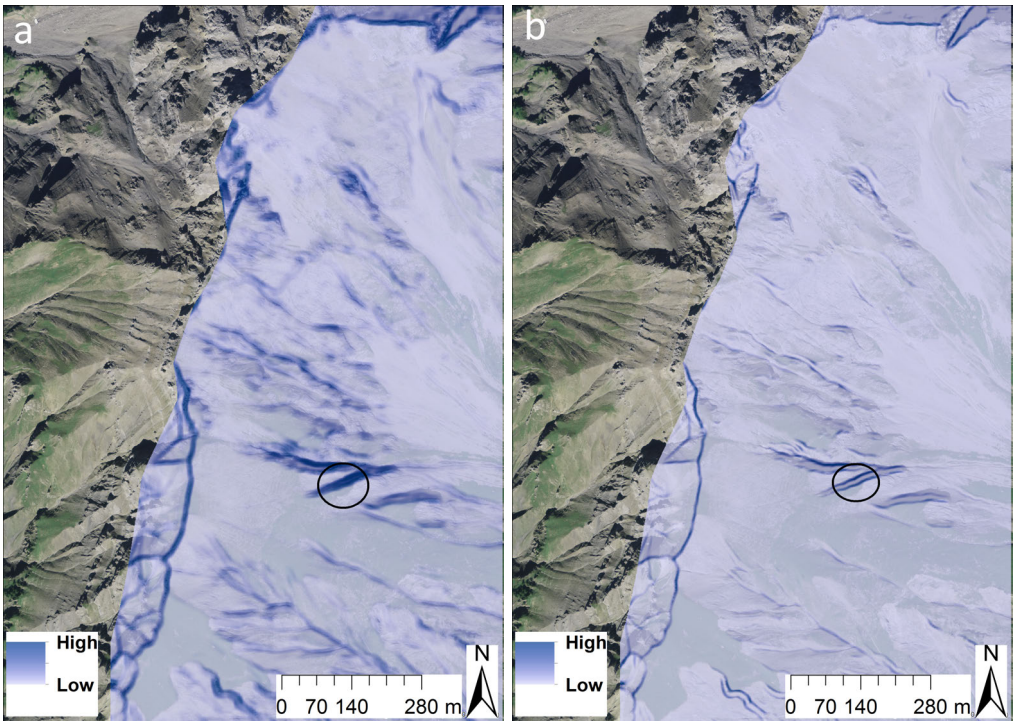

FIGURE 6.2: Terrain roughness calculated at a scale of 15 m with (**a**) the method of (Sappington et al., 2007) and (**b**) the new enhanced multi-scale roughness measure. Black circles show the large gully in the CB1 basin.

We observe that the new method produces a more crisp output, significantly reducing the blurring effects. As an example, it clearly distinguishes the two transitions of the gully flanks at the top and the bottom of the large gullies of CB1 (black circles). In contrast, the traditional method classifies the whole gully, including the even parts on the flanks between the top and bottom of the gully as rough. In our view, this behaviour more realistically approximates the smoothing effect of snow on terrain roughness. In the next chapter, we evaluate the extent to which this new measure is suitable for the modelling of the winter terrain.

6.2 Modeling of snow surface roughness from summer terrain

Chapter 4 shows that terrain smoothing processes are related to scale as a function of snow depth and snow depth variability. This relationship is used to evaluate whether we can relate the scale of terrain roughness to given snow cover scenarios; in other words, is there an optimal scale related to snow depth and its variability?

Methodological approach

We calculate roughness for all winter terrain surfaces of the Steintälli and the Vallée de la Sionne fieldsites using a window of 3x3 grid cells for slope and aspect. We use a basic resolution of 2 m for the elevation models in order to overcome the high variability for small scale winter terrain surface, such as local drift features. The scale, corresponding to a 3x3 grid cell window, is 6 m. Furthermore, we calculate terrain roughness for scales, ranging between 6 m and 26 m.

Following, we calculate the coefficient of correlation R^2 between the different terrain roughness surfaces to the 6 m - scale roughness snow cover scenarios. In addition, we calculate the ratio between modelled and measured surface roughness to determine whether the two measures produce similar absolute values.

In the last step, focus is directed towards the spatial organisation of the modelled snow surface roughness. We visually compare maps of modelled snow surface roughness with its corresponding measured winter terrain. We also evaluate how a modelled winter terrain performs to define potential release areas. In mind of this purpose, we apply the same approach as in section 5.1.2 in an effort to classify surface roughness into the classes PRA and nPRA. The classification result is evaluated using the Jaccard index (section 2.5.3), comparing the results using the measured winter terrain from section 5.1.2. Again, we only considered the upper release zones, where the avalanches were triggered and excluded the lower release areas.

Results

Figure 6.3 shows the correlation coefficient R^2 and the ratio between multi-scale terrain roughness and snow surface roughness for a rough terrain (CB1), a smooth terrain (CB2) and the intermediate ST basin. We observe that, for every snow depth distribution, maximum correlation exists. Moreover, the scale of maximum correlation (characteristic scale) is increasing with greater snow depth. In smooth terrain (CB2), the characteristic scale is generally larger (10 m – 18 m) than in rough terrain (CB1, 6 m – 10 m). Further, R^2 is generally lower in smooth terrain and decreases with increasing

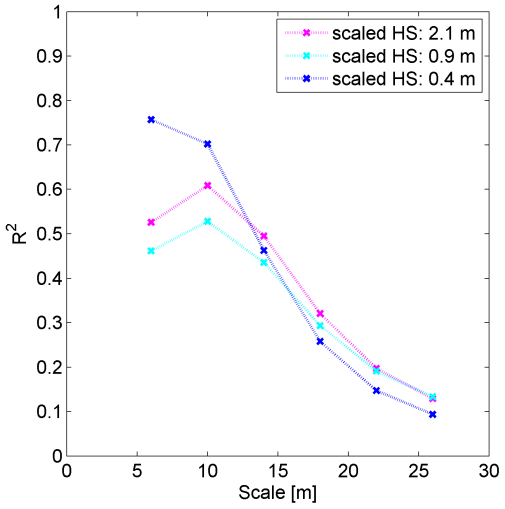

(**a**) R^2 in CB1

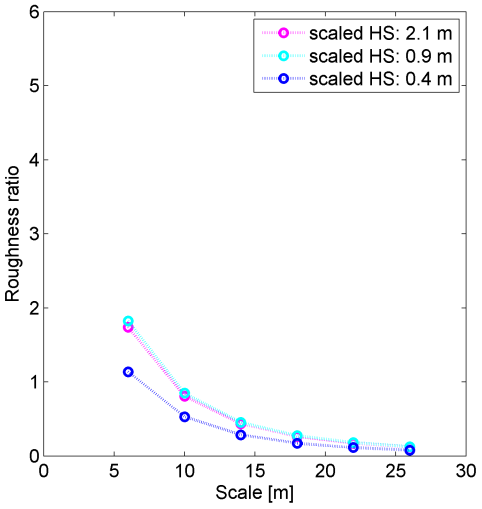

(**b**) roughness ratio, CB1

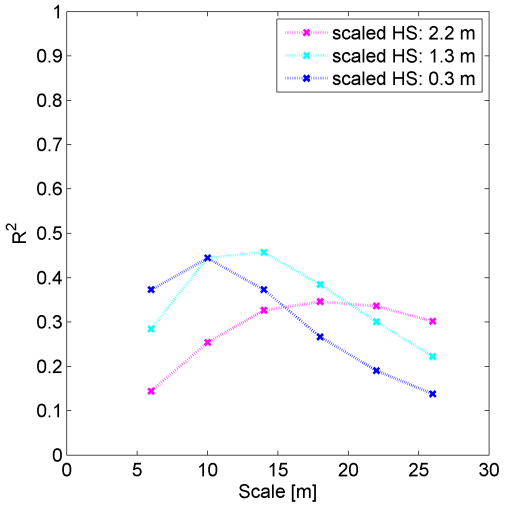

(**c**) R^2 in CB2

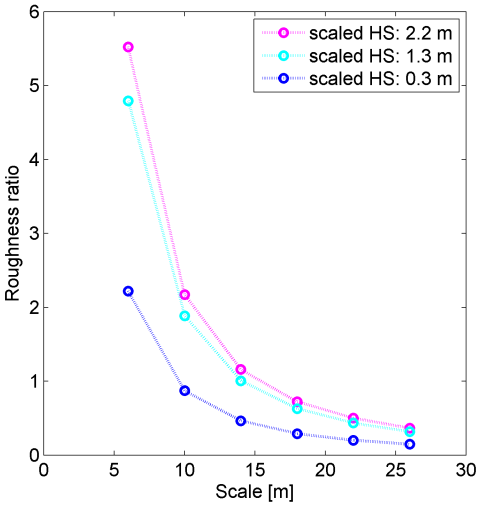

(**d**) roughness ratio, CB2

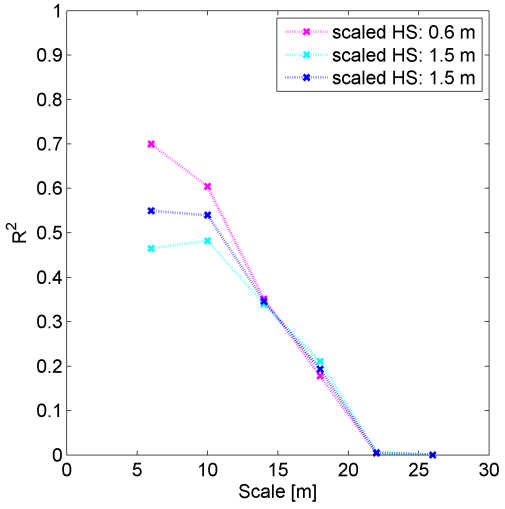

(**e**) R^2 in ST

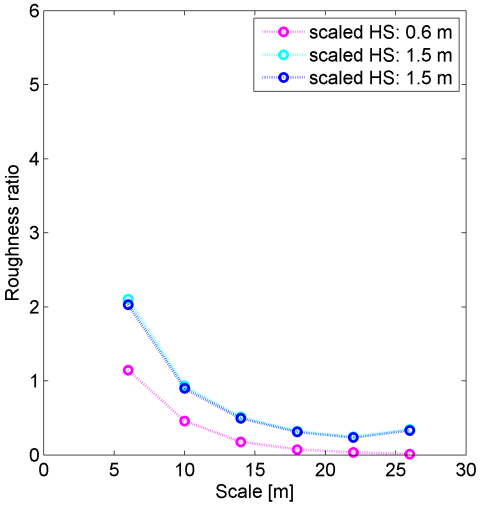

(**f**) roughness ratio, ST

FIGURE 6.3: Correlation of multi-scale terrain roughness with winter terrain roughness and ratio of mean winter terrain roughness and mean summer terrain roughness in the basins CB1 (**a**, **b**), CB2 (**c**, **d**) and ST (**e**, **f**). The three selected snow distributions for the basin ST are from 2 February 2011 (0.6 m), 11 January 2012 (1.5 m) and 20 March 2012 (1.5 m).

snow depth (distribution). This confirms the findings of chapter 4: in smooth terrain – and generally with a deeper snowpack – the snow surface becomes increasingly independent from its underlying terrain. Further, the roughness ratio at the characteristic scale is close to 1 (0.8 –1.2) for all snow distributions, indicating that the modelled winter terrain roughness produces reasonable approximations of the measured snow distributions. One exception is the snow distribution of 2.1 m in CB1, which shows a greater correlation with terrain than the snow distribution of 0.9 m. If we compare this with the roughness ratio, they produce a very similar smoothing degree. One possible explanation could be that, in very steep and rough terrain, such as CB1, the smoothing processes are limited to a certain level. Sluffing and avalanching might prevent the formation of a thicker snowpack and continuously redistribute snow from the steep flanks of gullies, downwards into the gully bottoms, preserving terrain roughness until the gullies are not fully filled with snow.

In an effort to illustrate the findings, the maps of modelled roughness were compared with the corresponding, measured winter terrain (Fig. 6.4).

By visual comparison, it can be observed that modelled winter terrain roughness reproduces remarkably well the measured snow surface roughness of the three snow cover scenarios. The cancelling out of finer scale terrain features in the models corresponds well to the situation in the snow covered terrain. Some differences can be observed in very steep regions, such as the very steep rockwall in the CB1 basin (black circles), where the modelled winter terrain overestimates the degree of smoothing. This can be explained by the steepness of the terrain ($> 50°$) where snow cannot accumulate and therefore smoothing due to snow does not occur. Therefore, this modelling procedure is only valid for steep terrain where snow is able to accumulate ($< 45°$).

In order to evaluate the performance of the modelled winter terrain for release area definition, it was compared with the measured winter terrain of 8 March 2006 (Figure 6.5).

We observe an almost identical classification result using the modelled winter terrain surface compared to the measured one. To confirm this qualitatively observed behaviour, we also calculated the Jaccard index between the classified PRA area and the observed release areas.

TABLE 6.1: Jaccard index between the classified PRA area and the observed release areas.

Reference dataset	Jaccard index
Terrain roughness, scale = 6 m	0.47
Modelled snow surface roughness	0.59
Measured snow surface roughness, scale = 6 m	0.63

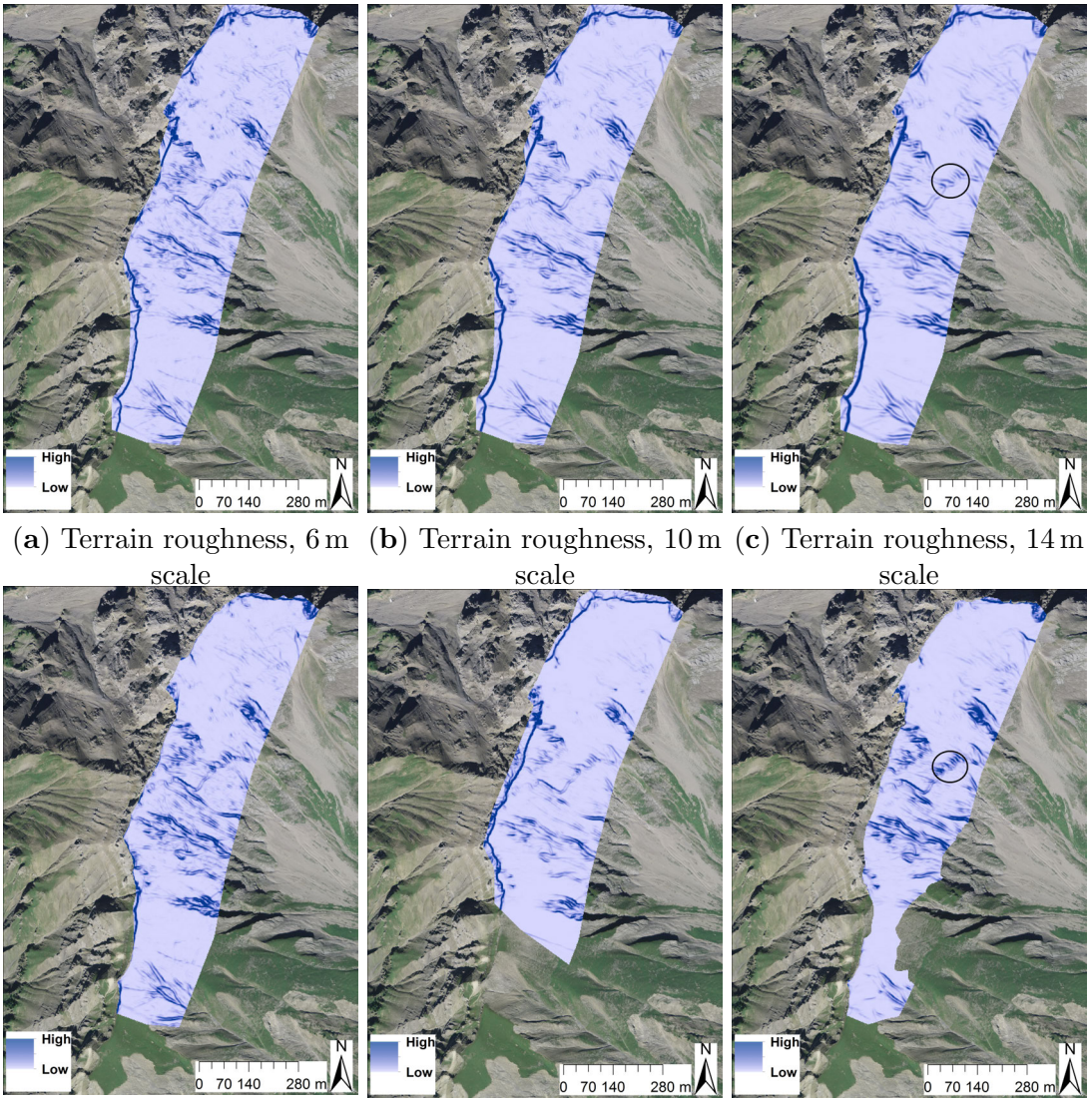

(**a**) Terrain roughness, 6 m scale (**b**) Terrain roughness, 10 m scale (**c**) Terrain roughness, 14 m scale

(**d**) Snow surface roughness, 8 Dec 2011 (**e**) Snow surface roughness, 25 Jan 2009 (**f**) Snow surface roughness, 8 Mar 2006

FIGURE 6.4: Terrain roughness at scales from 6 m to 14 m (**a** – **c**) compared to the corresponding snow cover situations (**d** –**f**). Black circles show the very steep rocky section in CB1.

Table 6.1 shows the Jaccard index for the measured and modelled snow surface roughness and terrain roughness. As already shown in section 5.1.2, the Jaccard index of measured winter terrain roughness increases from 0.47 to 0.63 when compared to summer terrain roughness, calculated at a scale of 6 m. However, when compared to modelled winter terrain roughness (which corresponds to summer terrain roughness at at a scale of 14 m), the Jaccard index is only slightly lower with a value of 0.59. This clearly shows that, if the scale of summer terrain is adapted to snow depth in the area, the quality of release zone estimation is almost as good as when using the measured winter terrain as a reference. This highlights the great potential of this simple procedure to be used for

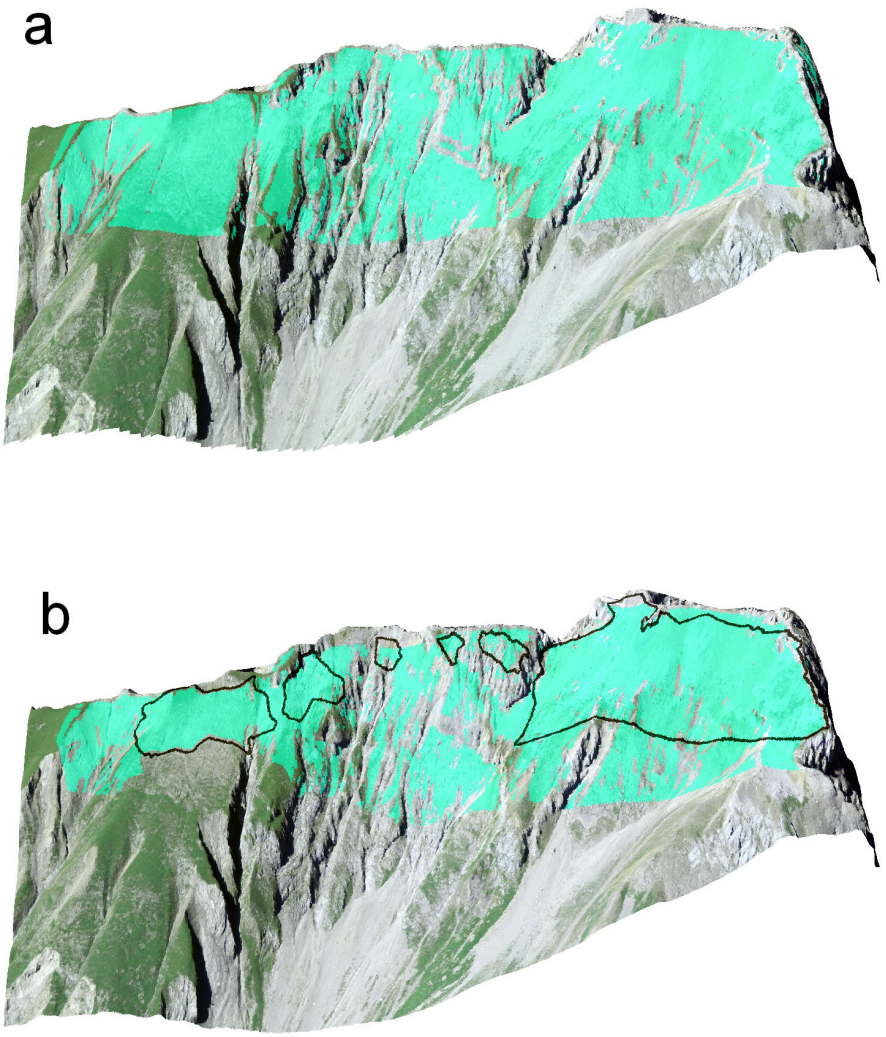

FIGURE 6.5: (**a**) PRA derived from modelled snow surface roughness representing a medium snow cover of 8 March 2006 (mean snow depth 2.9 m). (**b**) PRA derived from snow surface roughness calculated from measured snow surface of 08 March 2006. A threshold of 0.001 was applied to separate the class PRA from the class nPRA. In black the boundaries of the slab releases of the artificially triggered avalanches on 08 March 2006.

avalanche release definition.

In the next section we will implement winter terrain roughness into a new tool for release area estimation.

6.3 Algorithm for avalanche release area definition

In this chapter, the tool to define potential release areas is presented. It includes the snow depth dependent roughness parameter developed in the previous two paragraphs, and is completed by several other terrain parameters and a forest cover map. The framework is based on a fuzzy logic approach (section 2.5.2), assigning each pixel a membership grade to the class potential release area (PRA). We describe how the different terrain parameters are modelled form a fuzzy logic point of view and provide the reader with information about the process flow and the different calculation steps. We will further detail the required input data and discuss important settings. A main focus will be directed towards the validation of the algorithm, which also includes an example on the potential application of the tool in practice.

6.3.1 Fuzzy logic modelling of terrain variables

The design of current release area algorithms is mainly rule – based, considering expert knowledge and the past studies of topographical parameters of avalanche release areas. Due to the complexity of avalanche formation, it is very difficult to define precise rules, and expert decision– making still contains a significant degree of uncertainty. In order to deal with such imprecise data or diffuse rules, the fuzzy logic concept is well suited (section 2.5.2).

To define membership functions, bell shaped functions, defined by

$$\mu(x) = \frac{1}{1 + (\frac{x-c}{a})^{2b}}, \tag{6.14}$$

were selected and applied for the modelling of terrain parameters for potential release area (PRA) definition.

6.3.1.1 Slope

One of the most relevant terrain variables for the definition of avalanche starting zones is slope (Schweizer et al., 2003). Slope maps are regularly consulted in current avalanche hazard mapping practice as a basis for release area assessment. Slope values between 28° and 60° are considered potential release areas. The degree of membership $\mu_s(x)$ to the class PRA of slope is modelled using a generalised bell membership function with the parameters $a = 8$, $b = 3$ and $c = 40$ (Fig. 6.6).

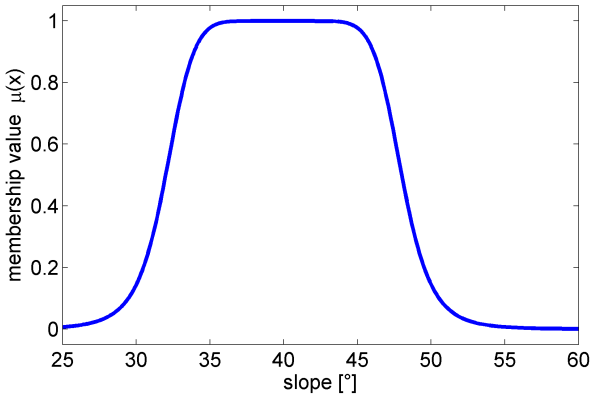

FIGURE 6.6: Fuzzy membership function for slope.

This function assigns the largest membership degrees to slopes between 35° and 45°. Slopes flatter than 30° and steeper than 50° are assigned low membership degrees as avalanches become increasingly unlikely for such slopes.

6.3.1.2 Wind shelter

The literature clearly reports the importance of wind – terrain interaction for avalanche release estimation. Many studies (Maggioni and Gruber, 2003; Vontobel, 2011) have established concave areas to be more prone for avalanche release. One possible reason is that snow under wind influence is mostly deposited in leeward slopes, in gullies or behind downslope terrain steepenings. Existing algorithms take into account these effects by using a curvature measure. Furthermore, studies for snow hydrological purposes demonstrated the good performance of terrain based wind-shelter parameters to reproduce patterns of snow accumulation to a remarkably well extent (Schirmer et al., 2011; Winstral et al., 2002). The use of a wind shelter parameter has, in our opinion, several advantages when compared with a curvature measure:

(1) A wind shelter parameter detects both wind sheltering effects due to changes of planar and profile curvature. Planar and profile curvature normally require two separate calculations.

(2) A wind shelter parameter calculates sheltering effects with regard to a given wind direction, which is not possible using curvature. This enables the user, for example, to define release area scenarios, taking into account the main wind direction for hazard mapping purposes or to define release scenarios with regard to the different directions of potential storm events for more short-term hazard mitigation measures.

In this study, the wind shelter parameter of Plattner et al. (2006) is utilised, which is a slightly modified version of the wind sheltering parameter of Winstral et al. (2002) of

the form:

$$index(S) = \arctan \frac{\max\left(z(x_0) - z(x)\right)}{|x_0 - x|} : x \in S \tag{6.15}$$

where $S = S(x_0, a, \delta a, d)$ is a subset of grid cells within a distance of δd and a range of direction of $a \pm \delta a$ from the central cell x_0. In our implementation we replaced the MAX function by the quantile function using the 3rd quantile instead of the MAX. This accounts for the fact that punctually very large sheltering effects might be outweighed in case the surrounding area is open to wind influence (e.g. large rocks in an otherwise open slope). The wind shelter index varies between -1.5 and 1,5 for complex alpine terrain. Negative values correspond to wind exposed terrain, positive values to wind sheltered terrain; therefore, the degree of membership $\mu_w(x)$ to the class PRA of wind shelter is modelled using a generalised bell membership function with the parameters $a = 2$, $b = 3$, $c = 2$ (Fig. 6.7).

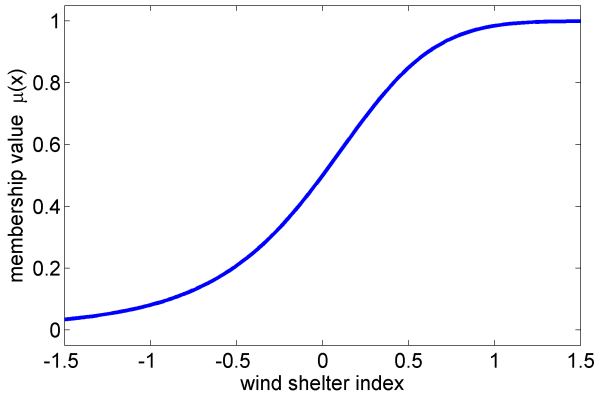

FIGURE 6.7: Fuzzy membership function for wind shelter.

6.3.1.3 Roughness

The third terrain parameter chosen is roughness. The literature review emphasised the importance of microtopography and its changes due to snow accumulation season for avalanche formation (2.3.4). In chapter 5 and section 6.2, adequate methods to capture and integrate this effect into release area definition were presented. The role of this parameter is to integrate microtopography together with its alteration under snow influence into release area definition. The relationship between snow depth and scale is used to adjust the roughness parameter as a function of a given snow depth. We further distinguish between concave terrain roughness (e.g. gullies), where snow accumulates, and convex terrain features, such as rocks or ridges, using a local wind shelter index. This index assigns positive roughness values for wind exposed features and negative roughness for wind sheltered roughness features representing potential accumulation zones of snow.

The degree of membership $\mu_r(x)$ to the class PRA of roughness is modelled using a generalised bell membership function with the parameters $a = 0.01$, $b = 3$, $c = -0.009$ (Fig. 6.8).

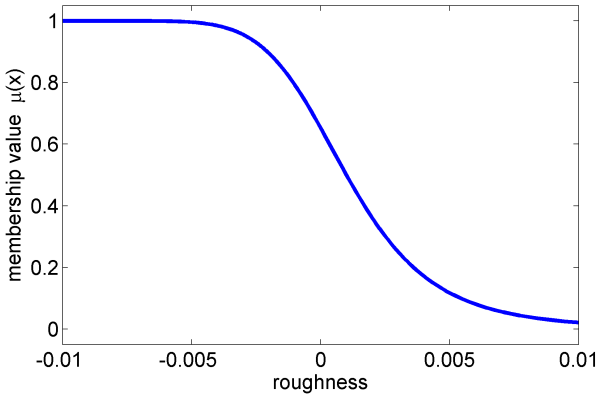

FIGURE 6.8: Fuzzy membership function for roughness.

According to the roughness values found in avalanche experiments and by expert interpretation, the roughness membership function assigns high membership degrees for concave and planar terrain features. Membership values strongly decrease for roughness between 0 and 0.005. Between 0.005 and 0.01, roughness values are assigned low membership degrees, accounting for the fact that avalanches are unlikely to happen but are possible in unfavourable conditions. Above 0.01, avalanches are considered to no longer occur.

6.3.1.4 Fuzzy operator

To define the membership degree to the class potential release area (PRA), the "fuzzy AND" operator, as defined by Werners (1988), is applied. For the three fuzzy sets slope $\mu_s(x)$, roughness $\mu_r(x)$ and wind shelter $\mu_w(x)$, the degree of membership to the class PRA is defined by:

$$\mu_{PRA}(x) = \gamma \times \min\left(\mu_s(x), \mu_r(x), \mu_w(x)\right) + \frac{(1-\gamma)(\mu_s(x) + \mu_r(x) + \mu_w(x))}{3}, x \in X, \gamma \in [0,1], \tag{6.16}$$

with γ defined as:

$$\gamma = 1 - \min\left(\mu_s(x), \mu_r(x), \mu_w(x)\right) \tag{6.17}$$

Depending on the value of γ, the operator varies between the minimum and the average of the three fuzzy sets. γ is function of the smallest membership value of the three fuzzy sets. The smaller the minimum value, the more the operator tends towards the minimum operator. The larger the minimum value, the more the operator resembles an averaging operator. The behaviour of this operator– and, in particular, the role of γ– can be best illustrated using an example. Let us imagine a medium steep slope of 32° with $\mu_r(x)$, = 0.5, which is situated in medium rough terrain ($\mu_r(x)$ = 0.5) and once in complete smooth terrain ($\mu_r(x)$= 0.8). If we use the classic minimum operator, both slopes would obtain the same membership value to the class PRA; by our own judgement, however, we would assume a generally higher release probability for the smooth slope. In contrast, our operator would assign a higher membership value to the smooth slope than to the rough slope as $\gamma = 0.5$ allows compensation from the larger roughness membership value. Assuming now the same two slopes show a gradient of 28° instead of 32°, resulting in $\mu_r(x) = 0.08$ and γ=0.92. A membership value to the class PRA close to 0.1 (0.13 and 0.11 respectively) would be assigned to both slopes. Due to the small γ value, the operator corresponds, in this case, almost to the minimum operator allowing for almost no compensation for the low slope value. This behaviour is, in our opinion, also reasonable, as a 28° slope produces an avalanche only in very rare cases –even when the slope would be perfectly smooth.

6.3.2 Software, workflow, input and output

The algorithm is programmed in the free software programming language R (version 3.0.3, http://www.r-project.org); in particular the RSAGA package (Brenning, 2008), providing access to the geocomputing and terrain analysis functions of the open source desktop GIS, SAGA (http://www.saga-gis.org), was used. Further, a Python interface (https://www.python.org/) was implemented to run the script as a tool in ESRI ArcGIS (ArcGIS 10.2 for Desktop). Figure 6.9 shows the toolbox in ArcGIS.

To perform a calculation of release areas, two mandatory inputs have to be provided: (1) A digital terrain model (DTM) and (2) a mean snow depth in the area. Optionally, a main wind direction and a forest mask can be provided to exclude forested areas from potential release areas. The development of this algorithm and its corresponding window sizes and scales are based on a relatively high DTM resolution of 2 m to allow calculations of early winter scenarios with very little snow depth where fine scale terrain features are relevant. If only coarser DEMs are available, resampling to a 2 m resolution is recommended. One still has to keep in mind that the calculation of early winter situations may not be very meaningful for scales smaller than the initial DEM resolution as small scale terrain features are not captured by the initially course DEM resolution.

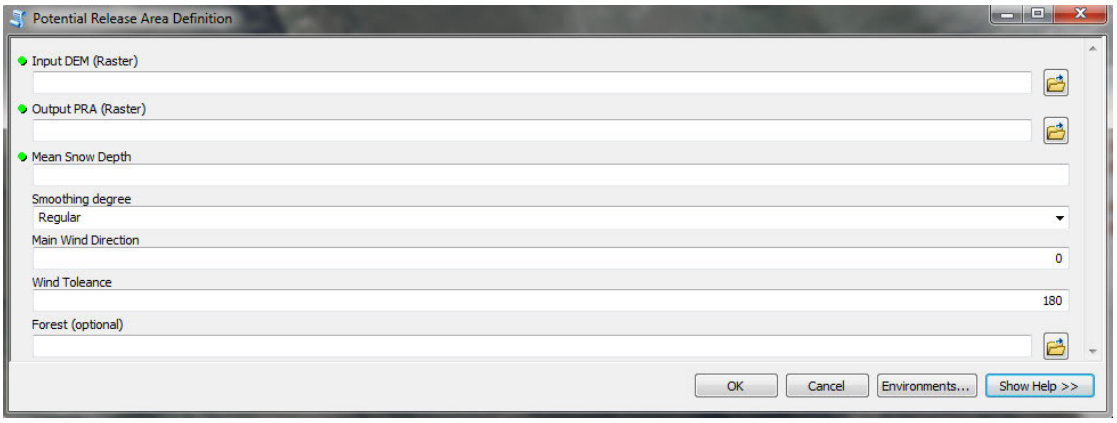

FIGURE 6.9: Input mask of the ArcGIS toolbox.

By default, a direction of 0° with a tolerance of 180° is set. This setting should be used if release area definition independent of a specific wind direction should be performed; it gives higher possibility to wind sheltered areas, such as gullies, being potential release area. If a specific wind direction should be used (such as to simulate potential release areas due to a storm event from a certain direction, for example) the wind direction can be set. As local winds often strongly deviate from the main wind direction, it is recommended that certain tolerance from the main wind direction of at least 30° is permitted. In case the local wind regime is known, it can already be taken into account in the input parameters.

The third input comprises an estimated snow depth HS in the area under examination. The input snow depth is associated with the corresponding scale for the calculation. Further, it is required to provide the degree of terrain smoothing. Two options exist; a regular degree of terrain smoothing (default) and low terrain smoothing. The latter should only be used for situations where significant snow distribution did not occur (e.g. first snowfalls in early season under little wind influence). In all other cases, the default setting should be chosen. Based on the measured snow distributions in Steintälli (Chapter 3), we select a coefficient of variation C_v of 0.35 for regular smoothing and a value of 0.2 for low terrain smoothing. The kernel window size S (measured in number of grid cells) as a function of snow distribution is obtained through the following empiric formula, based on the results of section 6.2:

$$S = 2 * \lceil HS^2 * C_v \rceil + 1 \tag{6.18}$$

This formula represents the case of medium terrain roughness (e.g. Steintälli). Characteristic scales can be larger for smooth terrain surfaces or smaller for very rough terrain.

The main steps executed within the algorithm are as follows:

(1) Determination of a characteristic scale (kernel window size S) as a function of snow depth and the degree of terrain smoothing.
(2) Calculation of roughness at the characteristic scale. Roughness at slopes steeper than 45° is calculated at a kernel window size of $S - 2$ to account for reduced terrain smoothing in very steep slopes.
(3) Calculation of slope at a 20 m scale. A scale of 20 m is selected in order to capture the large-scale characteristics of a slope. More fine-scale variations are captured with the roughness parameter.
(4) Calculation of wind shelter parameter as a function of input wind direction and tolerance at the characteristic scale.
(5) Calculation of degree of membership to the class PRA for every raster cell using the fuzzy operator.
(6) Exclusion of forested areas from the class PRA.
(7) Exclusion of potential PRAs $< 500m^2$ from the class PRA.
(8) Rendering the fuzzy output of the class PRA in four equally sized possibility classes. The classes were defined for visualization purposes only:

- PRA < 0.25: low possibility for PRA.
- $0.25 <$ PRA < 0.5: medium - low possibility for PRA.
- $0.5 <$ PRA < 0.75: medium - high possibility for PRA.
- PRA > 0.75: high possibility for PRA.

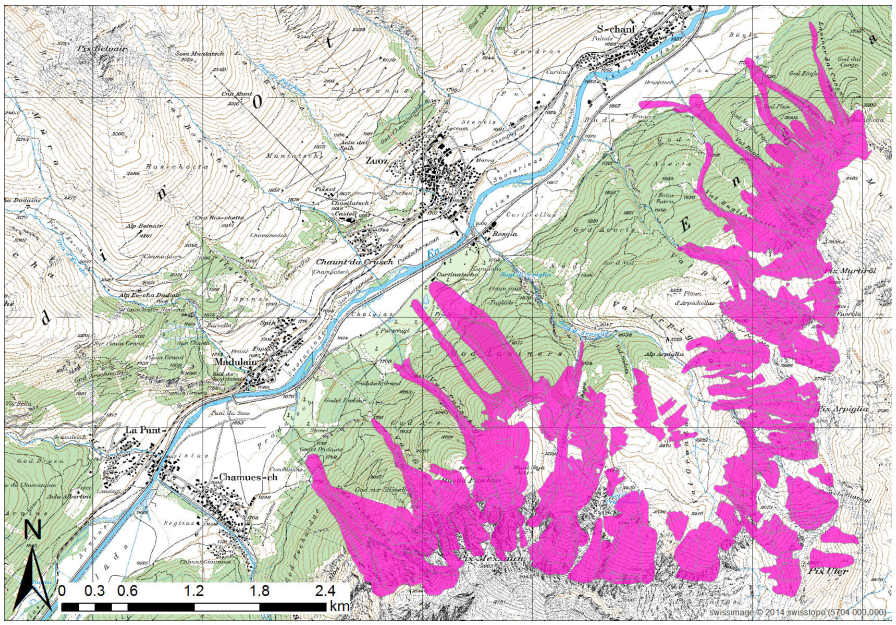

FIGURE 6.10: All avalanches observed within 30 years of observation south of Zuoz.

6.3.3 Validation

We provide, on the one hand a rather objective validation, comparing the modelled release area output to observed avalanches from the long-term database of Zuoz. On the other hand, we apply the algorithm to the recorded avalanches of 8 March 2006 in Vallée de la Sionne and assess its suitability for release area definition of single avalanche events.

6.3.3.1 ROC curves

To validate the algorithm, the database of Zuoz was utilised. The area in the southern part of the village was selected, as no artificial releases are performed in these avalanche paths. The observer normally maps the whole avalanche perimeter without specifying the release zone. Based on all avalanches, we built several reference datasets. As a first reference dataset, all avalanches, corresponding to the area which was at least once affected by an avalanche within the 30 years observation period, were selected. The selected area is shown in Figure 6.10.

For the second reference dataset, we impractically extracted the avalanche release areas from the first dataset. In order to do so, we identified the upper 80 height meters of every avalanche polygon and assigned this a release area. This is quite a conservative estimation of release area size; however, as we are mainly interested in the upper and lateral boundary, rather than the stauchwall, this rather conservative estimation can be considered appropriate. Likewise, as the size of the avalanches greatly varied between

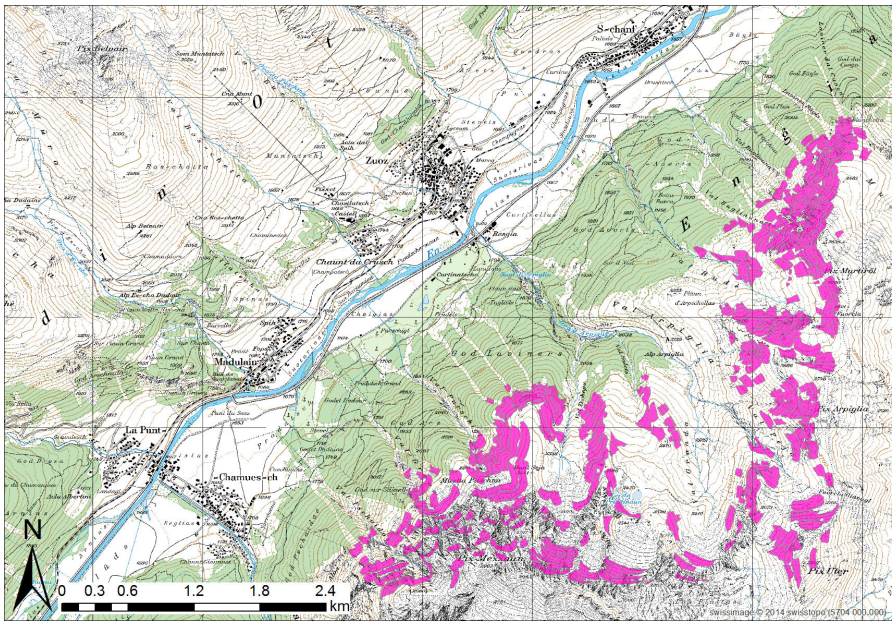

FIGURE 6.11: Extracted avalanche release areas based on all avalanches observed within 30 years of observation south of Zuoz.

small and very large avalanches, our identification method, instead to include significant parts of the avalanche track, rather excludes parts of the release area, which we consider less problematic than defining release areas containing significant parts of the avalanche track or run-out. The result of the release area extraction is shown in Figure 6.11.

Further, we selected two sub-data sets from the extracted release areas, depending on how often a certain area has released. In order to do so, we calculated the overlap of all avalanche release areas and assigned each pixel the number of overlapping polygons. This therefore corresponds to the frequency of how often this pixel was a part of an avalanche release area within 30 years of observation. The third dataset is therefore defined as the area that was at least twice included in an avalanche release area (Fig. 6.12).

The fourth dataset is defined as the area that released at least 5 times within 30 years of observation (Fig. 6.13).

In order to evaluate the performance of the algorithm, this was compared to a simple slope approach, which is often difficult to beat. Forested area was also excluded from being classified as release area in the slope approach. Further, we did not consider different snow depth scenarios for the validation process; rather we used a snow cover scenario with an input snow depth of 3 m to account for all possible situations from low to deep snow covers. Figure 6.14 shows the ROC curves for the algorithm and the slope approach using all avalanches as reference once and then the extracted release areas.

We observe that the PRA algorithm provides only little improvement over a slope approach, with a slightly better result using the whole avalanche perimeter as reference.

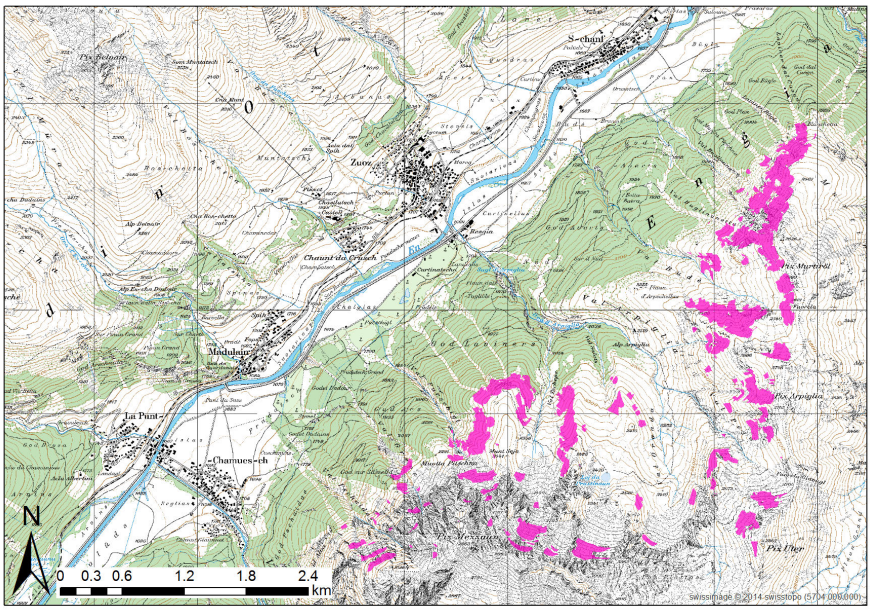

FIGURE 6.12: Extracted avalanche release area which released at least twice within 30 years of observation south of Zuoz.

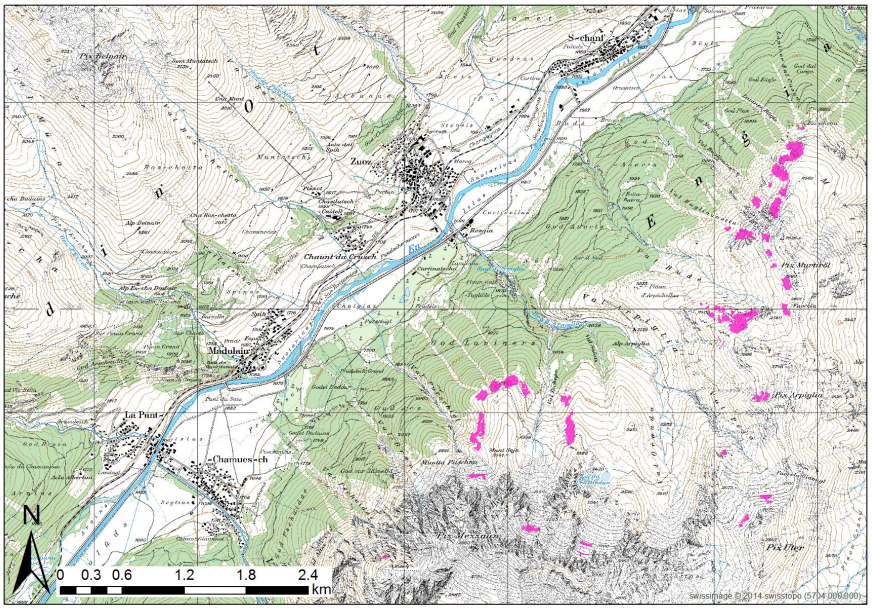

FIGURE 6.13: Extracted avalanche release area which released at least 5 times within 30 years of observation south of Zuoz.

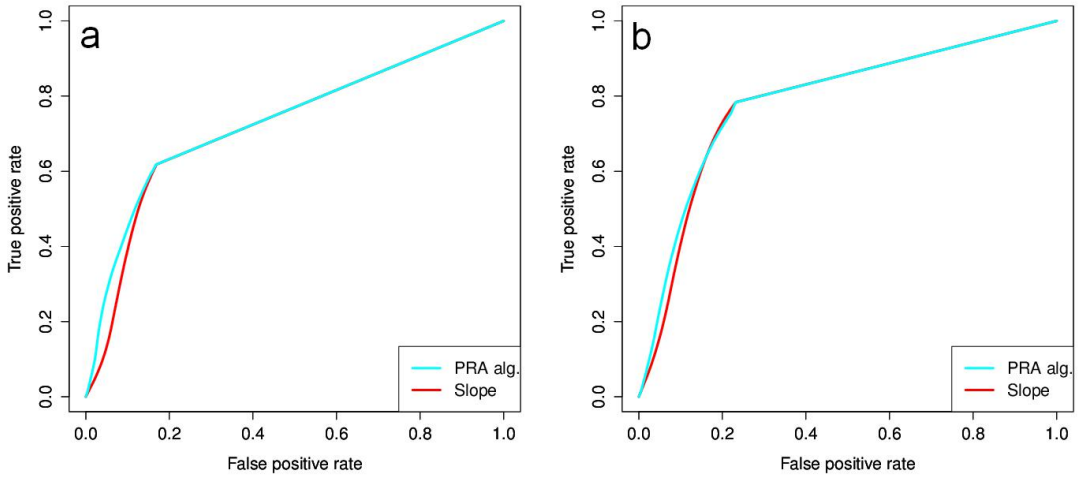

FIGURE 6.14: ROC curves for PRA algorithm and slope for (**a**) the whole avalanche perimeter and (**b**) the extracted release areas.

It is also observed that the true positive rate – even in the case of slope –is quite low with around 60% in the case of the whole avalanche perimeter and around 80% when the extracted release areas are taken as a reference. Whilst this can be explained with the significant proportion of avalanche track and run-out zone erroneously included in the reference dataset when using the full avalanche outline, this is not the case for the extracted release areas. In actual fact, a true positive rate of 80% for the slope classifier indicates that one fifth of the avalanches was mapped in areas flatter than 28° or steeper than 60°. As avalanches are very unlikely in such regions, this can be attributed to errors in the mapping process. Avalanches were mostly mapped from the road in the valley bottom on a 1:25000 m map. This most likely includes deviations of several tens of meters in the location of the avalanches, which could explain the erroneously mapped avalanches.

Furthermore, as we used a rather large snow depth scenario, the effect of roughness is lower compared to lower snow depth scenarios, where roughness has more influence on avalanche release. This explains why the algorithm reproduces only a slightly better result than a slope approach, indicating further that, in extreme situations, slope is still the most relevant and important parameter.
The role of the roughness parameter is further to identify borders between neighbouring release areas, such as ridges. However, the proportion of such features compared to the overall PRA zone is relatively low – at least in our study area. This suggests that the effect of roughness in a ROC curve is only little visible as the relative contribution of

such zones is small. Nevertheless, the identification of such features is crucial, and is one of main improvements of this algorithm.

Figure 6.15 shows the classification result for the release area that occurred at least 2 and at least 5 times, respectively.

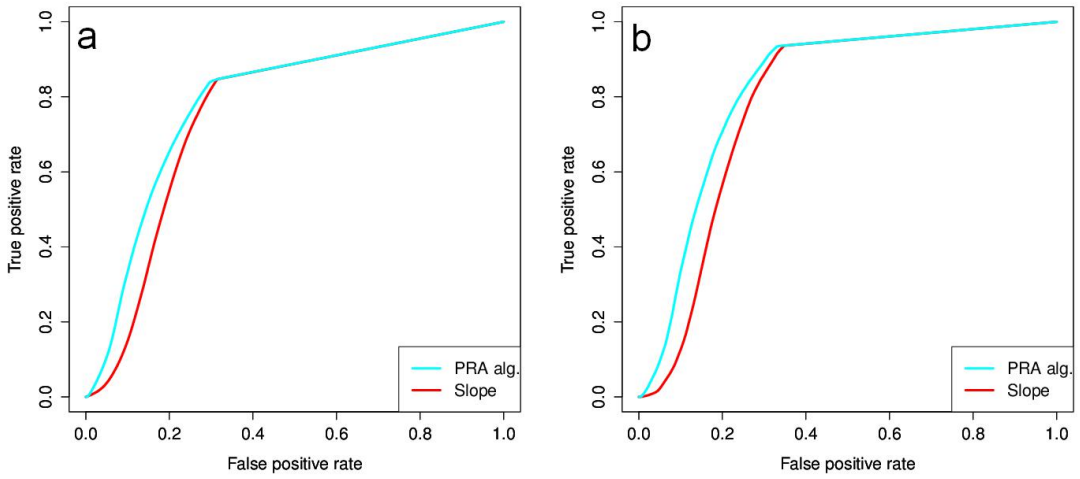

FIGURE 6.15: ROC curves for PRA algorithm and slope for release areas which occurred at least (**a**) twice and (**b**) 5 times.

In this case, we observe that the PRA algorithm shows a more pronounced improvement compared to the slope classifier supporting the hypothesis, where especially frequent avalanches are more reliably detected with the PRA algorithm. The fact that the true positive rate increases to around 90% in the case of the avalanches that released at least 5 times, shows that the mapping error is reduced by taking the overlay of several avalanches. Still, approximately 10% of the avalanches remain erroneously classified.

In order to quantify this visually observed behaviour, we calculate the area under the curve (AUC), which serves as an indicator for the quality of the classification. Table 6.2 shows the area under the curve (AUC) for all classifications.

TABLE 6.2: Area under the curve (AUC) for PRA and slope classifier.

avalanche outline	frequency	AUC (PRA alg.)	AUC (slope)
full perimeter	observed frequency: min. 1	73.5	72.4
release area	observed frequency: min. 1	79.2	78.6
release area	observed frequency: min. 2	78.5	75.5
release area	observed frequency: min. 5	82.3	78.6

The AUC calculation confirms that the performance of the PRA algorithm is increasing with increasing release area frequency. The difference between PRA and slope approach increases from 0.6 for all avalanches, to 3 for zones releasing at least twice and to 3.7 for zones releasing at least 5 times. This suggests that, despite the limitations mentioned in the reference data, the PRA algorithm can be considered more powerful over a classic slope approach – especially for the definition of more frequent avalanches.

6.3.3.2 Example Vallée de la Sionne

In this section we apply the algorithm to the avalanches of 8 March 2006, where snow distribution at the time of avalanche release is precisely known. Mean snow depth at the time of avalanche release across both basins CB1 and CB2 was 2,9 m, which was used for input snow depth. Strong west to northern winds brought significant new snow of around 90 cm. Therefore, we set a main wind direction NW with a tolerance of 45° to cover the whole NW sector. Figure. 6.16 shows the results of the PRA classification.

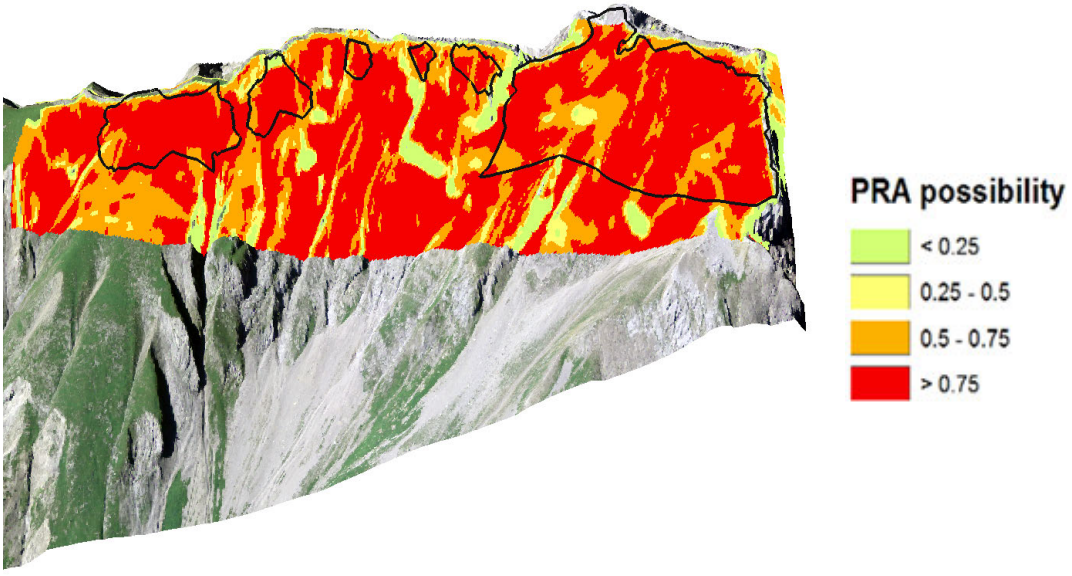

FIGURE 6.16: PRA possibility for a input snow depth of 2.9 m. Black boundaries show artificially released slab avalanches on 08 March 2006.

We observe that most of the release area is classified with high possibility of being PRA. Lateral boundaries of the slab are often classified with medium – low possibility, due to changes of morphology that might have been crucial for fracture arrest.

6.3.4 Practical example Canton Uri

The following example is taken from the current avalanche mitigation practice in Switzerland. It is a mountain road situated in the canton Uri, in the centre of Switzerland, close to the Gotthard pass. The mountain road has NE-SW orientation, and is threatened by the different avalanche paths of the Böschen avalanche (Fig. 6.17).

FIGURE 6.17: Avalanche path of the Böschen avalanche. The red circle shows the lower release zone which produces frequent avalanches affecting the road.

The avalanche path is NW – oriented and characterised by a lower release area zone (red circle) and a higher alpine avalanche zone separated by a flatter section in between. The lower release zone is covered with low bushes and characterised by many small gullies, which produce the majority of avalanches. The whole lower release zone is steeper than 30°, thus meaning that avalanches may occur everywhere. Due to its proximity to the main Alpine ridge, the slope is exposed to storm events from the NW direction, as well as Föhn situations from the S direction, often in combination with significant snowfalls. Generally, the S to SW storm events are more critical situations, responsible for the majority of avalanche events hitting the road. We analyse one typical avalanche period and apply the algorithm to the according wind and snow situation obtained from a nearby weather station at the time of avalanche release. On 2 February 2014, after a significant snowfall of around 40 cm, 11 small avalanches naturally released in the lower avalanche release zone (black outlines in Fig. 6.18) and hit the road. Snow depth in the area after the snowfall was 120 cm. Wind influence was rather low.

Figure 6.19a shows the result of a release area calculation with an input snow depth of 1.2 m and no main wind direction for the same area than shown in Fig. 6.18. We observe that the small channels in the lower release area are well detected and assigned mostly high possibility (red colour) being release area. This is in good agreement with the avalanches observed, which mostly released in the small gullies. Further, the algorithm indicates several areas with medium - low and low possibility (yellow and light green

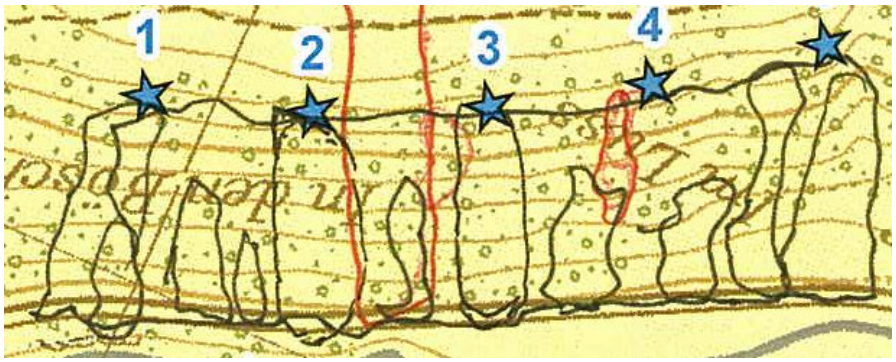

FIGURE 6.18: Observed avalanches on 2 February 2014, as mapped from local avalanche service (black boundaries). Stars represent areas where avalanche control is normally performed. The red boundaries delineate avalanches that were artificially released the day after the natural avalanches occurred.

colour) for some area in between the gullies, indicating that large, continuous avalanche releases are rather not to be expected under this snow scenario. If we assume a snow depth of 2.5 m as opposed to 1.2 m (Fig. 6.19b), the result would be a more continuous area of high possibility, indicating that under this scenario, larger release areas can potentially occur.

Release area calculations for different wind directions show that the main wind directions from SE to SW direction produce the largest possibility values of avalanche release (Fig. 6.20), indicating that such wind directions are the most critical for this slope.

Further, we calculated scenarios for a W wind direction and a NW wind direction with a snow depth of 1.2 m (Fig. 6.21). We observe that, for the NW scenario, the algorithm assigns low to medium - low possibility for the whole area. Due to the fact that the release area is completely wind exposed, the possibility of avalanche formation under these conditions is strongly reduced. For a W direction, we observe that the deeper gullies and the more N oriented slopes in particular are assigned medium - high possibility being a release area. This reflects the cross loading conditions which are often observed under this wind direction, also leading to avalanching.

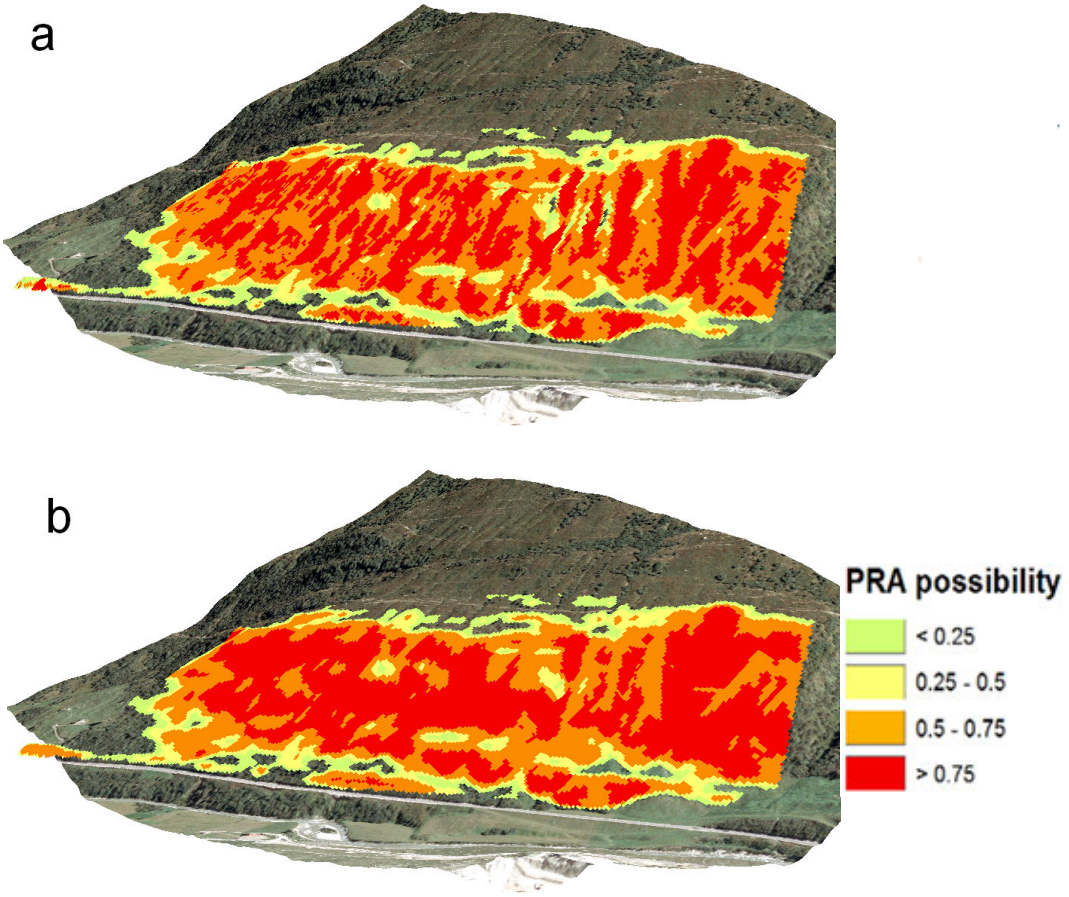

FIGURE 6.19: PRA possibility for a snow depth of (**a**) 1.2 m and (**b**) 2.5 m. No specific wind direction is set.

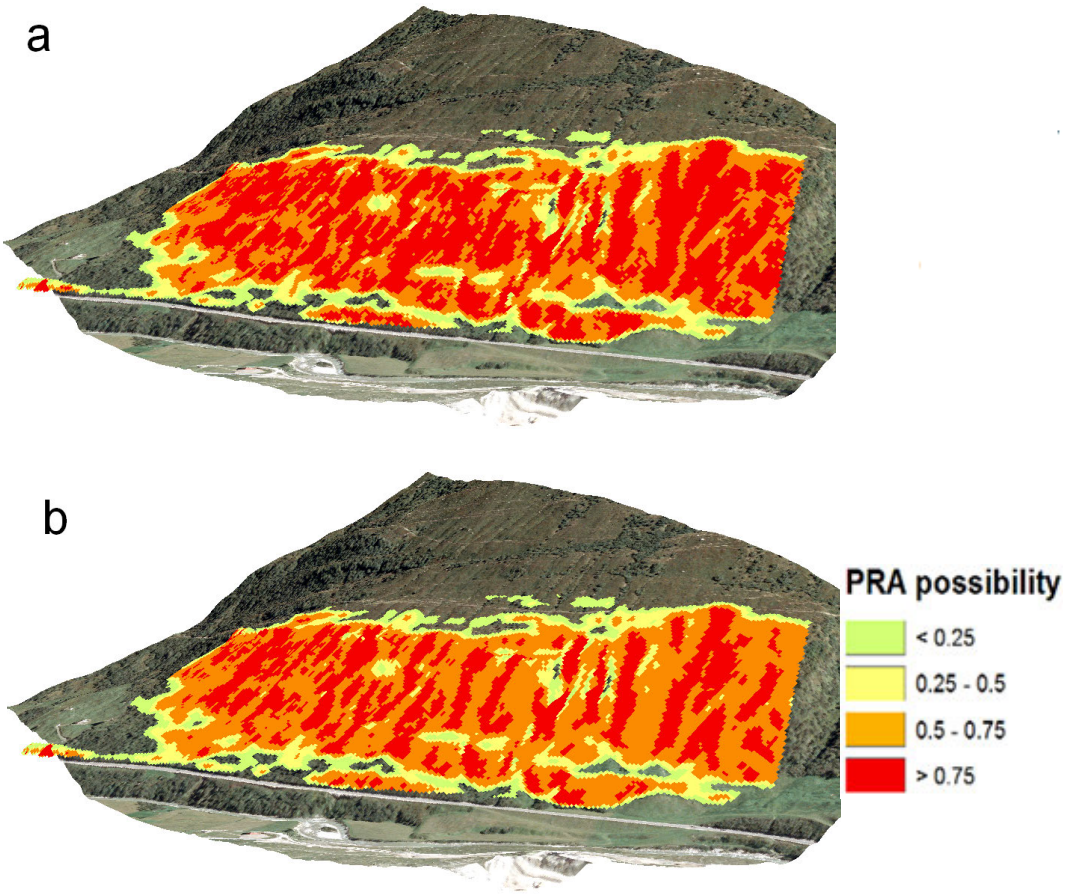

FIGURE 6.20: PRA possibility for (**a**) a S wind direction and (**b**) a SW wind direction. Snow depth is set to 1.2 m.

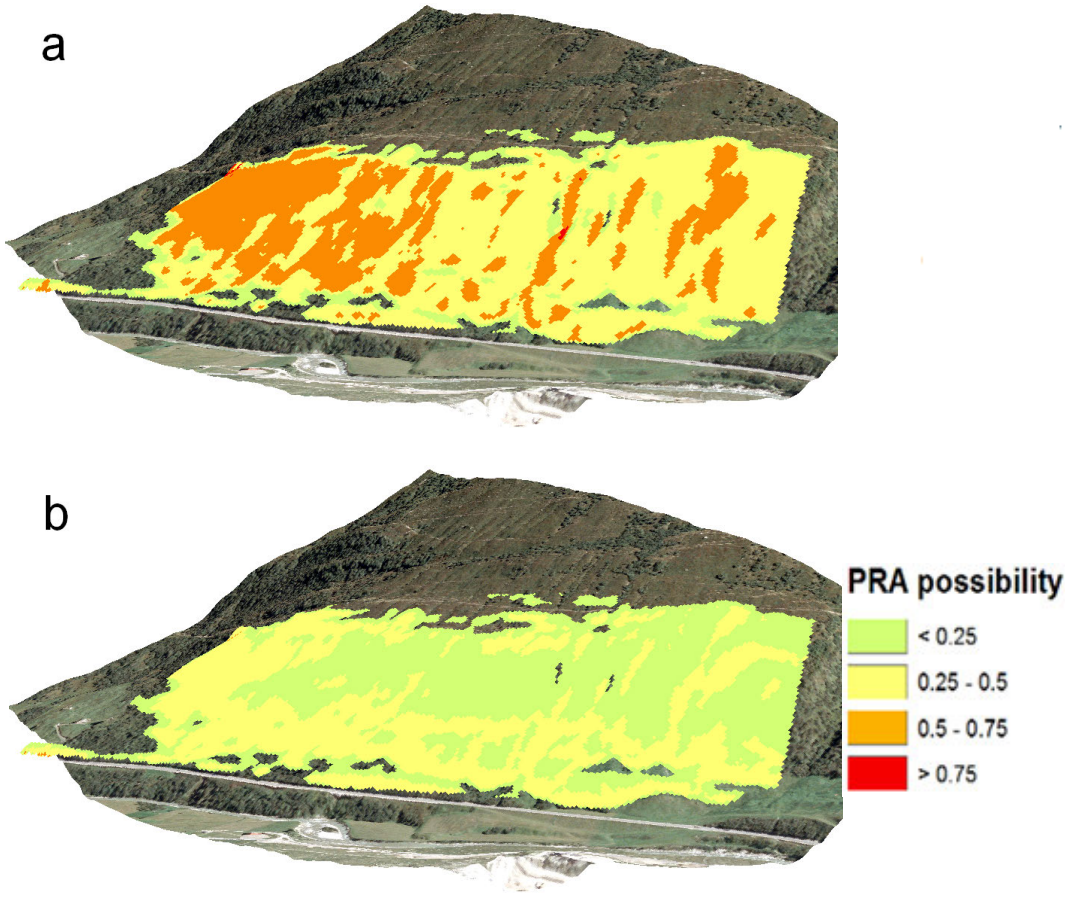

FIGURE 6.21: PRA possibility for (**a**) a W wind direction and (**b**) a NW wind direction. Snow depth is set to 1.2 m.

6.4 Key findings

We presented a new GIS tool for release area definition based on a fuzzy logic classification approach. In mind of this purpose, we developed an enhanced roughness parameter and a simple procedure to approximate winter terrain roughness from a summer DTM. We showed that, for given snow cover scenarios, a characteristic scale with maximum correlation between terrain roughness and snow surface roughness exists. This finding allows adapting scale of the roughness parameter as a function of snow depth.

The validation process showed that the release area algorithm provides an improvement over a traditional slope approach, especially in terms of identifying more frequent avalanches. The examples presented highlight the great potential over existing release area procedures:

(1) The algorithm detects fine-scale terrain features allowing the partitioning of the whole potential release in adequate sub basins.

(2) Terrain roughness is adjusted as a function of snow distribution allowing the assessment of the influence of terrain smoothing on potential release area size and location.

(3) It is possible to define release area scenarios as a function of a main wind direction.

In the next chapter, we will critically discuss our results; in particular the strengths and limitations of the release area algorithm. We will further recall the major research questions and evaluate the contribution of our results to the current scientific knowledge.

.

Chapter 7

Discussion

This chapter reviews the research findings from chapters 4 to 6 in the context of the underlying research questions. The methodologies and results are critically discussed, and their contribution to the state of the art is evaluated.

7.1 Snow influence on surface morphology of winter terrain

Research question 1. *How does snow distribution influence surface morphology of alpine terrain and how can such an effect be captured?*

So far, very little information relating to the effect of snow on terrain morphology can be found in scientific literature. Neither the effect of terrain smoothing has been quantified, nor the persistence of these effects assessed. As our results aimed to close this research gap, in this section we discuss the contribution of our findings to the state of the art knowledge .

7.1.1 Terrain smoothing

Our results suggest that snow distribution can be potentially linked to scale and magnitude of terrain smoothing as a function of snow depth and its variability. They further show that, in contrast to the indications given by Schweizer et al. (2003), terrain smoothing processes are not restricted to snow depths of 0.3 – 1 m, but are still observable in considerably thicker snowpacks; however, it is important to emphasise that this is dependent of the scale of terrain roughness under consideration. Considering the work of

Schirmer and Lehning (2011), we can confirm increasing terrain smoothing at increasing scales with a deeper and more variable snowpack; however we did not find a clear break separating scales, where terrain is smoothed or not smoothed. We rather observe a gradual decrease of terrain smoothing with increasing scales.

However, as our method to define terrain smoothing (section 4.1) is based on a regression analysis, a certain number of grid cells is required to obtain significant results. One limitation of this method is therefore that measuring terrain smoothing at a single point is not meaningful. In such cases, the simple ratio between summer and winter roughness should be applied. Further, we assumed a linear behaviour of the smoothing processes which is especially true for coarser scales. As the results showed increasing deviation from a linear behaviour at finer scales, the meaningfulness of slope of a regression line as an indicator for terrain smoothing is limited at a certain point.

This is in agreement with results on a local scale, where terrain smoothing cannot be unambiguously explained by snow depth and terrain roughness. It is rather controlled by morphological parameters of neighbouring pixels, which control together with meteorological factors, such as wind, the local redistribution of snow, depending on their arrangement at feature scale. Another reason is that terrain smoothing may vary strongly within an individual basin due to local wind conditions and their interaction with the underlying terrain features, which strongly influence deposition, redistribution (e.g. snow drift, saltation, preferential deposition (Lehning et al., 2008; Mott et al., 2010)) and/or wind erosion processes. Surface roughness therefore might be influenced by drift features (dunes, cornices) or sastrugi. This complex behaviour is not captured by a simple power law, as shown in chapter 4. Therefore, our results are limited to scales larger than individual drift features. Further, the selection of basin size and location is crucial for the observed smoothing behaviour. Terrain smoothing is likely to vary with snow-climatical conditions, terrain characteristics or vegetation cover (e.g. Trujillo et al. (2007)).

One potential to capture fine-scale snow distribution lies in physical models able to calculate snow redistribution in 3-D terrain (e.g. Alpine 3-D; Lehning et al., 2006). However, the physical modelling of snow distribution requires extensive computational effort, limiting applications over long time periods. They further require high resolution meteorological input parameters (Magnusson et al., 2010; Raderschall et al., 2008) which restrict its application to selected, well–equipped areas. This justifies the potential of simpler, statistical methods for practical applications, such as avalanche hazard assessment. Despite their generality and stated limitations, they can be widely and easily applied.

7.1.2 Interannual consistency of snow distribution and surface roughness

The analysis of persistence of snow distribution and surface roughness delivered interesting insight into snow- terrain interaction processes. Generally, we found strong inter and intraannual persistence of the snow distribution, supporting the hypothesis that snow distribution converges towards a site-specific, characteristic pattern. Further, we showed that the persistence of snow distribution is transferred to surface roughness patterns. A DSM of a winter terrain can therefore partly explain the variance between snow surface roughness in a winter terrain and terrain roughness, highlighting its relevance for integration into practical applications.

The high persistence of snow distribution is in agreement with previous studies, which often found very high interannual persistence of snow distribution at the end of the accumulation season (Deems et al., 2008; Winstral and Marks, 2014), with correlations of up to 0.97 (Pearson's correlation coefficient; Schirmer et al., 2011). In comparison, interannual persistence at peak accumulation is slightly lower in the Steintälli basin ($R^2 = 0.65$); this may be explained by large glide cracks in the winter season 2011/12, affecting the snow depth distribution during the whole winter season. In addition to previous studies, we further showed that high persistence can also exist significantly before peak accumulation (R^2 up to 0.69), and that rough terrain generally showed higher persistence than smooth terrain.

The main weakness of this outcome is the relatively small number of data sets with limited spatial and temporal extent restricting the generality of our results. Other studies exist (Pomeroy et al., 2004; MacDonald et al., 2009), where important variation of snow distributions between different years are observed. These studies mainly identify changing directions of major snowstorms as a main source of variation. This suggests that the persistence of snow distribution is dependent on climatic conditions and synoptic-scale weather patterns. A larger number of scans obtained in all possible snow cover situations, covering different terrain types and snow climates, therefore would be necessary to confirm and strengthen the significance of our findings. Nevertheless, new technologies to derive high-resolution DSMs over a wide area – even in a winter terrain – are currently being developed (Bühler et al., 2012; Bühler, 2012), making it more feasible in the future to obtain DSMs at significantly lower cost than lidar techniques. This would allow the extension of such studies.

7.2 Terrain smoothing and its role for release area size and location

Research question 2. *What is the influence of the morphological differences between the snow free summer terrain and the snow-covered winter terrain on avalanche release area size and location?*

In chapter 5, the potential of the winter terrain to define potential release areas was evaluated. Preliminary results, relating measured slab thickness and variability to the underlying terrain, illustrated the connection between terrain surface, slab geometry and the potential release size (Fig. 5.4). Compared to the summer terrain, winter terrain roughness further revealed an improved capacity to delimit release areas. This supports the hypothesis that increasingly smoother surfaces reduce slab and weak layer variability, subsequently leading to potentially larger release areas (Simenhois and Birkeland, 2008). This further emphasises that the reduced mechanical support of a smooth winter surface may have an influence on release area size and location (McClung and Schaerer, 2002).

One factor we did not consider in our analysis is snow stability. As an example, previous avalanches could have significantly disturbed the layering of the snowpack, especially in very steep areas where frequent avalanches are regularly observed. This also would have had an influence on observed release area size and location. However, studies on the relation between snowpack conditions and terrain indicate that, in a homogeneous terrain, rather homogeneous stability patterns can be expected (Harvey et al., 2012), emphasising the importance of (winter) terrain as a main parameter for release area definition. This is supported by recent mechanically based statistical modelling of the slab–weak-layer system, which emphasises the important role of small changes in terrain morphology in the definition of release area size (Gaume, 2012).

In an effort to overcome the limitations of only one set of detailed snow distribution measurements within avalanche release areas, we statistically assessed the influence of terrain smoothing through relation of release area size with daily point measurements of snow depth. In the area of Zuoz, more than 100 avalanches were available in each avalanche path. allowing for statistical analysis. The results highlighted the potential influence of terrain smoothing on release size – especially for surface slabs; however, basal weak layers produced large avalanches also in shallow snowpacks and deep slabs often showed very large release area sizes. This is in agreement with observations from other countries, such as Canada (Tracz and Jamieson, 2010). Generally larger release area sizes for deep slabs compared to other slab avalanche types were also found. The main limitation concerning the significance of our results is the representation of snow depth measurements from a flat fieldsite for neighbouring slopes.

Many studies show that flat field stations generally overestimate snow distribution in adjacent catchments (Grünewald and Lehning, 2014), especially when located in wind sheltered areas. The altitude difference between the measurement station in the valley and the release zones in high alpine areas may be another factor restricting the representativity of the measurement location. Generally, an increase of precipitation (Sevruk, 1997; Pipp and Locke, 1998; Wastl and Zängl, 2008) and a relatively increasing proportion of snow in precipitation events with altitude (López-Moreno and Stähli, 2008; Grünewald and Lehning, 2011) lead to deeper snowpacks in higher elevations . However, recent studies (Grünewald et al., 2014) show that the snow distribution is not simply a function of altitude but rather typically show a positive trend with altitude only up to certain level, where the increase of wind distribution (Gauer, 2001; Lehning et al., 2008) and complex terrain generally outweigh the altitudinal influence on snow depth. In such terrain, avalanches, sluffing or creeping (Bernhardt and Schulz, 2010; Gruber and Bartelt, 2007; Schweizer et al., 2003) redistribute snow downwards from often very steep slopes, even leading to a decrease of snow depth for the highest regions on a mountain. At the same time, these regions constitute the areas where avalanches most likely release, emphasising the importance of redistribution processes for the estimation of snow distribution in avalanche prone terrain.

Another factor is specifically related to the location of Zuoz. The area is mostly under the influence of snow storms originating from either Mediterranean or North Atlantic depressions. Whilst the former are related to a Southern direction, the latter are characterised by North-Western directions. Depending on the type of snow storm, the measurement station either under- or overestimates the amount of snow in the neighbouring slopes.

This reveals that, in the case of the Zouz database, many, commonly conflicting factors, contribute to the representativity of the snow depth measurement for the neighbouring avalanche paths and that the importance of each factor may further vary for every avalanche event, depending on the preceding snow-meteorological history and avalanche activity of the winter season. Nevertheless, we believe that snow depth measurements presumably serve as valid indicator of the amount of snow present on a mountain site, and are able to reproduce general trends of the snow situation.

7.3 Integration of snow cover into release area definition

Research question 3. *How can potential release area modelling be improved by taking into account the influence of snow distribution on surface morphology?*

This research question arose due to the limitations of tools available (Maggioni and Gruber, 2003; Ghinoi and Chung, 2005; Bühler et al., 2013) to assist avalanche professionals in the definition of potential release area size and location. In section 6.3, we showed how the results and methodologies developed in chapter 4, chapter 5 and section 6.2 can be exploited and integrated into a new tool for improved release area definition; therefore, in this section, we discuss the improvements over existing release area algorithms. We evaluate the various strengths and limitations of the new algorithm, and the potential for practical applications.

7.3.1 Evaluation of release area algorithm

In this section we provide a comprehensive evaluation of the algorithm including a comparison with existing tools. We discuss strengths and limitations with regard to algorithm design and output quality.

7.3.1.1 Comparison with existing tools

In this section we discuss the improvements of the developed release area algorithm (section 6.3) over existing release area tools from Maggioni and Gruber (2003); Ghinoi and Chung (2005); Bühler et al. (2013). The algorithms of Maggioni and Gruber (2003) and Ghinoi and Chung (2005) were based on terrain parameters, such as slope, aspect and curvature derived from course resolution DTMs ($> 20\,\mathrm{m}$). Such course resolutions cannot capture finer scale features, such as rocks, smaller ridges or gullies, thus limiting the application of algorithms to define extreme avalanches where smaller scale features can be neglected. The algorithm of Bühler et al. (2013) partly overcomes this limitation by using a resolution of 5 m and the introduction of a roughness parameter, allowing the capture of finer scale terrain features to define smaller avalanches. Still, by using a constant DTM resolution and constant scale of terrain roughness, the release area definition is derived for only one, predefined scale; however, as shown in chapter 4 and section 6.2, characteristic scales vary considerably with snow distribution, requiring the adaptation of scale (or DTM resolution) as a function of snow depth. This is so far lacking in all existing algorithms meaning that the output is not associated to a specific snow cover scenario.

Our algorithm, by using a multi-scale roughness parameter where scale is further adapted to snow depth, accounts for these effects allowing for a more realistic estimation of potential release areas. Release area definition therefore can be performed for very different snow cover situations, ranging from shallow early winter snowpacks, where

rocks and boulders stabilise the snowpack, to deeper snowpacks, where microtopography is largely smoothed out.

Further, most existing algorithms (with the exception of Ghinoi and Chung (2005), who also implemented a fuzzy logic approach) adopt a binary classification approach, thus distinguishing only between areas where avalanches are possible and where they are not. Consequently, terrain with very little suitability of being a release area (e.g. slopes between 28° and 30°) and which only rarely produce avalanches, cannot be distinguished from terrain that is more prone to avalanche release, such as steep slopes between 35° and 45°). Therefore, existing release areas mainly produce worst case scenarios, including all possible area that can release. Whilst this may be appropriate for an extreme situation, it makes it very difficult for decision– makers to identify the proportion of release area, which is relevant in a less extreme situation. Still, in order to efficiently allocate and apply mitigation measures, a certain prioritisation of the release zone would be very helpful.

By using a fuzzy logic approach, accounting for the degree of suitability of a terrain being a release area is possible; therefore, the presented release area algorithm is not restricted to the calculation of extreme avalanches, but rather can also be applied to define more frequent avalanches, which affect roads or ski runs on a more regular basis. This is further refined by the introduction of a wind shelter index, which accounts for the influence of a main wind direction. Snow storms or drift events mostly produce avalanches in leeward aspects where snow can accumulate, whereas wind exposed areas are less affected. This means that not all aspects are equally prone to avalanche release. Taking into account this effect in release area definition further enhances the specificity of the output with regard to given snow cover/ wind scenarios, thus providing the user with the particularly relevant release zones.

7.3.1.2 Strengths of release area algorithm

According to Li et al. (2010), a successful model has to fulfil seven criteria: accuracy, realism, precision, robustness, generality, fruitfulness and simplicity. Some of this factors can be analytically assessed, many of which are evaluated through application of the model for different purposes, scales or environments. We will use these seven points to discuss the strengths of the algorithm.

"Accuracy - is the model output correct or nearly correct?"

Accuracy deals with the question of whether or not results are correct (or nearly correct). Throughout the validation process, the algorithm was evaluated so as to detect

release areas that occurred in an observation period spanning more than 30 years. The selected database of Zuoz is one of the most detailed and long-term database comprising observation records of avalanches. The fact that the observer remained the same person across the whole observation period induces some consistency in the observation method; therefore, with regard to the quality of the reference data, we selected one of the best documented datasets available. We found that around 80% of observed avalanches could be detected. The reason for the non– detected avalanches was already given in chapter 6, and was identified as being mainly attributed to mapping errors. On the other side, we observed that the algorithm produced a false positive rate of around 10% when validated with the full avalanche outline, thus meaning that 10% of the area classified as potential release area by the algorithm did not release within the 30–year observation period; however, as indicated in the literature review, this does not necessarily represent a wrong classification result; rather, it could also indicate avalanche- prone terrain that has not yet released. The comparison with a simpler slope approach revealed that a greater accuracy can be achieved through the use of the PRA algorithm – especially for frequent avalanches. As slope is still considered the most reliable terrain parameter in the identification of avalanche starting zones, we believe that the accuracy of the algorithm is good with regard to the generally high inherent uncertainties associated with slab release area estimation.

"Realism: is the model based on realistic assumptions?"

This question can clearly be answered with a yes. Within the selection process of the model parameters, we based our decision on previous studies concerning avalanche formation, expert rules and the results gained throughout this thesis. Our model is further based on state-of-the-art knowledge within avalanche science. The realistic assumptions were a crucial factor in designing the algorithm as it is decisive about the acceptance by practitioners.

However, estimating single avalanche release events showed that not all of the observed avalanche release areas could be explained. This is due to the fact that meteorological effects and snowpack stability are not integrated within this algorithm –although those factors are highly relevant for release area size in a given situation. Still, the overall validation showed that, for a more long-term application, the algorithm provides improved results over a conventional slope approach – especially for frequent avalanches.

"Precision: Are the outputs best possible unbiased predictions?"

We showed in the literature review that many different statistical approaches exist to tackle a modelling problem. They all have advantages and disadvantages and are more or less suited to a given problem; however, the statistically best predictor may, at the

same time, not always be the simplest and most comprehensible. As our main aim was to obtain a map with spatial locations of release areas, we opted for a classification approach. Further, the reference data were often limited, such as in the case of roughness values from avalanche experiments,for example, or were not very precise, such as in the case of our reference avalanches for the validation. Therefore, the decision was made to not fully rely on the statistical estimation of potentially biased data, but to model terrain parameters using a fuzzy logic approach. The membership function of each terrain parameter integrates expert rules and scientific studies, which are the condensed result from countless avalanches in all kinds of possible snow conditions and terrain characteristics.

"Robustness: Is the model oversensitive to the errors and blunders in the data?"

The fuzzy logic concept assures that small changes to the parameters do not result in significant changes of the model result. By using bell –shaped curves, we aimed to reduce sharp transitions in the membership values of the single terrain parameters. Further, the modelling of the terrain parameters considered certain margins to account for rare, unusual situations such as releases in very flat terrain ($< 30°$). These margins at the borders of the parameter range assure that smaller errors in the input DEM do not automatically result in the omission of large areas for potential release area; however the algorithm is dependent on high resolution ($<= 2\,\mathrm{m}$), good quality elevation models. Gross errors in the DEM will evidently produce erroneous model results.

"Generality: Is the model applicable to various case studies and scales?"

We provided several examples of potential application for different types of terrain and practical problems, reflecting the generality of the algorithm. As the algorithm is mainly based on a summer terrain model, it can be applied wherever high resolution terrain models are available. As an example, Switzerland nowadays is covered with a 2 m resolution DTM. In the future, DTMs are likely to be available at further decreasing costs, through large- area remote sensing applications, such as airborne lidar. This guaranties that the algorithm can be applied over a wide range of scales, from the evaluation of a single avalanche path to large scale hazard assessment of transport networks. Further, the fuzzy logic principle allows for the easy adaptation of the algorithm to other conditions by simply adjusting the membership functions. As an example, in a more maritime snowpack, snow can adhere to the terrain at significantly steeper slopes than in the more continental climates, such as the Alps. Adaptation to different snow climates could be easily realised by a simple shift of the membership curve towards steeper slope angles. Further, the extension of the algorithm is also possible through the integration of other variables or rules within the current fuzzy logic design. This might be interesting for

specific locations where other variables are more significant than those presented in this thesis.

"Simplicity: is the model the simplest possible model (smallest numbers of parameters)?"

The algorithm comprises only three terrain parameters. The wind shelter index captures both profile and plan curvature, which would normally require two separate calculation steps. The input requires only a DEM and an estimation of snow depth in the area. Wind direction and forest cover are optional. Further, there are no "black box" calculations involved, delivering predictable and explainable results, which are important requirements for being accepted by avalanche practitioners. It was further shown that slope and roughness are independent terrain measures (Sappington et al., 2007). Therefore, we estimate the redundancy of the parameters to be quite low.

"Fruitfulness: Are the outputs useful and do they help users and decision makers solve problems?"

The introduction of a snow distribution dependent roughness parameter and a wind shelter index significantly enhances the capabilities of this tool compared with the previous approaches, as shown in section 7.3.1.1. How the aforementioned improvements of the developed algorithm over existing procedures affect practical applications, such as hazard mapping or short-term hazard assessment, will be discussed in section 7.3.2.

However, prior to directing focus towards the practical applications, we want to provide the user in the following section with the limitations of this approach so that he can fully apprehend the capability of the algorithm.

7.3.1.3 Limitations of release area algorithm

The release area algorithm defines release areas as a function of snow depth and wind direction. The statistical assessment of terrain smoothing, as well as a terrain based shelter index, contain various inherent limitations with regard to the precision of the results:

- Terrain smoothing modelling by adaptation of scale cannot model several effects present in a winter terrain. As an example, modifications by the winter terrain, such as large avalanches or extensive formation of drift features beyond the normal filling of terrain depressions (dunes, cornices), are not included in our approach. Such effects are strongly site-dependent and further vary from winter season to

winter season. This still needs to be assessed by experts knowledgeable in the local conditions in the study area.

- The function to adjust terrain smoothing is mainly based on measurements from predominantly leeward slopes. Whereas the effect of wind on release area possibility is taken into account by a shelter index, the same underlying terrain smoothing is applied to wind exposed and wind sheltered slopes. That might not always be true – especially for consistently wind exposed terrain, which might show a different smoothing behaviour to that found in our measurements. More studies in wind exposed terrain would be necessary in an effort to understand terrain smoothing in such a type of terrain.

- Wind influence is strongly variable and often deviates from the main wind direction (Mott and Lehning, 2011). Local winds strongly affect precipitation patterns near to the ground (Mott et al., 2014). In addition, wind speeds and course-scale sheltering effects through neighbouring mountain ridges also affect snow distribution. Such effects cannot be captured by a geomorphometric wind shelter index; this would require the physical modelling of the snow cover. Nevertheless, local experts aware of local wind effects and the loading behaviours of avalanche– prone slopes may integrate this knowledge through adequate setting of the wind shelter parameter.

- The implementation of a fuzzy logic approach, despite the aforementioned advantages such as a continuous classification output, requires a defuzzyfication of the model output. This task consists in defining adequate thresholds in view of the purpose of the model. The determination of thresholds is not easy and often requires a solid amount of reference data which is not always available. It is thus an additional source of uncertainty in the model design.

7.3.2 Implications for avalanche hazard mitigation practice

To finalise this chapter, we discuss in this section how the developed algorithm contributes to avalanche hazard mitigation practice.

7.3.2.1 Relevance for hazard mapping

One of the biggest challenges nowadays in hazard mapping is the partitioning of the release area as a function of return period. By taking into account microtopography and its smoothing under snow influence, the algorithm provides valuable support in the definition of avalanche hazard scenarios with different return periods. However, return

period of an avalanche release area cannot (yet) be directly obtained from the algorithm output, as this depends, in addition to terrain, on snow-climatological conditions, which are neglected by the algorithm. Still, it appears feasible to calibrate the tool to a given fieldsite with its inherent snow climatology and thus to relate PRA possibility values to return period. This has to be assessed in future studies, but would represent a very promising application of this tool.

Nonetheless, the problem of release area partitioning in the case of a very homogenous release zone, without distinct topographical features remains. As terrain features are missing, the partitioning is mainly based on the expert judgement of an avalanche specialist. Such decisions are very demanding and contain a significant degree of uncertainty. The support of a geomorphometric tool, despite being potentially useful in many situations, is limited for such purposes. This highlights that some difficulties in hazard mapping practice have to be tackled by approaches different to those presented in this thesis. It further emphasises that tools such as that presented in this thesis cannot replace the expert judgement and experience of avalanche specialists.

7.3.2.2 Relevance for short-term hazard assessment

Many avalanches, affecting roads or ski runs today, are small to midsize, frequent avalanches. Tools therefore must be capable of coping with this type of avalanche. Several improvements to the developed algorithm are particularly suited for application for the purpose of short-term hazard assessment. The detection of fine scale terrain features, often considered as delimiting borders in release area definition, allows a better assessment of frequent release areas. Another major outcome of this thesis is the quantification of the strong smoothing of fine scale topography by snow, the integration of which further allows obtaining varying potential release areas for different levels of terrain smoothing. In addition, a wind shelter index allows the formulation of scenarios for different types of storm events, originating from different directions. This illustrates the practical usefulness of the tool for short-term hazard assessment. The example of Canton Uri in section 6.3.4 further shows that the algorithm is able to realistically reproduce single avalanche events with only a DTM and snow depth as input parameter.

However, simple procedures, such as this algorithm, are based on several assumptions, which may not always be satisfying. With regard to the example of Canton Uri (section 6.3.4), snow depth was obtained from a weather station measurement in a flat field. This is subject to the representativity of a flat fieldsite for neighbouring slopes, as discussed in section 7.2. In an effort to overcome this limitation, snow depth could alternatively

be measured in the slope or otherwise may be adjusted as a function of a flat field measurement.

Further, in a real-time situation, snowpack stability and meteorological conditions are highly influential in terms of whether or not an avalanche releases, as well as concerning the potential size of the release area. As information about snowpack stability is not integrated in the algorithm, the application of the tool for forecasting purposes at the level of a single avalanche path is clearly limited. Still, the fuzzy logic output providing continuous values of release possibility raises the question concerning the extent to which the PRA possibility values can be related to snow stability. To link the different classes of release area possibility with snowpack stability could allow the formulation of release area scenarios also as a function of snowpack conditions, which is, in our opinion, a very interesting future research direction with high practical relevance.

Chapter 8

Conclusions and Outlook

This thesis presents approaches to capturing and modelling the influence of snow distribution on terrain morphology and to assessing its effect on avalanche release area size and location. The overall goal was to develop a new framework for release area definition, including morphological changes introduced by the snow distribution. In this chapter, the achievements and insights gained through this research are presented. Furthermore, an outlook on possible future research directions, concerning long- and short-term hazard assessment of avalanches is provided.

In an effort to quantify terrain smoothing, we established a dataset of high-resolution snow distribution measurements, performed by terrestrial lidar, in a high alpine catchment, spanning across three winter seasons. Such datasets, characterised by a high spatial and temporal resolution, are very valuable in assessing the multi-temporal evolution of the snow cover, which is highly relevant for avalanche hazard management, hydrological and ecological purposes.

The evaluation of terrain smoothing, based on lidar snow depth measurements, lead to the following major insights: First, surface roughness, at scales larger than fine scale drift features, is to some degree persistent between winter seasons. Persistence of the smoothing behaviour is a precondition for systematical integration into applications related to terrain smoothing processes, such as release area estimation or avalanche dynamics simulations. Second, the degree and the scale of terrain smoothing in a topographical basin could be linked to mean snow depth and its variability. This enables the potential integration of winter terrain not only into release area definition, but also into avalanche simulations (e.g. RAMMS; Christen et al., 2010), leading to more accurate calculations owing to a more realistic estimation of topography. For example, the disappearance of small channels observed in a winter terrain can have a large influence on the main

direction taken by the flow in 2-D or 3-D simulations (Maggioni et al., 2013). Moreover, the estimation of friction parameters could also be significantly improved. Terrain smoothing modelling could further be applied as a quantitative method to adjust DTM resolution used in dynamics calculations. A more realistic winter terrain will further improve modelling of wind-ground interaction in snow-covered terrain and be important for better snow redistribution simulation (Mott et al., 2010), which can be valuable for water resources assessment or ecology purposes.

Detailed lidar measurements from avalanche release zones showed that surface roughness of the winter terrain is capable of defining observed size and location of avalanche release areas, suggesting the importance of this parameter for release area definition. Moreover, the comparison of point snow depths measurements to observed avalanche release area sizes suggests that terrain smoothing may be an influential factor for the potential size of slab avalanches – especially for surface slabs. However, large-area slab releases, occurring in shallow snowpacks when basal weak layers, such as depth hoar, are present, show that exceptions are possible under particular critical snowpack conditions. As data about snow conditions and surface roughness in avalanche release zones was generally limited in our study, more studies need to be conducted in the future to strengthen this finding.

Based on the aforementioned findings, we developed a new algorithm for the estimation of potential slab avalanche release areas, using a fuzzy logic classification approach. Morphological changes introduced by snow distribution were integrated through a snow depth dependent roughness parameter. The evaluation of the release area algorithm demonstrated the improved capacity of the algorithm compared with traditional approaches – especially for the definition of frequent avalanches. With regard to hazard mapping, the algorithm provides additional criteria for the partitioning of the whole potential release in adequate sub-basins, by detecting fine scale terrain features, which serve as delimiting borders for less extreme avalanches. The algorithm further allows the assessment of the influence of snow distribution on terrain morphology and, consequently, the potential release area size and location. Both factors provide additional information for an avalanche expert in charge of designing design events with different return periods. This further enables avalanche experts to objectivize and justify their decisions. However, the challenge of release area partitioning in very homogeneous terrain remains, as the algorithm can only consider terrain changes as possible separation borders.

With respect to short-term hazard assessment, we could show that the new tool is able to potentially reproduce avalanche release areas, where microtopography plays a decisive role. The preliminary results suggest that the influence of the snow cover is realistically

modelled. The integration of a wind shelter index enables the user to define release area scenarios as a function of the main direction, enabling, for example, safety personnel, to assess release areas as a function of single storm events. However, the algorithm is not applicable as a forecasting tool as snow stability is currently not included in the parameters. Nevertheless, as different classes of release area possibility are provided, the definition of release area scenarios as a function of snowpack conditions seems possible – at least statistically.

Whilst the algorithm cannot replace local expert knowledge, it can serve as a basis for experts to combine it with local observations. When local knowledge is not available, the algorithm nonetheless provides valuable support, at least for a first recognition of the potentially dangerous areas. The output of such an analysis can later on serve as a basis for further on-site investigations of the problematic zones.

In order to ultimately improve release area definition, the integration of snow cover properties seems crucial. Future research directions could follow several strategies: In recent years, mechanical- statistical modelling of the slab - weak layer system has been providing increasing insight into relevant parameters for slab avalanche release size (Gaume et al., 2014c). As an example, they indicate that for denser slabs, rather topographical features such as rocks or terrain breaks and inhomogeneities in the snow distribution control the potential size of a slab release, whereas for low density slabs, release area size is rather controlled by snow mechanical properties. The integration of such findings might allow, in the future, the refinement of the release area definition, not only as a function of snow distribution, but also as a function of snow properties, such as density.

Another approach could be to integrate the output of snow cover models. Models, such as the one-dimensional numerical snow cover model SNOWPACK (Lehning et al., 2008) or the three-dimensional atmospheric and surface process model Alpine3D (Lehning et al., 2006), are applied with increasing success for diverse purposes such as studies on spatial snow distribution (Mott et al., 2010) or avalanche forecasting (Bellaire et al., 2011) and have shown to successfully model snow cover parameters (Steinkogler et al., 2014). They would not only provide a more precise estimation of the snow cover distribution, but could further allow the integration of snowpack stability as an additional parameter into existing release area algorithms.

This may allow in the future the simulation of realistic snow cover-avalanche scenarios, including the influence of the snow cover properties on both algorithms to calculate avalanche starting zones and avalanche dynamics simulations. This could open up new perspectives for the management of small and medium-sized avalanches, where the connection of snow cover properties and avalanche dynamics is of fundamental importance.

Appendix A

Snow cover and roughness maps

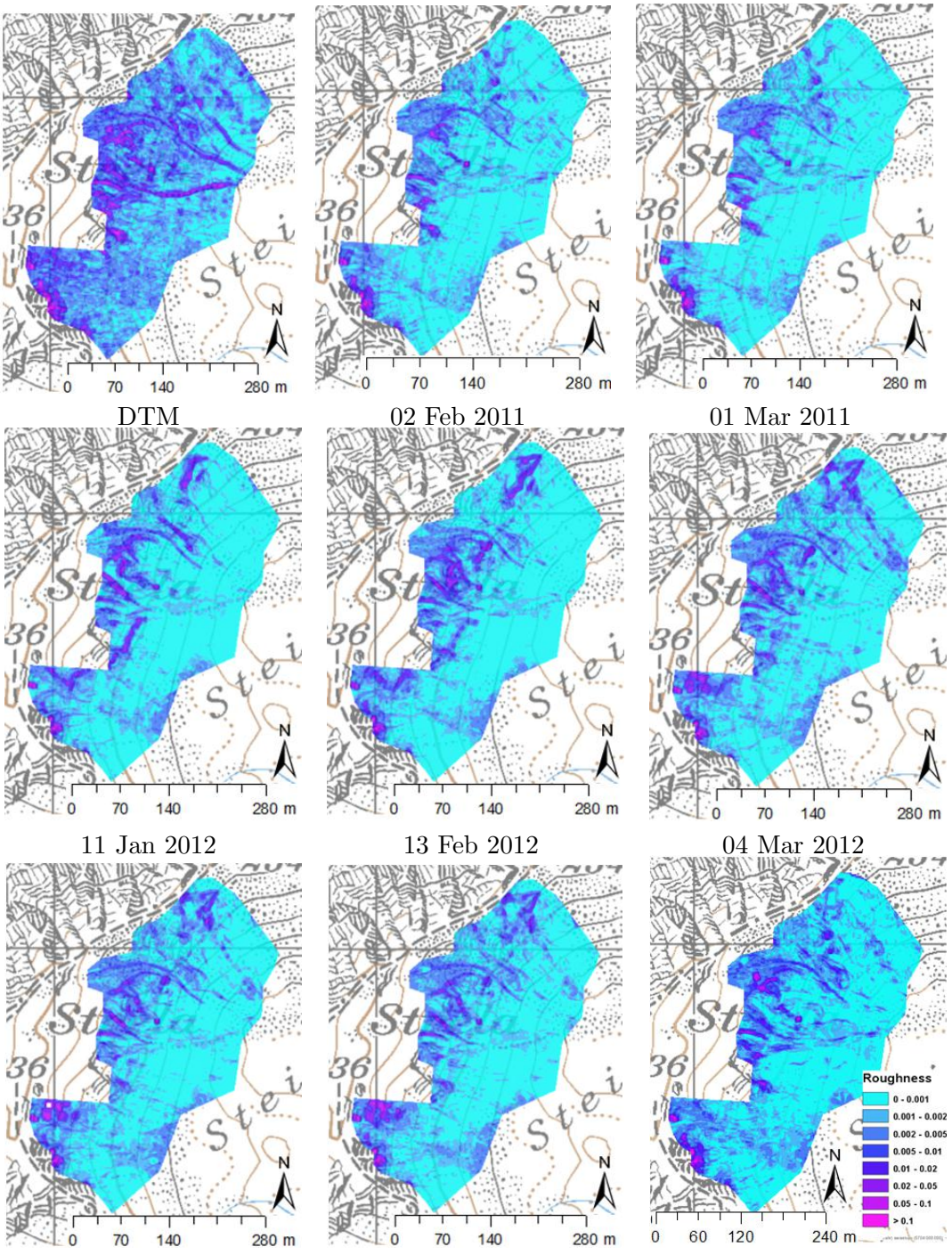

FIGURE A.1: Surface roughness of summer terrain and winter terrain at a scale of 5 m in the basin ST. Pixmaps 2013 swisstopo (5704 000 000).

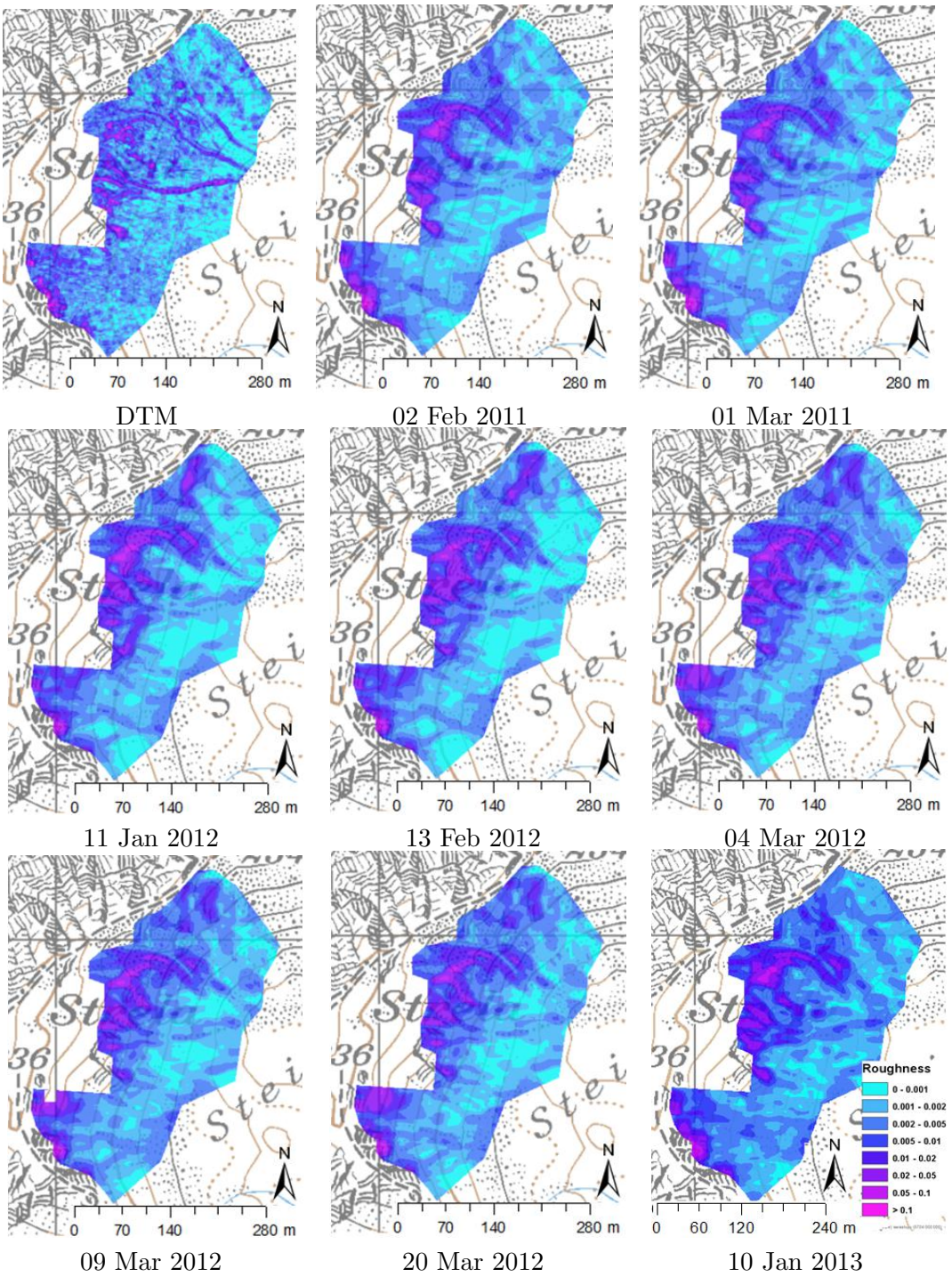

FIGURE A.2: Surface roughness of summer terrain and winter terrain at a scale of 15 m in the basin ST. Pixmaps 2013 swisstopo (5704 000 000).

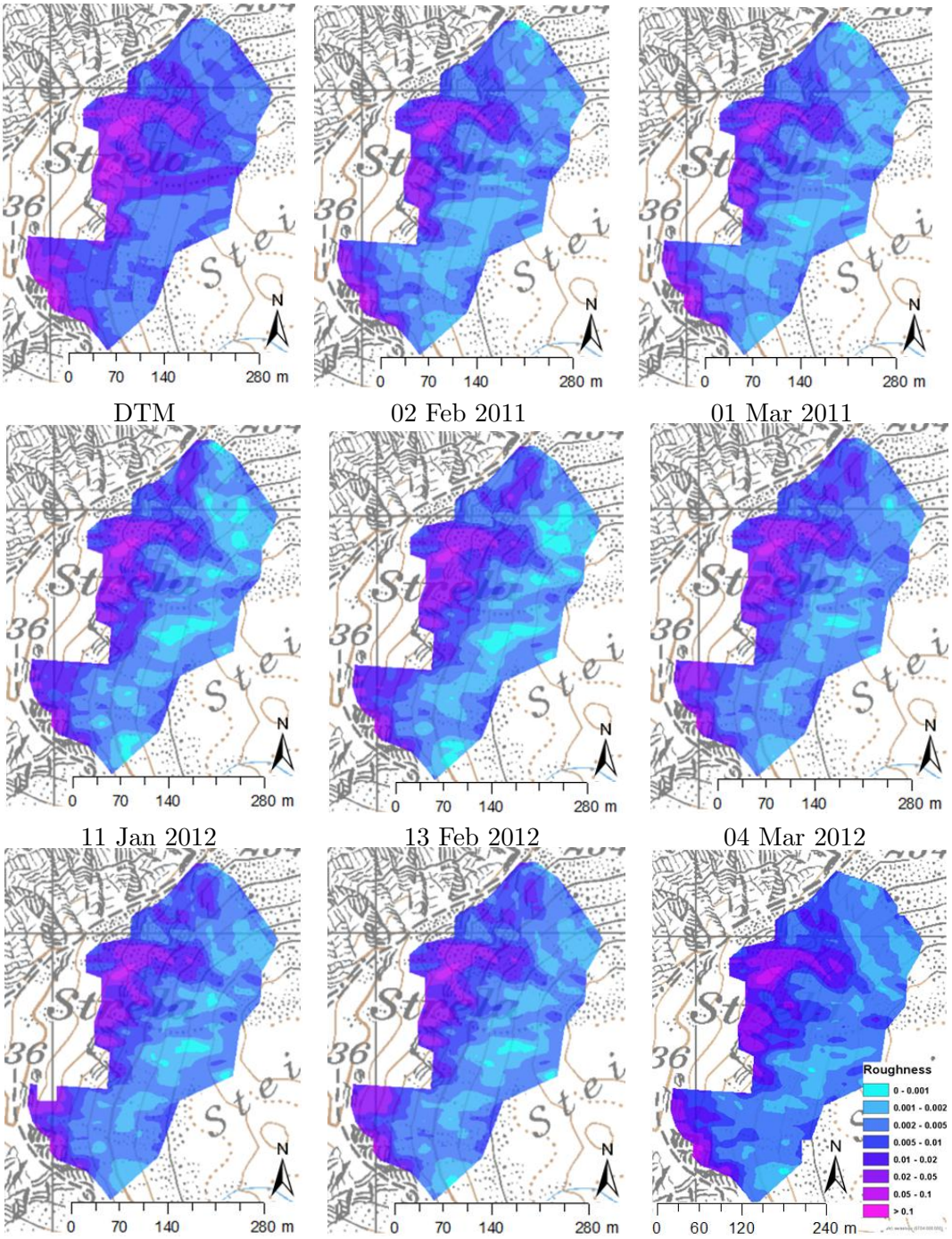

FIGURE A.3: Surface roughness of summer terrain and winter terrain at a scale of 25 m in the basin ST. Pixmaps 2013 swisstopo (5704 000 000).

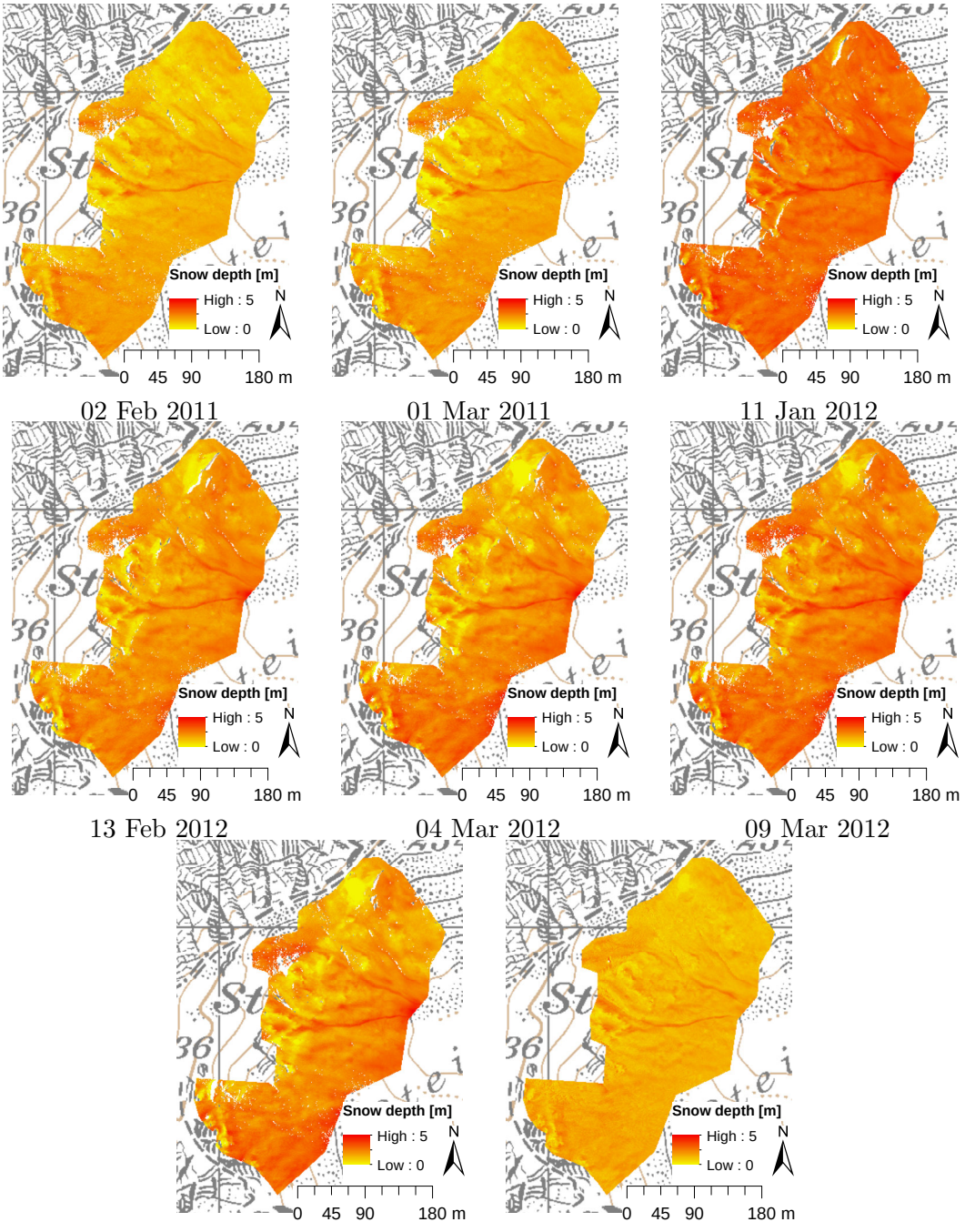

FIGURE A.4: Snow depth distributions in the basin ST. Pixmaps 2013 swisstopo (5704 000 000).

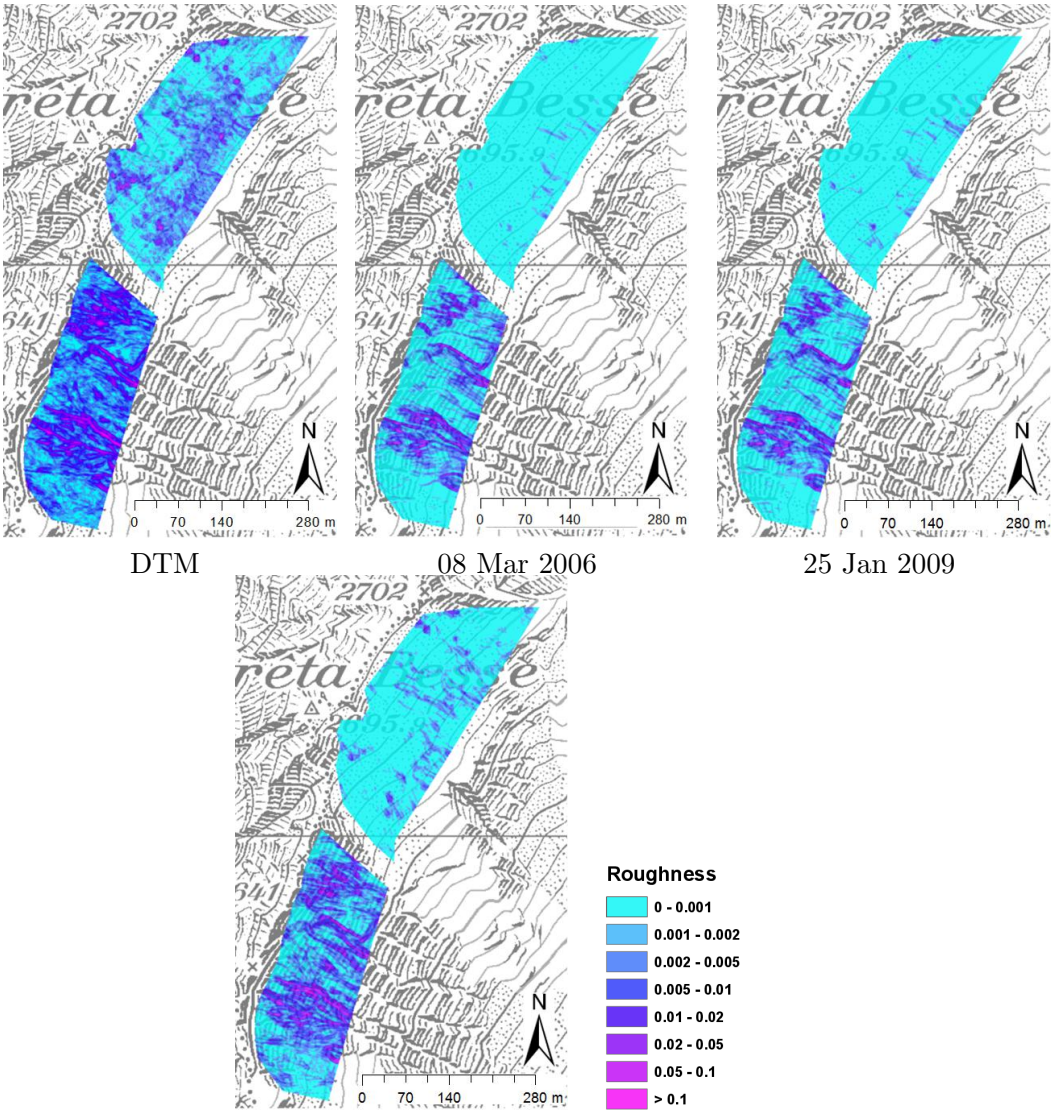

FIGURE A.5: Surface roughness of summer terrain and winter terrain at a scale of 5 m in basins CB1 and CB2. Pixmaps 2013 swisstopo (5704 000 000).

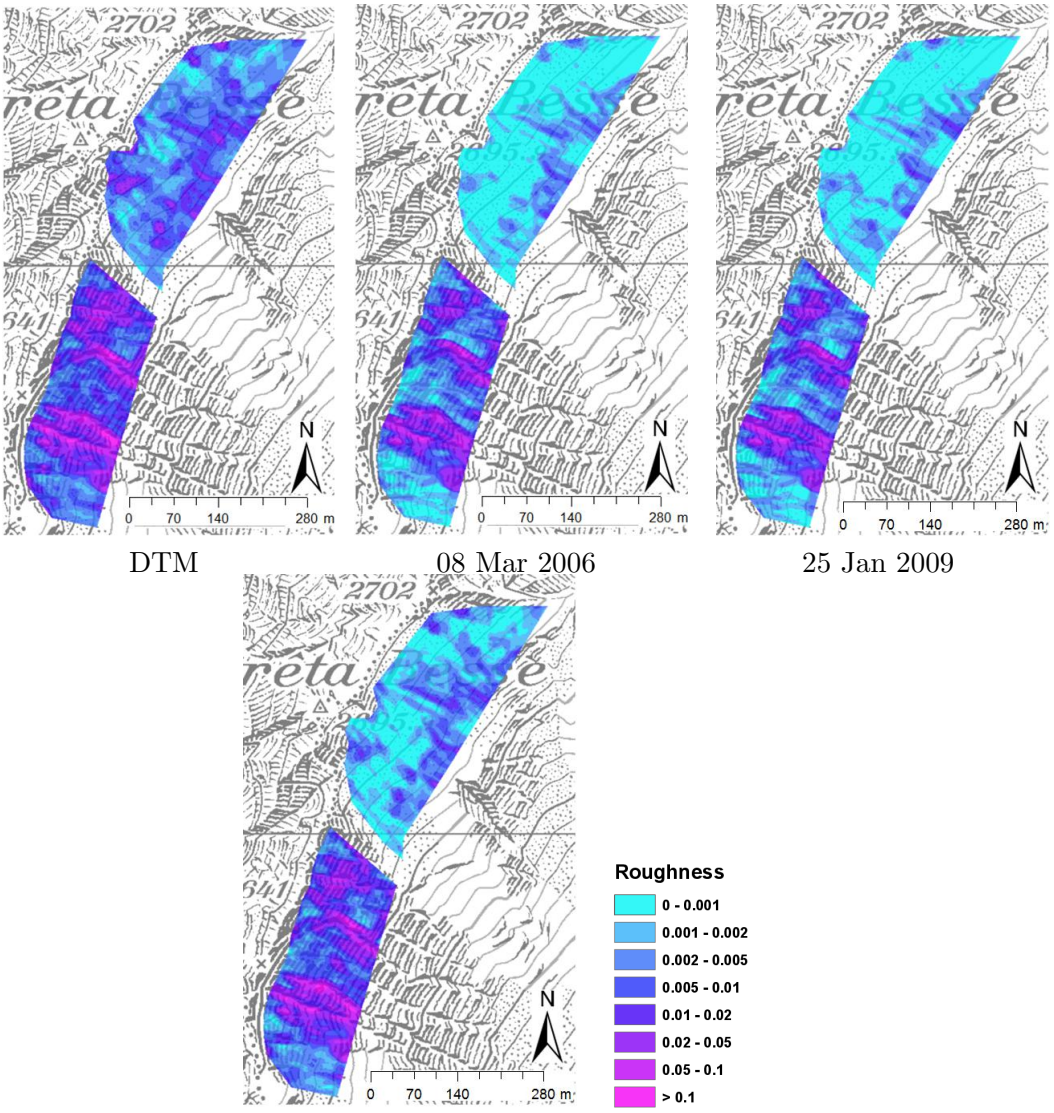

DTM 08 Mar 2006 25 Jan 2009

08 Dec 2011

FIGURE A.6: Surface roughness of summer terrain and winter terrain at a scale of 15 m in basins CB1 and CB2. Pixmaps 2013 swisstopo (5704 000 000).

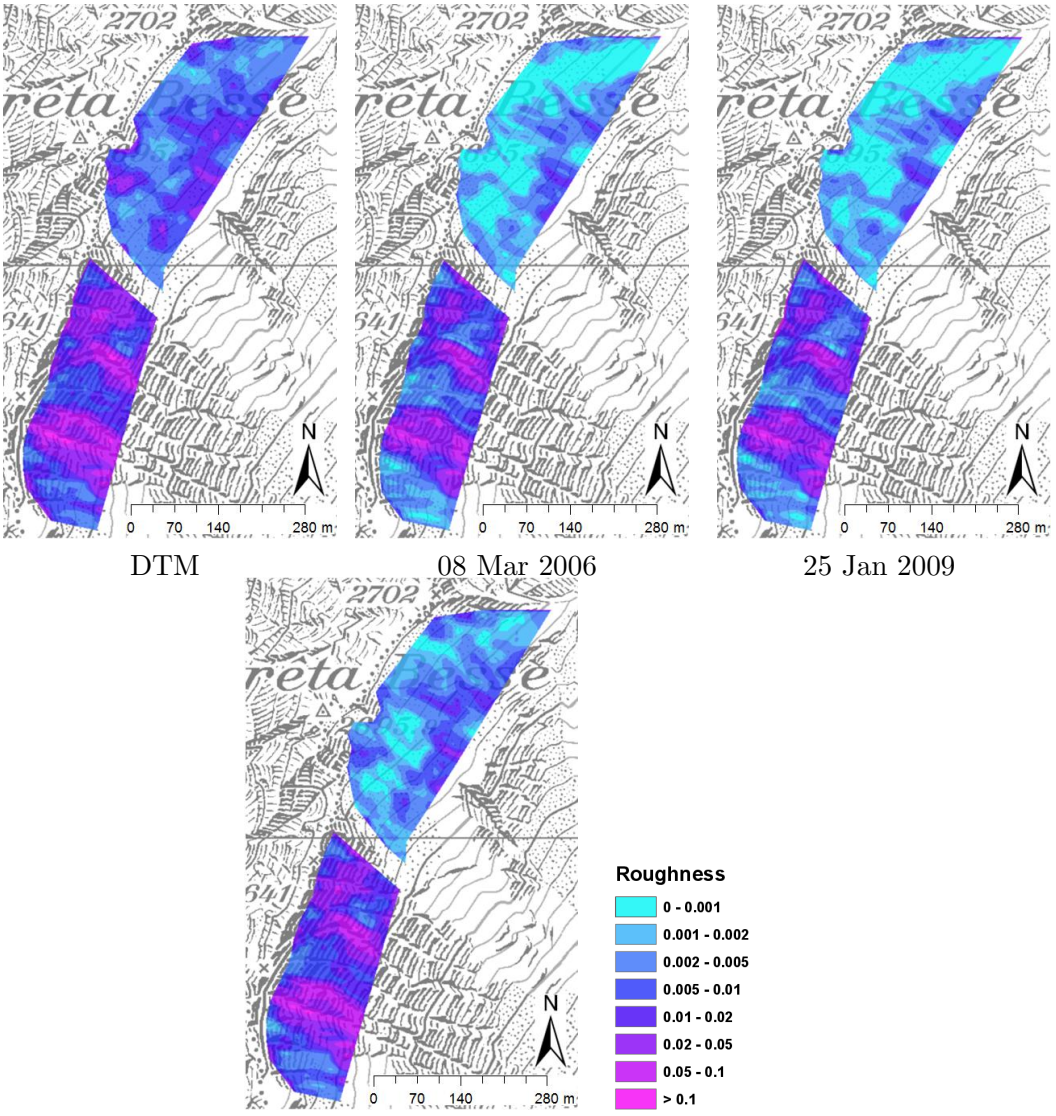

DTM 08 Mar 2006 25 Jan 2009

08 Dec 2011

FIGURE A.7: Surface roughness of summer terrain and winter terrain at a scale of 25 m in basins CB1 and CB2. Pixmaps 2013 swisstopo (5704 000 000).

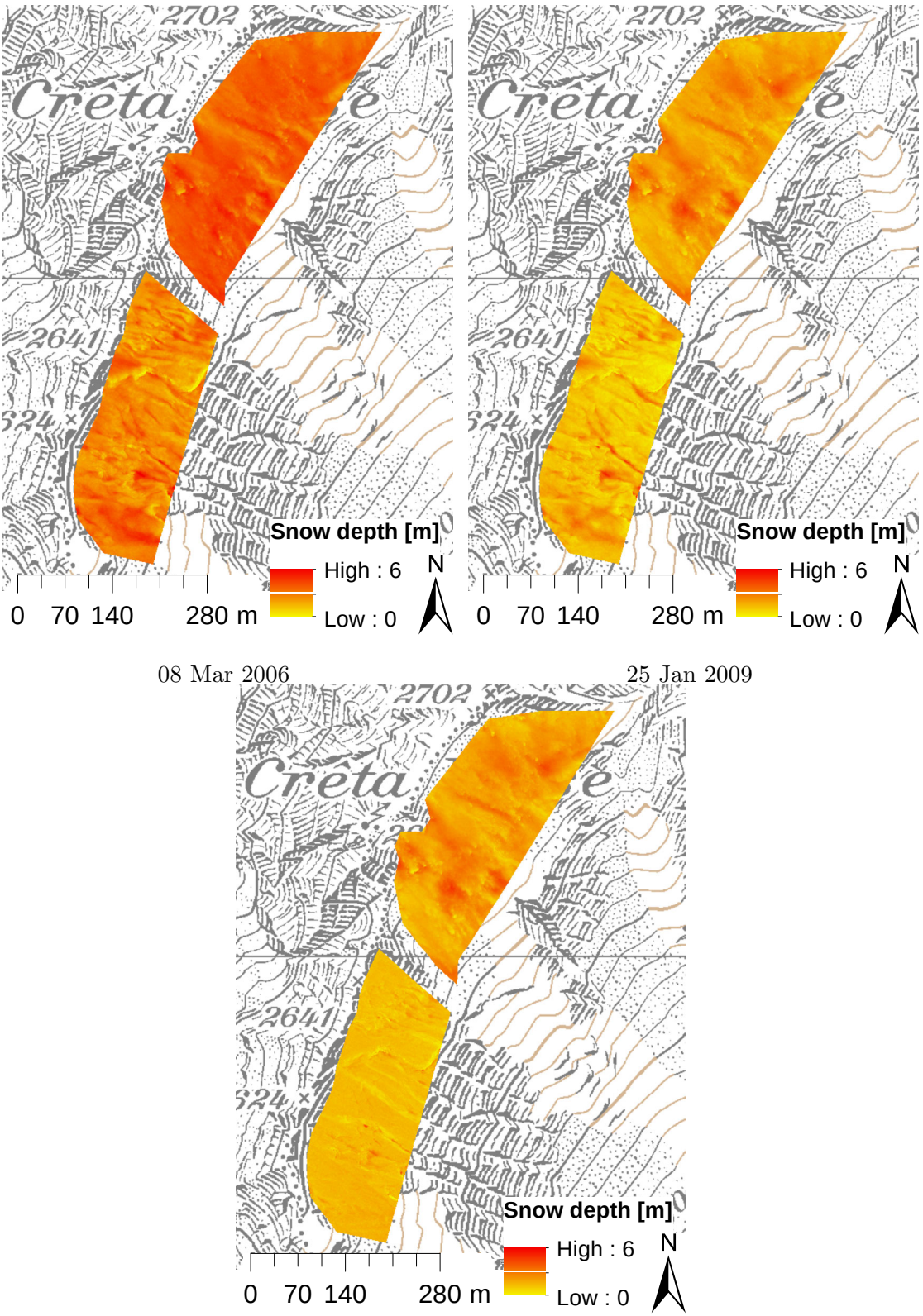

FIGURE A.8: Snow depth distributions in the basins CB1 and CB2. Pixmaps 2013 swisstopo (5704 000 000).

Bibliography

Ancey, C., Meunier, M., and Richard, D.: Inverse problem in avalanche dynamics models, Water Resources Research, 39, doi:10.1029/2002WR001749, URL http://dx.doi.org/10.1029/2002WR001749, 2003.

Anttila, K., Manninen, T., Karjalainen, T., Lahtinen, P., Riihel, A., and Siljamo, N.: The temporal and spatial variability in submeter scale surface roughness of seasonal snow in Sodankyl Finnish Lapland in 20092010, Journal of Geophysical Research: Atmospheres, 119, 9236–9252, doi:10.1002/2014JD021597, URL http://dx.doi.org/10.1002/2014JD021597, 2014.

Balk, B. and Elder, K.: Combining binary decision tree and geostatistical methods to estimate snow distribution in a mountain watershed, Water Resources Research, 36, 13–26, doi:10.1029/1999WR900251, URL http://dx.doi.org/10.1029/1999WR900251, 2000.

Bartelt, P., Meier, L., and Buser, O.: Snow avalanche flow-regime transitions induced by mass and random kinetic energy fluxes, Annals of Glaciology, 52, 159–164, doi:doi:10.3189/172756411797252158, URL http://www.ingentaconnect.com/content/igsoc/agl/2011/00000052/00000058/art00023, 2011.

BBF and SLF: Richtlinien zur Bercksichtigung der Lawinengefahr bei raumwirksamen Ttigkeiten, Bundesamt fr Forstwesen; Eidg. Institut f. Schnee- und Lawinenforschung, Bern, Eidg. Drucksachen- und Materialzentrale, 1984.

Beguera, S.: Validation and Evaluation of Predictive Models in Hazard Assessment and Risk Management, Natural Hazards, 37, 315–329, doi:10.1007/s11069-005-5182-6, URL http://dx.doi.org/10.1007/s11069-005-5182-6, 2006.

Bellaire, S., Jamieson, J. B., and Fierz, C.: Forcing the snow-cover model SNOWPACK with forecasted weather data, The Cryosphere, 5, 1115–1125, doi:10.5194/tc-5-1115-2011, URL http://www.the-cryosphere.net/5/1115/2011/, 2011.

Bernhardt, M. and Schulz, K.: SnowSlide: A simple routine for calculating gravitational snow transport, Geophysical Research Letters, 37, doi:10.1029/2010GL043086, URL http://dx.doi.org/10.1029/2010GL043086, 2010.

Birkeland, K. W., Hansen, K. J., and Brown, R. L.: The spatial variability of snow resistance on potential avalanche slopes, J. Glaciol., 41, 183–190, 1995.

Birks, H.: Recent methodological developments in quantitative descriptive biogeography, Annales Zoologici Fennici, 24, 165–178, 1987.

Blöschl, G.: Scaling issues in snow hydrology, Hydrological Processes, 13, 2149–2175, 1999.

Brenning, A.: Statistical geocomputing combining R and SAGA: The example of landslide susceptibility analysis with generalized additive models, in: SAGA – Seconds Out (= Hamburger Beitraege zur Physischen Geographie und Landschaftsoekologie, vol. 19), pp. 23–32, J. Boehner, T. Blaschke, L. Montanarella, 2008.

Bründl, M., McAlpin, M., Gruber, U., and Fuchs, S.: Application of the marginal cost-approach and cost-benefit analysis to measures for avalanche risk reduction–A case study from Davos, Switzerland, RISK21–Coping with risks due to natural hazards in the 21st century. Taylor & Francis, London, pp. 155–168, 2006.

Bühler, Y.: Remote sensing tools for snow and avalanche research, Proceedings of the 2012 International Snow Science Workshop, Anchorage, Alaska., pp. 264–268, 2012.

Bühler, Y., Marty, M., and Ginzler, C.: High Resolution DEM Generation in High-Alpine Terrain Using Airborne Remote Sensing Techniques, Transactions in GIS, 16, 635–647, 2012.

Bühler, Y., Kumar, S., Veitinger, J., Christen, M., Stoffel, A., and Snehmani: Automated identification of potential snow avalanche release areas based on digital elevation models, Natural Hazards and Earth System Science, 13, 1321–1335, 2013.

Carrara, A. and Pike, R. J.: {GIS} technology and models for assessing landslide hazard and risk, Geomorphology, 94, 257 – 260, doi:http://dx.doi.org/10.1016/j.geomorph.2006.07.042, URL http://www.sciencedirect.com/science/article/pii/S0169555X07002668, {GIS} technology and models for assessing landslide hazard and risk, 2008.

Caswell, H.: The validation problem, Systems analysis and simulation in ecology, 4, 313–325, 1976.

Christen, M., Kowalski, J., and Bartelt, P.: RAMMS: Numerical simulation of dense snow avalanches in three-dimensional terrain, Cold Regions Science and Technology, 63, 1 – 14, 2010.

Clark, M. P., Hendrikx, J., Slater, A. G., Kavetski, D., Anderson, B., Cullen, N. J., Kerr, T., Örn Hreinsson, E., and Woods, R. A.: Representing spatial variability of snow water equivalent in hydrologic and land-surface models: A review, Water Resources Research, 47, 2011.

Deems, J. S., Fassnacht, S. R., and Elder, K. J.: Fractal Distribution of Snow Depth from Lidar Data, Journal of Hydrometeorology, 7, 2006.

Deems, J. S., Fassnacht, S. R., and Elder, K. J.: Interannual Consistency in Fractal Snow Depth Patterns at Two Colorado Mountain Sites, J. Hydrometeor, 9, 977–988, 2008.

Dreier, L., Bühler, Y., Steinkogler, W., Feistl, T., and Bartelt, P.: Modelling Small and Frequent Avalanches, Proceedings of the 2014 International Snow Science Workshop, Banff, Alberta, Canada., 2014.

Eastman, J.: Multi-criteria evaluation and GIS, Geographical information systems, 1, 493–502, 1999.

Eckerstorfer, M., Farnsworth, W. R., and Birkeland, K. W.: Potential dry slab avalanche trigger zones on wind-affected slopes in central Svalbard, Cold Regions Science and Technology, 99, 66 – 77, doi:http://dx.doi.org/10.1016/j.coldregions.2013.12.005, URL `http://www.sciencedirect.com/science/article/pii/S0165232X13002048`, 2014.

Eckert, N., Parent, E., and Richard, D.: Revisiting statistical - topographical methods for avalanche predetermination: Bayesian modelling for runout distance predictive distribution, Cold Regions Science and Technology, 49, 88 – 107, doi:http://dx.doi.org/10.1016/j.coldregions.2007.01.005, URL `http://www.sciencedirect.com/science/article/pii/S0165232X07000080`, selected Papers from the General Assembly of the European Geosciences Union (EGU), Vienna, Austria, 25 April 2005, 2007.

Erath, A., Birdsall, J., Axhausen, K. W., and Hajdin, R.: Vulnerability assessment methodology for Swiss road network, Transportation Research Record: Journal of the Transportation Research Board, 2137, 118–126, 2009.

Erickson, T. A., Williams, M. W., and Winstral, A.: Persistence of topographic controls on the spatial distribution of snow in rugged mountain terrain, Colorado, United

States, Water Resources Research, 41, doi:10.1029/2003WR002973, URL http://dx.doi.org/10.1029/2003WR002973, 2005.

Evans, I. S.: An integrated system of terrain analysis and slope mapping, Zeitschrift für Geomorphologie, Suppl. Bd. 36, 274–295, 1980.

Fassnacht, S., Williams, M., and Corrao, M.: Changes in the surface roughness of snow from millimetre to metre scales, Ecological Complexity, 6, 221 – 229, 2009.

Fawcett, T.: An introduction to {ROC} analysis, Pattern Recognition Letters, 27, 861 – 874, doi:http://dx.doi.org/10.1016/j.patrec.2005.10.010, URL http://www.sciencedirect.com/science/article/pii/S016786550500303X, {ROC} Analysis in Pattern Recognition, 2006.

Fischer, L., Eisenbeiss, H., Kääb, A., Huggel, C., and Haeberli, W.: Monitoring topographic changes in a periglacial high-mountain face using high-resolution DTMs, Monte Rosa East Face, Italian Alps, Permafrost and Periglacial Processes, 22, 140–152, 2011.

Föhn, P., Stoffel, M., and Bartelt, P.: Formation and Forecasting of Large (Catastrophic) New Snow Avalanches, Proceedings of the 2002 International Snow Science Workshop, Penticton, British Columbia, Canada, pp. 591–598, 2002.

Fyffe, B. and Zaiser, M.: The effects of snow variability on slab avalanche release, Cold Regions Science and Technology, 40, 229 – 242, doi:http://dx.doi.org/10.1016/j.coldregions.2004.08.004, URL http://www.sciencedirect.com/science/article/pii/S0165232X04000916, 2004.

Fyffe, B. and Zaiser, M.: Interplay of basal shear fracture and slab rupture in slab avalanche release, Cold Regions Science and Technology, 49, 26 – 38, doi:http://dx.doi.org/10.1016/j.coldregions.2006.09.011, URL http://www.sciencedirect.com/science/article/pii/S0165232X06001595, selected Papers from the General Assembly of the European Geosciences Union (EGU), Vienna, Austria, 25 April 2005, 2007.

Ganju, A. and Dimri, A.: Prevention and Mitigation of Avalanche Disasters in Western Himalayan Region, Natural Hazards, 31, 357–371, doi:10.1023/B:NHAZ.0000023357.37850.aa, URL http://dx.doi.org/10.1023/B%3ANHAZ.0000023357.37850.aa, 2004.

Gauer, P.: Numerical modeling of blowing and drifting snow in Alpine terrain, Journal of Glaciology, 47, 97–110, doi:10.3189/172756501781832476, URL http://www.ingentaconnect.com/content/igsoc/jog/2001/00000047/00000156/art00011, 2001.

Gaume, J.: Evaluation of avalanche release depths. Combined statistical mechanical modeling, Ph.D. thesis, Universit é de Grenoble, 2012.

Gaume, J., Chambon, G., Eckert, N., and Naaim, M.: Influence of slab tensile strength and weak layer variability on slab tensile failure propensity, Naaim-Bouvet, F.; Durand, Y. ; Lambert, R. (eds) International Snow Science Workshop 2013, October, 2013 7th-11th. Proceedings. ISSW 2013. Grenoble - Chamonix Mont Blanc. Grenoble, ANENA., pp. 12–16, 2013a.

Gaume, J., Chambon, G., Eckert, N., and Naaim, M.: Influence of weak-layer heterogeneity on snow slab avalanche release: application to the evaluation of avalanche release depths, Journal of Glaciology, 59, 423–437, 2013b.

Gaume, J., Chambon, G., I., R., van Herwijnen, A., and Schweizer, J.: On the failure criterion of weak-snow layers using the discrete element method, Proceedings of the 2014 International Snow Science Workshop, Banff, Alberta, Canada., 2014a.

Gaume, J., Schweizer, J., van Herwijnen, A., Chambon, G., Reuter, B., Eckert, N., and Naaim, M.: Evaluation of slope stability with respect to snowpack spatial variability, Journal of Geophysical Research: Earth Surface, doi:10.1002/2014JF003193, URL `http://dx.doi.org/10.1002/2014JF003193`, 2014b.

Gaume, J., van Herwijnen, A., Schweizer, J., Chambon, G., and Birkeland, K.: Discrete element modeling of crack propagation in weak snowpack layers, Proceedings ISSW, 2014c.

Ghinoi, A. and Chung, C.-J.: STARTER: a statistical GIS-based model for the prediction of snow avalanche susceptibility using terrain features–application to Alta Val Badia, Italian Dolomites, Geomorphology, 66, 305 – 325, doi:10.1016/j.geomorph.2004.09.018, geomorphological hazard and human impact in mountain environments, 2005.

Gleason, J.: Terrain parameters of avalanche starting zones and their effect on avalanche frequency, Proceedings of the 1994 International Snow Science Workshop, Snowbird, Utah, USA, pp. 393–404, 1995.

Goodchild, M. F. and Quattrochi, D. A.: Scale, multiscaling, remote sensing, and GIS, Scale in remote sensing and GIS, pp. 1–11, 1997.

Grohmann, C., Smith, M., and Riccomini, C.: Multiscale Analysis of Topographic Surface Roughness in the Midland Valley, Scotland, IEEE Transactions on Geoscience and Remote Sensing, 49, 1200–1213, 2011.

Gruber: Using GIS for avalanche hazard mapping in Switzerland, in: Proceedings of the 2001 ESRI International User Conference, San Diego, USA, 2001.

Gruber, S.: A mass-conserving fast algorithm to parameterize gravitational transport and deposition using digital elevation models, Water Resources Research, 43, doi: 10.1029/2006WR004868, URL http://dx.doi.org/10.1029/2006WR004868, 2007.

Gruber, S., Huggel, C., and Pike, R.: Chapter 23 Modelling Mass Movements and Landslide Susceptibility, in: Geomorphometry Concepts, Software, Applications, edited by Hengl, T. and Reuter, H. I., vol. 33 of *Developments in Soil Science*, pp. 527 – 550, Elsevier, doi:http://dx.doi.org/10.1016/S0166-2481(08)00023-8, URL http://www.sciencedirect.com/science/article/pii/S0166248108000238, 2009.

Gruber, U. and Bartelt, P.: Snow avalanche hazard modelling of large areas using shallow water numerical methods and GIS, Environmental Modelling & Software, 22, 1472 – 1481, doi:10.1016/j.envsoft.2007.01.001, modelling, computer-assisted simulations, and mapping of dangerous phenomena for hazard assessment, 2007.

Gruber, U. and Margreth, S.: Winter 1999: a valuable test of the avalanche-hazard mapping procedure in Switzerland, Annals of Glaciology, 32, 328–332, doi:10.3189/172756401781819238, 2001.

Grünewald, T. and Lehning, M.: Altitudinal dependency of snow amounts in two small alpine catchments: can catchment-wide snow amounts be estimated via single snow or precipitation stations?, Annals of Glaciology, 52, 153–158, 2011.

Grünewald, T. and Lehning, M.: Are flat-field snow depth measurements representative? A comparison of selected index sites with areal snow depth measurements at the small catchment scale, Hydrological Processes, doi:10.1002/hyp.10295, URL http://dx.doi.org/10.1002/hyp.10295, 2014.

Grünewald, T., Schirmer, M., Mott, R., and Lehning, M.: Spatial and temporal variability of snow depth and ablation rates in a small mountain catchment, The Cryosphere, 4, 215–225, 2010.

Grünewald, T., Bühler, Y., and Lehning, M.: Elevation dependency of mountain snow depth, The Cryosphere Discussions, 8, 3665–3698, doi:10.5194/tcd-8-3665-2014, URL http://www.the-cryosphere-discuss.net/8/3665/2014/, 2014.

Guy, Z. M. and Birkeland, K. W.: Relating complex terrain to potential avalanche trigger locations, Cold Regions Science and Technology, 86, 1 – 13, doi:http://dx.doi.org/10.1016/j.coldregions.2012.10.008, URL http://www.sciencedirect.com/science/article/pii/S0165232X12002042, 2013.

Hageli, P. and McClung, D. M.: Hierarchy theory as a conceptual framework for scale issues in avalanche forecast modeling, Annals of Glaciology, 38, 209–214, doi:10.3189/172756404781815266, 2004.

Harvey, S., Rhyner, H., and Schweizer, J.: Lawinenkunde, Bruckmann Verlag GmbH, 2012.

Heierli, J., Purves, R. S., Felber, A., and Kowalski, J.: Verification of nearest-neighbours interpretations in avalanche forecasting, Annals of Glaciology, 38, 84–88, 2004.

Heierli, J., Gumbsch, P., and Zaiser, M.: Anticrack Nucleation as Triggering Mechanism for Snow Slab Avalanches, Science, 321, 240–243, doi:10.1126/science.1153948, 2008.

Hengl, T.: A practical guide to geostatistical mapping of environmental variables, JRC Scientific and Technichal Reports. Office for Official Publication of the European Communities, Luxembourg, 2007.

Hengl, T. and MacMillan, R.: Chapter 19 Geomorphometry A Key to Landscape Mapping and Modelling, in: Geomorphometry Concepts, Software, Applications, edited by Hengl, T. and Reuter, H. I., vol. 33 of *Developments in Soil Science*, pp. 433 – 460, Elsevier, doi:http://dx.doi.org/10.1016/S0166-2481(08)00019-6, URL `http://www.sciencedirect.com/science/article/pii/S0166248108000196`, 2009.

Hobson, R. D.: Surface roughness in topography: a quantitative approach, pp. 221–245, Harper & Row, 1972.

Huggel, C., Kääb, A., Haeberli, W., Krummenacher, B., et al.: Regional-scale GIS-models for assessment of hazards from glacier lake outbursts: evaluation and application in the Swiss Alps, Natural Hazards and Earth System Science, 3, 647–662, 2003.

Jaccard, P.: Nouvelles recherches sur la distribution florale, Bulletin de la Sociète Vaudense des Sciences Naturelles, 44, 223–270, 1908.

Jamieson, B. and Geldsetzer, T.: Avalanche Accidents in Canada 1984-96, Canadian Avalanche Association, Revelstoke, BC, 4, 203pp, 1996.

Jamieson, J. and Schweizer, J.: Texture and strength changes of buried surface hoar layers with implications for dry snow-slab avalanche release., Journal of Glaciology, 46, 151–160, 2000.

Jamieson, J. B. and Johnston, C. D.: Snowpack characteristics associated with avalanche accidents., Canadian Geotechnical Journal, 29, 862–866, 1992.

Jang, J.-S. R. and Sun, C.-T.: Neuro-fuzzy and Soft Computing: A Computational Approach to Learning and Machine Intelligence, Prentice-Hall, Inc., Upper Saddle River, NJ, USA, 1997.

Jóhannesson, T., Gauer, P., Issler, D., and Lied, K.: The design of avalanche protection dams, Tech. rep., Report of the European commission, 2009.

Lehning, M., Vlksch, I., Gustafsson, D., Nguyen, T. A., Sthli, M., and Zappa, M.: ALPINE3D: a detailed model of mountain surface processes and its application to snow hydrology, Hydrological Processes, 20, 2111–2128, 2006.

Lehning, M., Löwe, H., Ryser, M., and Raderschall, N.: Inhomogeneous precipitation distribution and snow transport in steep terrain, Water Resources Research, 44, 2008.

Lehning, M., Grünewald, T., and Schirmer, M.: Mountain snow distribution governed by an altitudinal gradient and terrain roughness, Geophys. Res. Lett., 38, L19504, 2, 2011.

Li, Z., Zhu, C., and Gold, C.: Digital terrain modeling: principles and methodology, CRC press, 2010.

López-Moreno, J. I. and Stähli, M.: Statistical analysis of the snow cover variability in a subalpine watershed: Assessing the role of topography and forest interactions, Journal of Hydrology, 348, 379–394, 2008.

MacDonald, M. K., Pomeroy, J. W., and Pietroniro, A.: Parameterizing redistribution and sublimation of blowing snow for hydrological models: tests in a mountainous subarctic catchment, Hydrological Processes, 23, 2570–2583, doi:10.1002/hyp.7356, URL `http://dx.doi.org/10.1002/hyp.7356`, 2009.

Maggioni, M. and Gruber, U.: The influence of topographic parameters on avalanche release dimension and frequency, Cold Regions Science and Technology, 37, 407 – 419, 2003.

Maggioni, M., Freppaz, M., Christen, M., Bartelt, P., and Zanini, E.: Back-Calculation of Small-Size Avalanches with the 2D Avalanche Dynamics Model RAMMS: Four Events Artificially Triggered at the Seehore Test Site in Aosta Valley (NW Italy), Proceedings of the 2012 International Snow Science Workshop, Anchorage, Alaska, USA., pp. 591–598, 2012.

Maggioni, M., Bovet, E., Dreier, L., Buehler, Y., Godone, D., Bartelt, P., M., F., Chiaia, B., and Segor, V.: Influence of summer and winter surface topography on numerical avalanche simulations, Naaim-Bouvet, F.; Durand, Y. ; Lambert, R. (eds) International Snow Science Workshop 2013, October, 2013 7th-11th. Proceedings.

ISSW 2013. Grenoble - Chamonix Mont Blanc. Grenoble, ANENA., pp. 591–598, 2013.

Magnusson, J., Jonas, T., Lopez-Moreno, I., and Lehning, M.: Snow cover response to climate change in a high alpine and half-glacierized basin in Switzerland, 2010.

Malczewski, J.: GIS and multicriteria decision analysis, John Wiley & Sons, 1999.

Manninen, T., Anttila, K., Karjalainen, T., and Lahtinen, P.: Automatic snow surface roughness estimation using digital photos, Journal of Glaciology, 58, 993–1007, 2012.

Margreth, S., Stoffel, L., and Wilhelm, C.: Winter opening of high alpine pass roadsanalysis and case studies from the Swiss Alps, Cold Regions Science and Technology, 37, 467 – 482, doi:http://dx.doi.org/10.1016/S0165-232X(03)00085-5, URL `http://www.sciencedirect.com/science/article/pii/S0165232X03000855`, {ISSW} 2002: International Snow Science Workshop, 2003.

McClung, D.: Characteristics of terrain, snow supply and forest cover for avalanche initiation caused by logging, Annals of Glaciology, 32, 223–229, 2001.

McClung, D. M.: Shear fracture precipitated by strain softening as a mechanism of dry slab avalanche release, Journal of Geophysical Research: Solid Earth, 84, 3519–3526, doi:10.1029/JB084iB07p03519, URL `http://dx.doi.org/10.1029/JB084iB07p03519`, 1979.

McClung, D. M. and Schaerer, P. A.: The Avalanche Handbook, Seattle, WA, the mountaineers edn., 2002.

Mott, R., M. S. and Lehning, M.: Scaling properties of wind and snow depth distribution in an Alpine catchment, J. Geophys. Res., 116, D06106, 2, 2011.

Mott, R., Schirmer, M., Bavay, M., Grünewald, T., and Lehning, M.: Understanding snow-transport processes shaping the mountain snow-cover, The Cryosphere Discussions, 4, 865–900, 2010.

Mott, R., Scipin, D., Schneebeli, M., Dawes, N., Berne, A., and Lehning, M.: Orographic effects on snow deposition patterns in mountainous terrain, Journal of Geophysical Research: Atmospheres, 119, 1419–1439, doi:10.1002/2013JD019880, URL `http://dx.doi.org/10.1002/2013JD019880`, 2014.

Murphy, A. H.: What is a good forecast? An essay on the nature of goodness in weather forecasting, Weather and forecasting, 8, 281–293, 1993.

Peev, C. D.: Der Einfluss von Hangneigung und Exposition auf die Lawinenbildung, Geographische Berichte, Heft 12, 138 – 150, 1959.

Perla, R.: Slab avalanche measurements, Canadian Geotechnical Journal, 14, 206–213, doi:10.1139/t77-021, URL http://dx.doi.org/10.1139/t77-021, 1977.

Pipp, M. J. and Locke, W. W.: Local scale variability in storm snowfall and seasonal snowpack distribution in the Bridger Range, Montana, in: Proceedings of the 66th Annual Western Snow Conference, pp. 26–37, 1998.

Plattner, C., Braun, L., and Brenning, A.: The spatial variability of snow accumulation at Vernagtferner, Austrian Alps, in winter 2003/2004, Zeitschrift für Gletscherkunde und Glazialgeologie, 39, 1, URL http://www.geophysik.uni-muenchen.de/~plattner/downloads/variabilitysnowaccumulation.pdf, 2006.

Pomeroy, J., Essery, R., and Toth, B.: Implications of spatial distributions of snow mass and melt rate for snow-cover depletion: observations in a subarctic mountain catchment, Annals of Glaciology, 38, 195–201, doi:10.3189/172756404781814744, 2004.

Pomeroy, J. W., Gray, D. M., Shook, K. R., Toth, B., Essery, R. L. H., Pietroniro, A., and Hedstrom, N.: An evaluation of snow accumulation and ablation processes for land surface modelling, Hydrological Processes, 12, 2339–2367, doi:10.1002/(SICI)1099-1085(199812)12:15⟨2339::AID-HYP800⟩3.0.CO;2-L, URL http://dx.doi.org/10.1002/(SICI)1099-1085(199812)12:15<2339::AID-HYP800>3.0.CO;2-L, 1998.

Prokop, A.: Assessing the applicability of terrestrial laser scanning for spatial snow depth measurements, Cold Regions Science and Technology, 54, 155 – 163, 2008.

Prokop, A., Schirmer, M., Rub, M., Lehning, M., and Stocker, M.: A comparison of measurement methods: terrestrial laser scanning, tachymetry and snow probing for the determination of the spatial snow-depth distribution on slopes, Annals of Glaciology, 49, 210–216, 2008.

Purves, R., Barton, J., Mackaness, W., and Sugden, D.: The development of a rule-based spatial model of wind transport and deposition of snow, Annals of Glaciology, 26, 197–202, 1998.

Raderschall, N., Lehning, M., and Schr, C.: Fine-scale modeling of the boundary layer wind field over steep topography, Water Resources Research, 44, doi:10.1029/2007WR006544, URL http://dx.doi.org/10.1029/2007WR006544, 2008.

Reuter, B., Proksch, M., Loewe, H., van Herwijnen, A., and Schweizer, J.: On how to measure snow mechanical properties relevant to slab avalanche release, Naaim-Bouvet, F.; Durand, Y. ; Lambert, R. (eds) International Snow Science Workshop 2013, October, 2013 7th-11th. Proceedings. ISSW 2013. Grenoble - Chamonix Mont Blanc. Grenoble, ANENA., pp. 7–11, 2013.

Rykiel Jr, E. J.: Testing ecological models: the meaning of validation, Ecological modelling, 90, 229–244, 1996.

Salm, B., Burkard, A., and Gubler, H. U.: Berechnung von Fliesslawinen: eine Anleitung fuer Praktiker mit Beispielen, Mittlg. No. 47, Eidg. Institut f. Schnee- und Lawinenforschung, CH–7260 Davos Dorf, 1990.

Sampl, P. and Granig, M.: Avalanche Simulation with Samos-AT. International Snow Science Workshop, Proceedings, Davos, Switzerland, 2009.

Sampl, P. and Zwinger, T.: Avalanche simulation with SAMOS, Annals of glaciology, 38, 393–398, 2004.

Sappington, J., Longshore, K., and Thomson, D.: Quantifiying Landscape Ruggedness for Animal Habitat Anaysis: A case Study Using Bighorn Sheep in the Mojave Desert, J. Wildl. Manage., 71, 1419 –1426, 2007.

Sargent, R. G.: A tutorial on verification and validation of simulation models, in: Proceedings of the 16th conference on Winter simulation, pp. 114–121, IEEE Press, 1984.

Schaer: Avalanche activity during major avalanche events - A case study for hydroelectric reservoirs, Les apports de la recherche scientifique la scurite neige, glace et avalanche, Actes de Colloque, Chamonix, France, 30 mai3 juin 1995, p. 133138, 1995.

Schernthanner, H.: Fuzzy Logic Method for Landslide Susceptibility Mapping, Rio Blanco, Nicaragua, in: Proceedings of 9th International Conference on GeoComputation,, 2007.

Schirmer, M. and Lehning, M.: Persistence in intra-annual snow depth distribution: 2.Fractal analysis of snow depth development, Water Resources Research, 47, 2011.

Schirmer, M., Wirz, V., Clifton, A., and Lehning, M.: Persistence in intra-annual snow depth distribution: 1.Measurements and topographic control, Water Resources Research, 47, 2011.

Schweizer, J.: Review of dry snow slab avalanche release, Cold Regions Science and Technology, 30, 43 – 57, doi:DOI:10.1016/S0165-232X(99)00025-7, 1999.

Schweizer, J.: On the predictability of snow avalanches, in: Proceedings Whistler 2008 International Snow Science Workshop September 21-27, 2008, pp. 688–692, 2008.

Schweizer, J. and Jamieson, J.: Snow cover properties for skier triggering of avalanches, Cold Regions Science and Technology, 33, 207 – 221, doi:http://dx.doi.org/10.1016/S0165-232X(01)00039-8, URL `http://www.sciencedirect.com/science/article/pii/S0165232X01000398`, {ISSW} 2000:International Snow Science Workshop, 2001.

Schweizer, J. and Lütschg, M.: Characteristics of human-triggered avalanches, Cold Regions Science and Technology, 33, 147 – 162, doi:10.1016/S0165-232X(01)00037-4, 2001.

Schweizer, J., Bruce Jamieson, J., and Schneebeli, M.: Snow avalanche formation, Reviews of Geophysics, 41, 2003.

Schweizer, J., Kronholm, K., Jamieson, J. B., and Birkeland, K. W.: Review of spatial variability of snowpack properties and its importance for avalanche formation, Cold Regions Science and Technology, 51, 253–272, 2008.

Schweizer, J., Mitterer, C., and Stoffel, L.: On forecasting large and infrequent snow avalanches, Cold Regions Science and Technology, 59, 234 – 241, doi:10.1016/j.coldregions.2009.01.006, international Snow Science Workshop (ISSW) 2008, 2009.

Sevruk, B.: Regional dependency of precipitation-altitude relationship in the Swiss Alps, in: Climatic Change at High Elevation Sites, pp. 123–137, Springer, 1997.

Simenhois, R. and Birkeland, K. W.: The effect of changing slab thickness on fracture propagation, Proceedings of the 2008 International Snow Science Workshop, Whistler, B.C., pp. 755–760., 2008.

SLF: Winterbericht 1951, Mittlg. No. 15, Eidg. Institut f. Schnee- und Lawinenforschung, CH–7260 Davos Dorf, 1951.

SLF: Der Lawinenwinter 1999. Ereignisanalyse, Eidg. Institut f. Schnee- und Lawinenforschung, CH–7260 Davos Dorf, 2000.

Sovilla, B., Burlando, P., and Bartelt, P.: Field experiments and numerical modeling of mass entrainment in snow avalanches, J. Geophys. Res., 111, 2006.

Sovilla, B., McElwaine, J. N., Schaer, M., and Vallet, J.: Variation of deposition depth with slope angle in snow avalanches: Measurements from Vallée de la Sionne, J. Geophys. Res., 115, 2010.

Sovilla, B., Sonatore, I., Bühler, Y., and Margreth, S.: Wet-snow avalanche interaction with a deflecting dam: field observations and numerical simulations in a case study, Natural Hazards and Earth System Science, 12, 1407–1423, 2012.

Stehman, S. V.: Selecting and interpreting measures of thematic classification accuracy, Remote Sensing of Environment, 62, 77 – 89, doi:http://dx.doi.org/10.1016/S0034-4257(97)00083-7, URL `http://www.sciencedirect.com/science/article/pii/S0034425797000837`, 1997.

Steinkogler, W., Sovilla, B., and Lehning, M.: Influence of snow cover properties on avalanche dynamics, Cold Regions Science and Technology, 97, 121 – 131, doi:http://dx.doi.org/10.1016/j.coldregions.2013.10.002, URL http://www.sciencedirect.com/science/article/pii/S0165232X13001535, 2014.

Stoffel, A., Meister, R., and Schweizer, J.: Spatial characteristics of avalanche activity in an alpine valley-a GIS approach, Annals of Glaciology, 26, 329–336, 1998.

Stoffel, L. and Margreth, S.: Beurteilung von Sekundärlawinen bei künstlicher Lawinenauslösung. Anleitung fr die Praxis, Bundesamt fr Umwelt, Bern. Umwelt-Wissen Nr. 1222: 62 S., 2012.

Tracz, D. and Jamieson, J.: Characteristics of old-deep-slab avalanches., Proceedings of the 2010 International Snow Science Workshop, Squaw Valley, CA, USA, pp. 148–154, 2010.

Trujillo, E., Ramirez, J. A., and Elder, K. J.: Topographic, meteorologic, and canopy controls on the scaling characteristics of the spatial distribution of snow depth fields, Water Resources Research, 43, 2007.

Vallet, J.: Quick Deployment Heliborne Handheld LiDAR System for Natural Hazard Mapping, 3-7 May, in: Gi4DM - Geoinformation for Disaster management Conference, Antalya, Turkey, 2011.

van Herwijnen, A. and Heierli, J.: Measurement of crack-face friction in collapsed weak snow layers, Geophysical Research Letters, 36, 2009.

van Herwijnen, A., Schweizer, J., and Heierli, J.: Measurement of the deformation field associated with fracture propagation in weak snowpack layers, Journal of Geophysical Research: Earth Surface, 115, doi:10.1029/2009JF001515, URL http://dx.doi.org/10.1029/2009JF001515, 2010.

Vera Valero, C., Feistl, T., Steinkogler, W., Buser, O., and Bartelt, P.: Thermal temperature in avalanche flow, Proceedings of the 2012 International Snow Science Workshop, Anchorage, Alaska, USA., pp. 32–37, 2012.

Vontobel, I.: Geländeanalysen von Unfalllawinen, Master's thesis, Department of Geography, University of Zurich, 2011.

Vontobel, I., Harvey, S., and Purves, R.: Terrain analysis of skier-triggered avalanche starting zones, Naaim-Bouvet, F.; Durand, Y. ; Lambert, R. (eds) International Snow Science Workshop 2013, October, 2013 7th-11th. Proceedings. ISSW 2013. Grenoble - Chamonix Mont Blanc. Grenoble, ANENA., pp. 371–375, 2013.

Wastl, C. and Zängl, G.: Analysis of mountain-valley precipitation differences in the Alps, Meteorologische Zeitschrift, 17, 311–321, 2008.

Werners, B.: Aggregation Models in Mathematical Programming, in: Mathematical Models for Decision Support, edited by Mitra, G., Greenberg, H., Lootsma, F., Rijkaert, M., and Zimmermann, H., vol. 48 of *NATO ASI Series*, pp. 295–305, Springer Berlin Heidelberg, doi:10.1007/978-3-642-83555-1_19, URL `http://dx.doi.org/10.1007/978-3-642-83555-1_19`, 1988.

Whiteman, C. A.: Cold region hazards and risks, John Wiley & Sons, 2011.

Wilhelm, C.: Quantitative risk analysis for evaluation of avalanche protection projects, in: Proceedings of the Anniversary Conference, vol. 25, pp. 288–293, 1998.

Winkler, K. and Schweizer, J.: Comparison of different snow stability tests including the extended column test, in: Proceedings of the Int. Snow Science Workshop, Whistler BC, Canada, 2008.

Winstral, A. and Marks, D.: Long-term snow distribution observations in a mountain catchment: Assessing variability, time stability, and the representativeness of an index site, Water Resources Research, 50, 293–305, doi:10.1002/2012WR013038, URL `http://dx.doi.org/10.1002/2012WR013038`, 2014.

Winstral, A., Elder, K., and Davis, R. E.: Spatial Snow Modeling of Wind-Redistributed Snow Using Terrain-Based Parameters, J. Hydrometeor, 3, 524–538, 2002.

Wipf, S., Stoeckli, V., and Bebi, P.: Winter climate change in alpine tundra: plant responses to changes in snow depth and snowmelt timing, Climatic Change, 94, 105–121, doi:10.1007/s10584-009-9546-x, URL `http://dx.doi.org/10.1007/s10584-009-9546-x`, 2009.

Wirz, V., Schirmer, M., Gruber, S., and Lehning, M.: Spatio-temporal measurements and analysis of snow depth in a rock face, The Cryosphere Discussions, 5, 1383–1418, doi:10.5194/tcd-5-1383-2011, 2011.

Wood, J.: The Geomorphological Characterisation of Digital Elevation Models, Ph.D. thesis, University of Leicester, 1996.

Wood, J.: Visualization of scale dependencies in the surface models, in: 19th International Cartographic Association Annual Conference. Ottawa, http://www. soi. city. ac. uk/˜ jwo/ica99, 1999.

Yager, R.: On ordered weighted averaging aggregation operators in multicriteria decisionmaking, Systems, Man and Cybernetics, IEEE Transactions on, 18, 183–190, doi:10.1109/21.87068, 1988.

Zadeh, L.: Fuzzy sets, Information and Control, 8, 338 – 353, doi:http://dx.doi.org/10.1016/S0019-9958(65)90241-X, URL http://www.sciencedirect.com/science/article/pii/S001999586590241X, 1965.

Zevenbergen, L. W. and Thorne, C. R.: Quantitative analysis of land surface topography, Earth Surface Processes and Landforms, 12, 47–56, doi:10.1002/esp.3290120107, URL http://dx.doi.org/10.1002/esp.3290120107, 1987.

Zimmermann, H.-J.: Fuzzy sets, decision making, and expert systems, Boston: Kluwer, 1987.

Zimmermann, H.-J. and Zysno, P.: Decisions and evaluations by hierarchical aggregation of information, Fuzzy Sets and Systems, 10, 243 – 260, doi:http://dx.doi.org/10.1016/S0165-0114(83)80118-3, URL http://www.sciencedirect.com/science/article/pii/S0165011483801183, 1983.

Zischg, A., Fuchs, S., Keiler, M., and Meißl, G.: Modelling the system behaviour of wet snow avalanches using an expert system approach for risk management on high alpine traffic roads, Natural Hazards and Earth System Science, 5, 821–832, 2005.

Curriculum Vitae

Jochen Veitinger
Date of birth: 20 April 1981
Place of birth: Ulm, Germany
Nationality: German

Education

2010 – 2014	PhD Student at University of Zurich (Geocomputation Group) and WSL Institute for Snow and Avalanche Research SLF.
2007 – 2010	Master of Science ETH in Geomatic Engineering and Planning, ETH Zurich. Majors: Photogrammetry and Remote Sensing, Geoinformation Science and Cartography. Master thesis: Methods for the Derivation of Snow Covered Area from Envisat/ASAR-Data.
2003 – 2006	Bachelor of Science BSc in Environmental Sciences and Engineering, EPF Lausanne.
1991 – 2000	Abitur, Lessing-Gymnasium Neu-Ulm, Germany

Publications

Veitinger, J.; Sovilla, B.; Purves, R., 2014:
Slab Avalanche Release Area Estimation: A new GIS Tool. In: International Snow Science Workshop 2014. A merging of Theory and Practice. September 29 - October 3, 2014. Banff, Alberta, Canada. Proceedings. ISSW. Banff, ISSW. 256-262.

Veitinger, J.; Sovilla, B.; Purves, R., 2014:
Influence of snow depth distribution on surface roughness in alpine terrain: a multi-scale approach. The Cryosphere, 8, 547-569, doi:10.5194/tc-8-547-2014.

Veitinger, J.; Sovilla, B.; Purves, R., 2013:
Winter terrain roughness as a new parameter to define location and size of avalanche release areas, In: Naaim-Bouvet, F.; Durand, Y. ; Lambert, R. (eds) International Snow Science Workshop 2013, October, 2013 7th-11th. Proceedings. ISSW 2013. Grenoble - Chamonix Mont Blanc. Grenoble, ANENA. 703-706.

Bühler, Y.; Marty, M.; Egli, L.; Veitinger, J.; Jonas, T.; Thee, P.; Ginzler, C.; 2014:
Spatially continuous mapping of snow depth in high alpine catchments using digital photogrammetry. The Cryosphere Discuss., 8, 3297-3333.

Bühler, Y.; Kumar, S.; Veitinger, J.; Christen, M.; Stoffel, A.; Snehmani, 2013:
Automated identification of potential snow avalanche release areas based on digital elevation models. Nat. Hazards Earth Syst. Sci. 13: 1321-1335.